MARSHALL
GRANT
IN-25-CR
118982

FINAL REPORT

for

SRB COMBUSTION DYNAMICS ANALYSIS COMPUTER PROGRAM (CDA-1)

NAG8-627

by

T. J. Chung and O. Y. Park

Department of Mechanical Engineering
The University of Alabama in Huntsville
Huntsville, AL 35899

prepared for

George C. Marshall Space Flight Center
National Aeronautics and Space Administration
Marshall Space Flight Center, AL 35812

(NASA-CR-179302)) SRB COMBUSTION DYNAMICS ANALYSIS COMPUTER PROGRAM (CDA-1) Final Report (Alabama Univ.) 130 p CSCL 21B

N88-15032

Unclas
G3/25 0118982

February 1988

ABSTRACT

A two-dimensional numerical model is developed for the unsteady oscillatory combustion of the solid propellant flame zone. Variations of pressure with low and high frequency responses across the long flame, such as in the double-base propellants, are accommodated. The formulation is based on a premixed, laminar flame with a one-step overall chemical reaction and the Arrhenius law of decomposition for the gaseous phase with no condensed phase reaction. Numerical calculations are carried out using the Galerkin finite elements, with perturbations expanded to the zeroth, first, and second orders. The numerical results indicate that amplification of oscillatory motions does indeed prevail in high frequency regions. For the second order system, the trend is similar to the first order system for low frequencies, but instabilities may appear at frequencies lower than those of the first order system. The most significant effect of the second order system is that the admittance is extremely oscillatory between moderately high frequency ranges.

TABLE OF CONTENTS

APPENDICES

LIST OF FIGURES

LIST OF TABLES

LIST OF SYMBOLS

a	speed of sound
B	frequency factor for gas phase reaction
C_p	specific heat at constant pressure for gas
C_s	specific heat of solid
Da	Damköhler number
E	gas phase activation energy, acoustic energy in Eq. (2.14)
E_s	surface activation energy
F	eigenvector
G	source term in numerical formulation
h	heat of combustion per unit mass
H	heat of reaction
I	order of perturbation
k	thermal conductivity, constant in Eq. (3.11), wave number (2.29)
k	reaction rate constant
ℓ	characteristic flame length
L	latent heat of vaporization, chamber length in Eqs. (2.25)
m	mass flux
M_b	Mach number
n	order of chemical reaction
P	pressure

Pr	Prandtl number
Q	dimensionless heat of gas phase reaction
r	burning rate
R	gas constant
R_c	dimensionless distance from surface in Eq. (3.22)
t	time
T	temperature
u	axial gas velocity
u_i	velocity vector
u_c	core velocity in Eq. (3.22)
v	normal gas velocity
V	total volume
w	reaction rate
W	molecular weight
x	axial distance parallel to the surface
X	solution vector, mole fraction
y	normal distance from the surface
Y	mass fraction of fuel species
z	oxidizer-fuel ratio, z-axis in cylindrical coordinate
α	thermal diffusivity
β	ratio of solid to gas density
Γ	ratio of heat capacity, surface area
δ	temperature exponent in Eq. (3.7)
γ	specific heat ratio
ϵ	perturbation parameter
ζ	$= k_s^* C_p^* / k^* C_s^*$

λ eigenvalue

λ_γ Lagrange multiplier

μ viscosity coefficient

ν stoichiometric coefficient

ξ $= k^*/k_s^*$

ρ density

ϕ scalar potential in Eq. (2.26), interpolation function

ω frequency

Ω interior volume

Subscripts and Superscripts

* dimensional quantity

- steady-state mean value

^ spatial variable

(i) i^{th} order perturbation coefficient

+ gas side of interface

- solid side of interface

c propellant cold side

D time-dependent variable

f fuel

h homogeneous solution

i,j vector quantity

I time-independent variable

O steady-state, oxidizer

p particular solution, product

r reference value

s	solid phase
$\alpha, \beta,$	
γ, δ	finite element global node number
†	complex conjugate

CHAPTER I

INTRODUCTION

Determination of oscillatory pressure and velocity variations from their mean values in solid propellant combustion chambers has been the subject of study for many years. Because of computational difficulties, however, rigorous and accurate methods of solution still remain in various stages of development. Often details of physics are obscured in complicated computational strategies. In view of the fact that reliable experimental measurements are difficult to obtain, it is crucial to possess an analytical tool to accurately predict combustion dynamics and combustion efficiency in designing successful solid propellant rocket motors.

Earlier works on combustion dynamics include Hart and McClure [1], Denison and Baum [2], Culick [3] and T'ien [4] among others. These studies are centered around one-dimensional, linear oscillatory burning. Culick [5,6], Baum and Levine [7], and Yang et al. [8] subsequently studied the nonlinear growth and limiting amplitude of acoustic waves in a combustion chamber. Nonlinear behavior as characterized by higher order perturbation expansions of governing equations has been investigated by Flandro [9] and Chung and Kim [10] in recent years. They assumed that the pressure varies sinusoidally with time, the pressure

amplitudes being a function of position.

In the present approach, the pressure is assumed to vary in the unstable state. This allows the presence of a long flame such as in double-base solid propellants, in which high pressures and high frequencies may be accommodated. Galerkin finite elements [11] are utilized to model numerically the geometries of burning surfaces and the flame thickness. The nonsteady governing equations are linearized by means of the zeroth, first, and second order perturbation expansions. The boundary conditions, including the burning surfaces and flame edges, are imposed by means of the Lagrange multipliers.

In the simple example problems demonstrated in this paper, the gaseous flame is assumed to follow the Arrhenius law with one-step forward chemical reactions. No condensed phase reaction is included in the formulation. The calculated results confirm the prediction reported by other investigators in the literature for the low frequency region. Extended studies are then carried out for the high frequency region. It has been found that amplification of oscillatory motions does prevail in the high frequency region. Discussions are presented in Section 4.

The present study does not include turbulent boundary layers which may play an important role in erosive burning and combustion instability; this is the subject of the current study.

CHAPTER II

PRELIMINARIES FOR COMBUSTION WAVES

2.1 Premixed Laminar Flame

Combustion is the chemical process which gives rise to the conversion of reactants into products. During combustion, chemical reactions are coupled with heat and mass transfer. Energy and species are transported with rapid chemical reactions occurring exothermically in single or composite phase. Most chemical reactions occur in a chain sequence composed of four basic processes: initiation, branching, propagation, and termination of the radicals. A chemical reaction to combustion can be written in the form

$$\sum_{\alpha=1}^{N} \nu'_{\alpha,m} Y_\alpha \rightleftarrows \sum_{\alpha=1}^{N} \nu''_{\alpha,m} Y_\alpha \tag{2.1}$$

where Y_α denotes the chemical species α and $\nu'_{\alpha,m}$ and $\nu''_{\alpha,m}$ represent the stoichiometric coefficients of species Y_α for the reactants and for the reaction products in the m^{th} reaction, respectively. The stoichiometric coefficients $\nu'_{\alpha,m}$ and $\nu''_{\alpha,m}$ must satisfy elemental material balances. The phenomenological principle of mass action states that the rate of reaction is proportional to the product of the concentration of the reactants. Thus, the reaction rate is

given by

$$w_\alpha = -W_\alpha \sum_{m=1}^{M} (\nu''_{\alpha,m} - \nu'_{\alpha,m}) k_m \prod_{\beta=1}^{N} \left(\frac{X_\beta P}{RT}\right)^{\nu'_{\beta,m}} \tag{2.2}$$

in which X_β is the mole fraction and k_m is the reaction rate constant, with m indicating the reaction order. The order of a reaction is determined by summing the exponents of the reactant mass fraction that express the reaction rate. The constant k_m for a single step reaction is empirically given by the Arrhenius law

$$k_m = A_m \exp\left(-\frac{E_m}{RT}\right) \tag{2.3}$$

with R being the universal gas constant, E_m the activation energy, and A_m the frequency factor for the reaction step. According to the theory related to the collison process and potential energy barrier of the reaction, E_m is the minimum barrier height which reactants must acquire before reaction process. The factor $\exp(-E_m/RT)$ represents the fraction of collisions between reactant molecules in which products can be formed. Generally, E_m is constant, but A_m depends on T such that

$$A_m = B_m T^{\delta_m} \tag{2.4}$$

where B_m and δ_m are constant. Combining those relations gives

$$w_\alpha = -W_\alpha \sum_{m=1}^{M} (\nu''_{\alpha,m} - \nu'_{\alpha,m}) B_m T^\delta m e^{-(E_m/RT)} \prod_{\beta=1}^{N} \left(\frac{X_\beta P}{RT}\right)^{\nu'_{\beta,m}} \tag{2.5}$$

in which the detailed reaction kinetics are neglected.

For a single step irreversible chemical reaction, the chemical process may be written in the form

$$\nu'_f F + \nu'_o O \rightarrow \nu''_p P \tag{2.6}$$

with F, O, and P being the species representing the fuel, oxidizer, and product. In this case, the overall reaction rate is given by

$$w_f = \frac{dY_f}{dt} = -BT^\delta Y_f{}^r Y_o{}^s \exp\left(-\frac{E}{RT}\right) \tag{2.7}$$

It is noted that the exponents r and s are not necessarily related to the stoichiometric coefficients ν_f' and ν_o'. In many cases, actual values of B, δ, r, s, and E are empirically determined. Based on this model, the local heat release rate Q_f can be determined from Eq. (2.7) and the heat of combustion per unit mass of fuel h_f,

$$Q_f = -\frac{h_f}{\rho}\frac{dY_f}{dt} \tag{2.8}$$

where Q_f represents heat addition to the system. Thus, Eqs. (2.7) and (2.8) can be used in conjunction with the species and energy transport equations, respectively.

2.2 Fluid Dynamically Excited Oscillations

The contribution of flow excitation is not usually distinguishable from that due to combustion. However, there are three rather distinct examples that indicate flow excitation by means other than combustion: (1) oscillations related to vortex shedding and transport from the segment-transition regions of the motor cavity in large segmented motors at low frequencies [13]; (2) excitation by the interaction between transverse flow oscillation and axial mean flow [14]; and (3) excitation by turbulence [15]. The contribution of flow excitation to oscillations is usually small compared to the combustion oscillations, primarily because flow excitation results from the kinetic energy flux in the mean flow, while combustion oscillation results from the much larger thermal energy flux in the combustion zone. However, flow excitation may play a role in initiation of combustion-driven oscillations and correspondingly affect stability limits.

2.3 Propellant Characteristics

Experience shows that combustion instability is highly dependent on propellant characteristics. It is clear that the effects can be due to either changes in combustion dynamics of the propellant or changes in damping. Although the stability is a property of the entire combustor and cannot generally be attributed to the propellant alone, the

variables involved in the response function are related to the characteristics of propellants. The growth constant in the response function shows that a high energy, fast burning propellant in a charge configuration with a large burning surface area will tend to be unstable unless the real part of the response function is small or the damping effect is large. It has been shown that the value of the response function for energetic propellants is high enough at some frequencies to cause motor instabilities. These propellants include ammonium perchlorate, double-base propellant, aluminized propellants, and combustion of propellants with other energetic oxidizers.

2.4 Acoustic Admittance

The acoustic wave equation for an adiabatic compressible inviscid flow is given as

$$\nabla^2 \phi - \frac{1}{a^2} \frac{\partial^2 \phi}{\partial t} = 0 \tag{2.9}$$

where a is the speed of sound and ϕ is a scalar potential defined as $u_i = \phi_{,i}$.

The corresponding acoustic pressure P' is

$$P' = -\rho \frac{\partial \phi}{\partial t} \tag{2.10}$$

Taking a partial derivative of Eq. (2.10) leads to

$$\frac{\partial u_i}{\partial t} = -\frac{1}{\rho} P'_{,i} \tag{2.11}$$

The general solution of Eq. (2.9) in the one-dimensional case is

$$\phi = Ae^{i(kx-\omega t)} + Be^{-i(kx+\omega t)} \tag{2.12}$$

in which A and B are complex quantities, k is the wave number, and ω is the frequency. If the positive going travelling wave is considered, it follows that

$$u = Ce^{i(kx-\omega t)} \tag{2.13}$$

Substituting Eq. (2.13) into Eq. (2.11) yields

$$P' = C\rho a e^{i(kx-\omega t)} \tag{2.14}$$

From Eqs. (2.13) and (2.14), we have

$$\frac{P'}{u} = \rho a \tag{2.15}$$

The quantity ρa is called the specific impedance in acoustics and the reciprocal of the normalized specific impedance is denoted as the admittance in combustion instability. Thus, the acoustic admittance Y' is given as

$$Y' = -\frac{u}{P'} \tag{2.16a}$$

Dividing by the steady-state value gives the non-dimensional form of Y',

$$Y = \frac{P_0}{u_0}\frac{u}{P'} \tag{2.16b}$$

where the subscript o indicates the mean flow.

The so-called response function F is defined as

$$F = Re(m'/m_0)/(P'/P_0) \tag{2.17}$$

where m is the mass flow rate and Re is the real part of the complex quantity. Both acoustic admittances and response functions are representative of the combustion instability. In what follows, however, we shall use the acoustic admittance as a measure of combustion wave instabilities.

CHAPTER III

COMBUSTION DYNAMICS

3.1 General

A numerical model is developed for the unsteady state combustion of a solid propellant subject to acoustic pressure oscillations in both low and high frequency ranges. The governing equations are perturbed to the second order and then solved by using the finite element method. After reproducing the analytical model given by Friedly and Petersen [16,17], the numerical results are verified for the one-dimensional case by comparison with the analytical solution. Thus, the work is extended for the multi-dimensional case where the critical assumptions required in the analytical method may be removed. As a result, the investigation of variable distributions in the flame zone is made possible and, consequently, the acoustic admittance is obtained to determine the combustion instability in a more realistic manner.

Discussions of governing equations and finite element solutions will be presented in the following sections.

3.2 Governing Equations

The governing equations for a premixed laminar flame are derived under the following assumptions: (1) the Mach

number is small, (2) body forces are negligible, (3) radiative heat transfer is negligible, (4) the Soret and Dufour effects are negligible, (5) diffusion caused by the pressure gradient is negligible, (6) the gas mixture is ideal and thermal coefficients are constant, and (7) the Lewis number is unity for the explicit relation between concentration and temperature. A schematic representation of the coordinate system for a one-dimensional model is shown in Fig. 3.1.

3.2.1 Gas Phase

For the simplicity of the combustion modeling of solid propellants, the gaseous flame is assumed to be multi-dimensional, premixed laminar, and calorically perfect, and a one-step forward chemical reaction occurs. The combustion of a solid propellant is approximated by the Arrhenius law. Thus, the conservation laws for the multi-component reactive system in the gas-phase are represented in the non-dimensional forms as follows (see Appendix A for details):

Continuity

$$\frac{\partial \rho}{\partial t} + (\rho u_i)_{,i} = 0 \qquad (3.1)$$

Momentum

$$\rho \frac{\partial u_i}{\partial t} + \rho u_{i,j} u_j + \frac{1}{\gamma M_b^2} P_{,i} - Pr\left(u_{i,jj} + \frac{1}{3} u_{j,ij}\right) = 0 \qquad (3.2)$$

Energy

$$\rho \frac{\partial T}{\partial t} + \rho u_i T_{,i} - \frac{\gamma - 1}{\gamma} \frac{\partial P}{\partial t} - T_{,ii} - wh = 0 \qquad (3.3)$$

Species

$$\rho \frac{\partial Y}{\partial t} + \rho u_i Y_{,i} - Y_{,ii} + w = 0 \qquad (3.4)$$

State

$$P = \rho T \qquad (3.5)$$

where the commas denote partial derivatives, the repeated indices imply summing, Pr is the Prandtl number, and Y represents the fuel mass fraction. Note that only one out of three species equations (fuel, oxidizer, and product) is taken into account from the simple chemical reaction model [4]. The following characteristic parameters are used to render the above equations dimensionless:

$$\rho = \rho^*/\rho_0^* \quad , \quad P = P^*/P_0^* \quad , \quad T = T^*/T_0^*$$

$$u_i = u_i^*/v_0^* \quad , \quad t = t^* v_0^*/\ell^* \quad , \quad x_i = x_i^*/\ell^* \qquad (3.6)$$

$$M_b = v_0^*/a_0^* \quad , \quad h = h^*/C_p^* T_0^* \quad , \quad w = w^* \alpha^*/\rho_0^* v_0^{*2}$$

in which ℓ^* is the flame thickness given by α^*/v_0^*, with α^* being the thermal diffusivity, M_b represents the Mach number; k^*, the thermal conductivity; a_0^*, the speed of sound; h^*, the combustion heat release; and w^*, the reaction rate, whose dimensionless form is

$$w = BzT^{\delta}\left(\frac{P}{T}\right)^{n} Y^n \exp[-E/T] \tag{3.7}$$

with z denoting the oxidizer-fuel ratio; n, the order of chemical reaction; E, the activation energy given by $E = E^*/RT_0^*$; and B, the rate constant. The superscript * represents dimensional quantities and subscript zero gives the mean value at the flame edge.

3.2.2 Solid Phase

The solid propellant is assumed to be homogeneous, with no condensed phase chemical reaction. The dimensionless form of the heat transfer equation in the solid phase is

$$\beta \frac{\partial T_s}{\partial t} + \beta u_i T_{s,i} - \zeta T_{s,ii} = 0 \tag{3.8a}$$

Furthermore, assuming that the heat transfer is one-dimensional gives

$$\beta \frac{\partial T_s}{\partial t} + r \frac{\partial T_s}{\partial y} - \zeta \frac{\partial^2 T_s}{\partial y^2} = 0 \qquad (3.8b)$$

where

$$\beta = \rho_s^*/\rho_0^* \quad , \quad \zeta = k_s^* C_p^*/k^* C_s^*$$
$$r = r^*/\bar{r}^* \quad \text{with} \quad \bar{r}^* = \rho_0^* v_0^*/\rho_s^*$$

Here, r denotes the burning rate at the solid surface and subscript s represents the solid phase. The decomposition process of the solid propellant at the surface is assumed to follow an Arrhenius law; thus,

$$r = \exp\left[-E_s \left(\frac{1}{T_s} - \frac{1}{\bar{T}_s} \right) \right] \qquad (3.9)$$

in which E_s is the dimensionless surface activation energy, $E_s = E_s^*/RT_0^*$, and $\bar{T}_s$ is the mean temperature at the surface. The solid-gas interface boundary conditions are determined by the dimensionless mass and energy balances across the interface, such that

$$\left(\frac{\partial T}{\partial y} \right)_+ = \frac{1}{\xi} \left(\frac{\partial T}{\partial y} \right)_- + rL \qquad (3.10)$$

with $\xi = k^*/k_s^*$ and $L = (H_+^* - H_-^*)/C_p^* T_0^*$. Here, L is the latent heat of vaporization of the propellant and H^* denotes the enthalpy changes. The subscripts + and - represent the gas and solid side at the interface,

respectively.

3.2.3 Perturbation Expansions

When a small pressure disturbance occurs in the combustion chamber, every field variable will be disturbed from its steady-state value and can be expressed in the form,

$$F = F^{(0)} + \epsilon F^{(1)} + \epsilon^2 F^{(2)} + \ldots \tag{3.11}$$

where $F = \{\rho, u_i, T, Y, P\}$ and ϵ represents the perturbation parameter. The superscripts in the parentheses indicate the perturbation order. Furthermore, assuming sinusoidal fluctuation of pressure with time renders the variables in a different form:

$$F^{(I)} = \hat{F}^{(I)} e^{iI\omega t} \quad , \quad I = 1,2,\ldots \tag{3.12}$$

It is important to recognize that the sources in the second order consist of inhomogeneous terms that describe the nonlinearities in terms of the product of two first order variables. Considering the physical quantity of $F^{(1)}$ leads to the separation of each inhomogeneous term into a time-independent term and a term oscillating at the frequency of the second harmonic. Because of the fact that only the real parts of $F_1^{(1)}$ and $F_2^{(1)}$ are the physical quantities, the product indicates, in reality, that

$$\begin{aligned}
\mathrm{Re}(F_1^{(1)})(F_2^{(1)}) &= \mathrm{Re}[\hat{F}_1^{(1)}e^{i\omega t}]\mathrm{Re}[\hat{F}_2^{(1)}e^{i\omega t}] \\
&= \mathrm{Re}[(F_{1r} + iF_1)(\cos\,\omega t + i\,\sin\,\omega t)]\mathrm{Re}[(F_{2r} + \\
&+ iF_2)(\cos\,\omega t + i\,\sin\,\omega t)] \\
&= \frac{1}{2}(F_{1r}F_{2r} + F_1F_2) + \frac{1}{2}(F_{1r}F_{2r} - F_1F_2)\cos\,\omega t \\
&- \frac{1}{2}(F_{1r}F_2 + F_1F_{2r})\sin\,\omega t
\end{aligned}$$

The right-hand side of the above equation equals the real part of $(1/2)(F_1^{(1)\dagger}F_2^{(1)} + F_1^{(1)}F_2^{(1)})$, where the dagger represents the complex conjugate. Thus, the product of $F_1^{(1)}$ and $F_2^{(1)}$ may be replaced by

$$\begin{aligned}
F_1^{(1)}F_2^{(1)} &= \frac{1}{2}(F_1^{(1)\dagger}F_2^{(1)} + F_1^{(1)}F_2^{(1)}) \\
&= \frac{1}{2}(\hat{F}_1^{(1)\dagger}\hat{F}_2^{(1)} + \hat{F}_1^{(1)}\hat{F}_2e^{i2\omega t}) \qquad (3.13)
\end{aligned}$$

and each product of two first order terms can be replaced by a similar expression. Since each nonlinearity yields a constant term and a term oscillating at the frequency of the second harmonic, the dependent variable $F_2^{(1)}$ may be rewritten as

$$F^{(2)} = \hat{F}_I^{(2)} + \hat{F}_D^{(2)}e^{i2\omega t} \qquad (3.14)$$

From the expression of Eq. (3.14), those equations for the second order system can be separated into two individual

equations, one for the time-independent equations and the other for the time- dependent equations. All the coefficients of the time- independent equation set are exactly the same as those of the first order set, except the inhomogeneous terms which consist of each product of two first order variables. For a higher order, the same argument is applicable.

Substituting Eqs. (3.11)-(3.14) into Eqs. (3.1)-(3.5) and rearranging separately in the order of perturbation yield the final form of the governing equations corresponding to each order.

Steady-State Governing Equations

The one-dimensional steady-state governing equations are given as follows:

Continuity

$$\rho^{(0)}v^{(0)} = 1 \tag{3.15}$$

Energy

$$\frac{\partial T^{(0)}}{\partial y} - \frac{\partial^2 T^{(0)}}{\partial y^2} = w^{(0)}h \tag{3.16}$$

Species

$$\frac{\partial Y^{(0)}}{\partial y} - \frac{\partial^2 Y^{(0)}}{\partial y^2} = -w^{(0)} \tag{3.17}$$

State

$$\rho^{(0)}T^{(0)} = 1 \tag{3.18}$$

Note that the uniform pressure is retained throughout the flame thickness ($P^{(0)} = 1$), and from Eqs. (3.6) and (3.11), both the dependent variables, $\rho^{(0)}$ and $T^{(0)}$, are equal to unity at the flame edge, which is far from the origin on the scale of ℓ^*. From Eqs. (3.15) and (3.18), we have

$$v^{(0)} = T^{(0)} \tag{3.19}$$

and from Eqs. (3.16) and (3.17), $Y^{(0)}$ can be expressed as

$$Y^{(0)} = \frac{1}{h}\,(1 - T^{(0)}) \tag{3.20}$$

Therefore,

$$w^{(0)} = \frac{1}{h^2}\,Bz\left(\frac{1 - T^{(0)}}{T^{(0)}}\right)^2 \exp[-E/T^{(0)}] \tag{3.21}$$

where $\delta = 0$ and the second order chemical reaction ($n = 2$) is assumed.

Now, the equations are expressed in terms of temperature in the steady-state; thus, only the solution of Eq. (3.16) is required. Flandro [9] suggests a simple analytical model of the mean flow field to facilitate multi-dimensional analysis in the higher order system. This model is given in the form

$$u_1^{(0)} = u_c[1 - \exp(-y/R_c)]\hat{i} + v^{(0)}\hat{j} \tag{3.22}$$

Here, u_c describes the flow speed along the local streamline and R_c is a dimensionless distance from the solid surface. The following boundary conditions are used in the steady-state solution:

At the flame edge,

$$Y^{(0)} = 0 \tag{3.23}$$

$$T^{(0)} = 1 \tag{3.24a}$$

or

$$\frac{dT^{(0)}}{dy} = 0 \tag{3.24b}$$

At the solid phase, Eq. (3.8) gives

$$T_s^{(0)} = (\bar{T}_s - T_c)e^{Y/\xi} + T_c \tag{3.25}$$

where T_c is the propellant cold side temperature. The continuous temperature condition at the interface requires that

$$T_{s-}^{(0)} = T_{+}^{(0)} = \bar{T}_s \tag{3.26}$$

The matching condition across the interface can be obtained by substituting Eq. (3.25) into Eq. (3.10), which yields

$$\left.\frac{dT^{(0)}}{dy}\right|_{+} = \frac{\bar{T}_s - T_c}{\zeta\xi} + L \qquad (3.27)$$

In solving Eq. (3.16), note that a correct rate constant B in Eq. (3.21) has to be determined such that the system satisfies the boundary conditions at the flame edge as well as at the interface.

Higher Order Governing Equations

The higher order governing equations can be expressed in a single form because only the source terms are different from each other. Presenting the source terms on the right-hand side of the equations in terms of G_s, the governing equations are represented as follows:

Continuity

$$iI\omega\hat{\rho}^{(I)} + (\rho^{(0)}\hat{u}_i^{(I)} + \hat{\rho}^{(I)}u_i^{(0)})_{,i} = G_1 \qquad (3.28)$$

Momentum

$$iI\omega\rho^{(0)}\hat{u}_i^{(I)} + [\rho^{(0)}u_{i,j}^{(0)}\hat{u}_j^{(I)} + \rho^{(0)}\hat{u}_{i,j}^{(I)}u_j^{(0)} + \hat{\rho}^{(I)}u_{i,j}^{(0)}u_j^{(0)}] + \frac{1}{\gamma M_b^2}\hat{P}_{,i}^{(I)} - Pr\left[\hat{u}_{i,jj}^{(I)} + \frac{1}{3}\hat{u}_{j,ij}^{(I)}\right] = G_{2i} \qquad (3.29)$$

Energy

$$iI\omega\rho^{(0)}\hat{T}^{(I)} + [\rho^{(0)}u_i^{(0)}\hat{T}_{,i}^{(I)} + \rho^{(0)}\hat{u}_i^{(I)}T_{,i}^{(0)} + \hat{\rho}^{(I)}u_i^{(0)}T_{,i}^{(0)}] - iI\omega\frac{\gamma-1}{\gamma}\hat{P}^{(I)} - \hat{T}_{,ii}^{(I)} - \hat{w}^{(I)}h = G_3 \qquad (3.30)$$

Species

$$iI\omega\rho^{(0)}\hat{Y}^{(I)} + [\rho^{(0)}u_i^{(0)}\hat{Y}_{,i}^{(I)} + \rho^{(0)}\hat{u}_i^{(I)}Y_{,i}^{(0)} + \hat{\rho}^{(I)}u_i^{(0)}Y_{,i}^{(0)}] - \hat{Y}_{,ii}^{(I)} + \hat{w}^{(I)} = G_4 \tag{3.31}$$

State

$$\hat{P}^{(I)} - \rho^{(0)}T^{(I)} - \hat{\rho}^{(I)}T^{(0)} = G_5 \tag{3.32}$$

and the reaction-rate is given by

$$\hat{w}^{(I)} = w^{(0)}\left[\frac{2}{\rho^{(0)}}\hat{\rho}^{(I)} + \frac{E}{T^{(0)2}}\hat{T}^{(I)} + \frac{2}{Y^{(0)}}\hat{Y}^{(I)}\right] + G_6 \tag{3.33}$$

Here, G_s is given as follows: for the first order system ($I = 1$), $G = 0$; for the second order system ($I = 2$),

$$G_1 = -(\hat{\rho}^{(1)}\hat{u}_i^{(1)})_{,i}$$

$$G_{2i} = -\{i\omega\hat{\rho}^{(1)}\hat{u}_i^{(1)} + \rho^{(0)}\hat{u}_{i,j}^{(1)}\hat{u}_j^{(1)} + \hat{\rho}^{(1)}u_{i,j}^{(0)}\hat{u}_j^{(1)} + \hat{\rho}^{(1)}\hat{u}_{i,j}^{(1)}u_j^{(0)}\}$$

$$G_3 = -\{i\omega\hat{\rho}^{(1)}\hat{T}^{(1)} + \rho^{(0)}\hat{u}_i^{(1)}\hat{T}_{,i}^{(1)} + \hat{\rho}^{(1)}u_i^{(0)}\hat{T}_{,i}^{(1)} + \hat{\rho}^{(1)}\hat{u}_i^{(1)}T_{,i}^{(0)}\}$$

$$G_4 = -\{i\omega\hat{\rho}^{(1)}\hat{Y}^{(1)} + \rho^{(0)}\hat{u}_i^{(1)}\hat{Y}_{,i}^{(1)} + \hat{\rho}^{(1)}u_i^{(0)}\hat{Y}_{,i}^{(1)} + \hat{\rho}^{(1)}\hat{u}_i^{(1)}Y_{,i}^{(0)}\}$$

$$G_5 = \hat{\rho}^{(1)}\hat{T}^{(1)}$$

$$G_6 = w^{(0)}\left\{\left(\frac{\hat{\rho}^{(1)}}{\rho^{(0)}}\right)^2 + \frac{2E}{\rho^{(0)}T^{(0)2}}\hat{\rho}^{(1)}\hat{T}^{(1)} + \frac{4}{\rho^{(0)}Y^{(0)}}\hat{\rho}^{(1)}\hat{Y}^{(1)}\right.$$
$$\left. + \frac{E}{T^{(0)}}\left(\frac{E}{2T^{(0)}} - 1\right)\left(\frac{\hat{T}^{(1)}}{T^{(0)}}\right)^2 + \frac{2E}{Y^{(0)}T^{(0)2}}\hat{Y}^{(1)}\hat{T}^{(1)} + \left(\frac{\hat{Y}^{(1)}}{Y^{(0)}}\right)^2\right\} \tag{3.34}$$

Note that, including the pressure coupling, the velocity coupling is significant in the source terms (Appendix B).

At the solid phase, Eq. (3.8) gives

$$iI\omega\beta\hat{T}_s^{(I)} + r^{(0)}\frac{\partial\hat{T}_s^{(I)}}{\partial y} + \hat{r}^{(I)}\frac{\partial T_s^{(0)}}{\partial y} - \zeta\frac{\partial^2\hat{T}_s^{(I)}}{\partial y^2} = G_7 \tag{3.35}$$

with

$$G_7 = -\hat{r}^{(1)}\frac{\partial\hat{T}_s^{(1)}}{\partial y}$$

Linearizing Eq. (3.9) results in

$$\hat{r}^{(I)} = r^{(0)}c_1(\hat{T}_s^{(I)} + G_8) \tag{3.36}$$

where

$$G_8 = \left(\frac{c_1}{2} - \frac{1}{\bar{T}_s}\right)\hat{T}_s^{(1)2}$$

Substituting Eq. (3.36) into Eq. (3.35) and solving analytically yield

$$\hat{T}_+^{(I)} = \left(\frac{\partial \hat{T}^{(I)}}{\partial y} \bigg|_+ + G_9 \right) \left[\frac{\lambda_I}{\xi} \left(1 + \frac{c_1 c_2}{iI\omega\beta} \right) - \frac{c_1 c_2}{iI\omega\beta\zeta\xi} + c_1 L \right]^{-1} \tag{3.37}$$

in which

$$G_9 = \frac{c_3 c_2}{iI\omega\beta\xi} \left(-\lambda_2 + \frac{1}{\zeta} \right) + \frac{1}{\xi} \left(\lambda_2 c_4 + c_5 - \frac{c_4}{\zeta} \right) - c_3 L$$

and

$$\lambda_I = \frac{1}{2\zeta} \left[1 + (1 + i4I\omega\beta\zeta)^{1/2} \right]$$

$$c_1 = E_s / \bar{T}_s^{\,2}$$

$$c_2 = \frac{1}{\zeta} (\bar{T}_s - T_c)$$

$$c_3 = c_1 \left(\frac{c_1}{2} - \frac{1}{\bar{T}_s} \right) \hat{T}^{(1)2}$$

$$c_4 = - \frac{c_2 \hat{r}^{(1)2}}{2\omega^2\beta^2\zeta}$$

$$c_5 = \frac{\lambda_1 (\lambda_2 - \lambda_1)}{(\zeta\lambda_1^{\,2} - \lambda_1 - i2\omega\beta)} \hat{r}^{(1)} \left(\hat{T}_s^{(1)} + \frac{c_2 \hat{r}^{(1)}}{i\omega\beta} \right)$$

Equation (3.37) gives a boundary condition at the surface; other conditions are as follows:

At the flame edge,

$$\hat{Y}^{(I)} = 0 \tag{3.38}$$

Assumption of an isentropic flow near the flame edge gives

the temperature conditions. Noting that the steady-state temperature gradient at the flame edge is almost zero, this condition can be expressed in the form

$$i\Gamma\omega\rho^{(0)}\hat{T}^{(1)} + \rho^{(0)}u_i{}^{(0)}\hat{T}_{,i}^{(1)} - i\Gamma\omega\frac{\gamma - 1}{\gamma}\hat{P}^{(1)} = G_{10} \quad (3.39)$$

with

$$G_{10} = -\frac{\gamma - 1}{\gamma^2}i\omega\hat{P}^{(1)2}$$

Since the flux of each reactant species is always a fixed fraction of the total flux, the fuel mass flux fraction m_f can be derived from Eq. (3.4) as

$$\rho u_i Y_{,i} - Y_{,ii} = 0 \quad (3.40)$$

For a one-dimensional expression, m_f is given as

$$m_f = Y - \frac{1}{m}\frac{dY}{dy} \quad (3.41)$$

where m is the mass flux equal to ρv, and assumption of the constant burning rate at an instant has been used. At the surface,

$$\hat{m}_f{}^{(1)} = \hat{Y}^{(1)} - \frac{1}{m^{(0)}}\frac{d\hat{Y}^{(1)}}{dy} + \frac{1}{m^{(0)2}}\hat{m}^{(1)}\frac{dY^{(0)}}{dy} + G_{11} \quad (3.42)$$

in which

$$G_{11} = \frac{1}{m^{(0)}} \left[\frac{\hat{m}^{(1)}}{m^{(0)}} \frac{d\hat{Y}^{(1)}}{dy} - \frac{dY^{(0)}}{dy} \left(\frac{\hat{m}^{(1)}}{m^{(0)}} \right)^2 \right]$$

Using the relationship $\hat{m}^{(I)} = \rho_s \hat{r}^{(I)}$ yields

$$\hat{Y}^{(I)} = \frac{d\hat{Y}^{(I)}}{dy} - c_1 \frac{dY^{(0)}}{dy} (\hat{T}_s{}^{(I)}) + G_{12} \tag{3.43}$$

with

$$G_{12} = -c_1 \frac{dY^{(0)}}{dy} \left(\frac{c_1}{2} - \frac{1}{\overline{T}_s} \right) \hat{T}_s^{(1)2} - c_1 \hat{T}_s^{(1)} \frac{d\hat{Y}^{(1)}}{dy} + \hat{T}_s^{(1)2} \frac{dY^{(0)}}{dy}$$

The normal velocity component is derived from the mass balance condition at the interface such that

$$\hat{v}_+^{(I)} = \left(\frac{E_s}{\overline{T}_s} + 1 \right) \hat{T}_+^{(I)} - \overline{T}_s \hat{P}^{(I)} + G_{13} \tag{3.44}$$

where

$$G_{13} = c_1 \left(\frac{E_s}{2\overline{T}_s} - 1 \right) \hat{T}_+^{(1)2} + (\hat{T}_+^{(1)} - \hat{v}_+^{(1)}) \left(\hat{P}^{(1)} - \frac{1}{\overline{T}_s} \hat{T}_+^{(1)} \right)$$

Moreover, the parallel velocity component may be obtained using the Taylor series expansion about the surface where the no-slip condition must be valid. Thus,

$$\hat{u}_+^{(I)} = \frac{1}{iI\omega\beta} \frac{\partial u^{(0)}}{\partial y} \bigg|_+ \hat{r}^{(I)} + G_{14} \tag{3.45}$$

with

$$G_{14} = \frac{1}{iI\omega\beta}\frac{\partial \hat{u}^{(1)}}{\partial y}\bigg|_{+}\hat{r}^{(1)} - \frac{1}{2I^2\omega^2\beta^2}\frac{\partial^2 u^{(0)}}{\partial y^2}\bigg|_{+}\hat{r}^{(1)2}$$

Note that $G_7 \sim G_{14}$ are valid only for $I = 2$. For higher order systems, Eqs. (3.37)-(3.39) and Eqs. (3.43)-(3.45) are used as boundary conditions to solve Eqs. (3.28)-(3.32). It is necessary to have more conditions for the density at both sides for better solutions, and the pressure fluctuation has to be forced at the flame edge. In the case of the second order time-independent system, care must be taken to use boundary equations (3.35) and (3.39). See Appendix C for details.

3.3 Finite Element Applications

The finite element method (FEM) is an approximate numerical procedure for solving partial differential equations of boundary and initial value problems. The basic idea resides in the application of variational principles or equivalent concepts such as weighted residual methods. It is well known that the most general approach to the finite element analysis is the Galerkin method, which is one of the methods of weighted residuals. In this scheme, test functions are the same as trial functions, known more popularly as interpolation functions. Typically, any scalar variable X is expressed as a linear combination of interpolation function ϕ_β and the nodal values of X_β such that

$$X = \phi_\beta X_\beta \tag{3.46}$$

where ß denotes the global nodes. The Galerkin finite element equations result from the inner product of the residual of a governing equation and the test function such as

$$(R, \phi_\alpha) = \int_\Omega R\phi_\alpha \, d\Omega = 0 \tag{3.47}$$

Integrating this equation by parts gives rise to the simultaneous algebraic equations. The Gaussian quadrature is employed for the integrations of the spatial finite

element domain. Consequently, the global finite element equations are of the form

$$[iI\omega A_{\alpha\beta} + B_{\alpha\beta}]X_{\beta} = G_{\alpha} \tag{3.48}$$

in which i denotes the imaginary part of the complex number, X_{β} represents the solution vector, $X_{\beta} = [\rho_{\beta}, u_{\beta i}, T_{\beta}, Y_{\beta}, P_{\beta}]$, and G_{α} is the inhomogeneous source term valid for the second order.

The algebraic finite element equations are modified for the boundary conditions. Implementation of complicated boundary conditions is achieved by adopting the Lagrange multipliers method. The solution variables included in the boundary conditions have to be provided in the global form of the nodal values. The boundary conditions are expressed in the form of the boundary matrix equations,

$$q_{\gamma\beta}X_{\beta} = b_{\gamma} \tag{3.49}$$

with $\gamma = 1,2,\ldots,m$, with m being the number of equations. Thus, the modified algebraic finite element equations have the final form:

$$\begin{bmatrix} iI\omega A_{\alpha\beta} + B_{\alpha\beta} & q_{\gamma\alpha} \\ q_{\gamma\beta} & 0 \end{bmatrix} \begin{bmatrix} X_{\beta} \\ \lambda_{\gamma} \end{bmatrix} = \begin{bmatrix} G_{\alpha} \\ b_{\gamma} \end{bmatrix} \tag{3.50}$$

In combination with the Lagrange multipliers method, it is also possible to impose additional Dirichlet boundary conditions. Implementation of Dirichlet conditions is

achieved by zeroing out the rows and columns of $A_{\alpha\beta}$ and $B_{\alpha\beta}$, placing 1 at the diagonal corresponding to the boundary nodes with all the boundary terms subtracted from G_α. The influence of this process is propagated to all other equations.

It is seen that Eq. (3.50) lends itself to a standard eigenvalue problem, the solution of which determines the existence of excited natural frequencies and modes. Using Eq. (3.48) with zero setting of G_α gives the eigenvalue ω which is the natural frequency of the given system.

The solution of Eq. (3.50) at a given frequency is obtained by imposing the Dirichlet condition of the pressure at the flame edge. The finite element formulation contains two different kinds of test function used to represent the volume and surface integrals in the domain. The total number of field variables would be reduced by one if the density or pressure were eliminated using the perfect gas law. However, the stability of the matrix system is doubtful.

Before calculations, the following is expected: since the Mach number is generally very small, the coefficient of the pressure term in Eq. (3.2) dominates the system unless the frequency considered is large enough such that other coefficients containing the frequency factor become comparable in magnitude. Therefore, in lower frequencies, the pressure gradient has to be negligible, thus resulting

in constant pressure. On the contrary, the gradient will become significant in higher frequencies; this results in pressure variance. In the latter case, severe pressure changes will occur if unbounded at the solid surface. Note that care must be exercised in expanding Eq. (3.9) due to the appearance of the exponential growth effect.

For the steady-state case, as mentioned earlier, we calculate the eigenvalue B in which necessary initial conditions are satisfied. However, as will be discussed later, the eigenvalue is referred from the results of reference [4] for this study. The Galerkin finite element formulation of the governing equations in each system is described in Appendix D.

CHAPTER IV

DISCUSSION

In the steady-state, the flame zone is governed by Eqs. (3.15) through (3.18). When an acoustic pressure wave at a certain frequency is imposed on the flame zone, the system will react according to Eqs. (3.28) through (3.32). The present computations on homogeneous solid propellants are performed for an adiabatic flame with a second order chemical reaction [Eq. (3.7)]. Instead of solving Eqs. (3.15) through (3.18), distributions of the field variables in the steady-state are calculated from the temperature given in Eq. (3.16). The coefficients used in this computation are chosen in such a way that the results may be compared with those in [4,9]. In view of this, the following parameters are utilized: $z = 1$, $\delta = 0$, $T_c = 0.15$, $\bar{T}_s = 0.35$, $\zeta = \xi = 1$, $E = 10$, $E_s = 4$, $L = 0.15$, $\beta = 1000$, $\gamma = 1.2$, $M_b = 0.003$, $u_c = 1.0$, $R_c = 5.0$, $Pr = 1.0$, and $h = 1.3$. Representative dimensional parameters corresponding to the above dimensionless values are given in Table 1, and these are based on a single-base propellant [12].

To demonstrate the validity of the theory presented above, a two-dimensional rectangular geometry, shown in Fig. 4.1, is analyzed, in which a burning surface and flame edge can be established as boundaries. This configuration was chosen to resemble a one-dimensional behavior so that

Table 1 Typical value and range of parameters

Parameter	Typical Value	Range	Physical Variable	Typical Value
ρ_s	1000	250-1000	-g/cm^3	1.5
ρ_g	1	-	g/cm^3	1.5 x 10^{-3}
T_c	0.15	-	^{0}K	300
T_s	0.35	-	^{0}K	700
T_f	1.0	-	^{0}K	2000
E	10	4-15	cal/gmole	40 x 10^3
E_s	4	2-10	cal/gmole	16 x 10^3
C_p	-	-	cal/g^{0}k	0.33
C_s	-	-	cal/g^{0}k	0.33
k_g	-	-	cal/cm^{0}ksec	5 x 10^{-4}
k_s	-	-	cal/cm^{0}ksec	5 x 10^{-4}
m_o	1	-	g/cm^{2}sec	0.4
P_o	1	-	atm	9.5
n	2	0.5-2	-	-
Y_f	0.5	0.4~0.85	-	-
ω	-	10^{-3}-10^2	H_z	-
γ	1.4	-	-	-
ΔH	0.15	0.05-0.3	cal/gmole	2.8 x 10^3

the results may be compared directly with those reported in the literature [4,9].

The computations begin with finding the natural frequencies of the system. The resonance frequencies of the system can be obtained by examining the acoustic admittance or response function at each natural frequency. As mentioned earlier, the natural frequencies of the system are given by the homogeneous solution of the total matrix equation (3.50), neglecting the boundary conditions. The frequency range of interest in this computation is shown to be between $\omega = 10^{-3}$ and $\omega = 10^{2}$, corresponding to approximately 80 Hz and 8 MHz, respectively. Thus, sixteen different frequencies in this range are chosen to evaluate the present study, and these are $\omega = 10^{-4}$, 5×10^{-4}, 10^{-3}, 5×10^{-3}, 10^{-2}, 5×10^{-2}, 10^{-1}, 5×10^{-1}, 1, 5, 10, 20, 30, 40, 50, and 100.

Figure 4.2 shows a typical steady-state distribution of the field variables and the reaction rate along the flame thickness. In general, these data may be obtained by solving the energy equation (3.16) together with the reaction rate in Eq. (3.21). Ideally, a fourth order Runge-Kutta scheme may be used for this purpose. The result will be used as the basis of further calculations for combustion instability in the unsteady-state.

Distributions of the field variables versus frequency for the first order system are shown in Figs. 4.3-4.8. These results are obtained by imposing an acoustic pressure

amplitude of unity at the flame edge as the Dirichlet condition. Conventionally, the thickness of the burning zone has been assumed to be negligibly small compared with the wavelength of the acoustic oscillation in the intermediate frequency range. Thus, the uniform pressure is approximated throughout the domain of study and is assumed to vary with time only. On the contrary, since the oscillatory pressure is regarded as a spatially nonhomogeneous time-dependent source in the present study, it is possible to investigate the response of a specific solid propellant at significantly high frequencies and to find the response even in the long flame of a double-base propellant. Figure 4.3 shows variations of the pressure distribution versus the acoustic frequencies. It is seen that the amplitude remains constant for $\omega < 10$. Random variations of these amplitudes occur for higher frequencies. Here, the imaginary parts representing the phase shift are zero.

Figure 4.4 demonstrates distributions of various component fluctuations of the first order system at $\omega = 1$. A pressure wave with a certain amplitude striking the solid surface will give rise to a response in the burning rate. Generally, the response of the burning rate is nonlinear and has a complete Fourier series form that may not be expressed by a single frequency component. In Fig. 4.4, however, the pressure is uniform in the flame zone, although significant variations may occur at higher

frequencies.

The temperature amplification at the surface changes the burning rate in Eq. (3.36), while the velocity at the flame edge represents the acoustic admittance for pressure coupling, whose magnitude and sign indicate the instability of the system. Since the pressure remains constant, implying that the acoustic wavelength is larger than the flame thickness in this case, the imaginary part of the velocity approaches a constant slope at the edge by the assumption of an isentropic condition at the flame edge. It is interesting to note that the trend of variations of temperature and velocity appears to be similar, which is inversely proportional to the variations of species and density as expected. These results are comparable to those of T'ien [4] and Flandro [9].

Density distributions for various frequencies are given in Fig. 4.5. At $\omega < 0.5$, changes of the distributions versus frequency are negligible; however, near $\omega = 1$ a significant reduction of the amplitude occurs, and then for $\omega > 1$ the amplitudes increase moderately. The distributions in the lower frequency region are very similar to those in the steady-state, from which the quasi-steady assumption may be deduced. Note that the reverse peak moves in the flame zone, which implies a change of the reaction zone. Close to the surface, the effect of preheat in the solid phase increases, resulting in a higher burning rate. Positive amplitudes at the interface in each

frequency are caused by the rise in pressure and/or the increase of the burning rate.

It is interesting to see that the amplitudes decrease while the frequency increases up to the unity and then increase along the frequency, from which the flame is expected to react sensitively at special frequencies. The negative amplitude is shown most notably at $\omega = 1$. This may result from the net blowing effect, and the velocity at that point should be positive (see Fig. 4.8).

The normal velocity distributions are shown in Fig. 4.8. The profile may be classified into positive and negative slopes, the only exception being at $\omega = 1$. The latter contains most of the distributions in the lower frequency region. Negative amplitudes appear mostly at the interface, relating to an increase of the density. Although the pressure remains constant in lower frequencies, the velocity varies severely. At $\omega > 20$, the variation is more significant since from that frequency the pressure varies in the flame zone. At $\omega = 0.01$, note that the slope is positive even though it is a lower frequency. This result implies instability of the system for the quasi-steady case. At $\omega = 1$, a positive amplitude near the interface results from adjusting between the density increase and the higher gasification rate. As indicated in Fig. 4.4, the slopes of the imaginary parts near the flame edge are constant.

Rearranging the real part of the velocity at the flame

edge gives the distribution of the acoustic admittance, whose magnitude and sign indicate the amplifications or damping ability of the flame subject to the acoustic disturbance. Figure 4.9 shows the curve-smoothed acoustic admittance and burning rate from Eq. (3.36) at each frequency.

At $\omega = 1$, there is a definite increase in the burning rate. The burning rate increases by increasing the heat transfer effect due to closer movement of the reaction zone to the surface. There are actually several secondary effects such as structural change in the solid phase and change of the chemical kinetics in the flame. These effects cause the feedback to the solid phase, resulting in a change of the burning rate. These effects, however, are not considered.

Figure 9 also reveals a resonance in the condensed phase near $\omega = 0.01$, indicating that the system is unstable. This verifies the result of Denison and Baum [2] and previous laboratory measurements which have shown that the response consists generally of a single peak in the range of frequency for which the quasi-steady approximation appears to be accurate. Some negative peaks exist at the other frequencies, implying that the resonance in the gas phase tends to damp the oscillatory motion. At most higher frequencies, the system seems to be unstable.

The real part of the burning rate shows a trend similar to the acoustic admittance at the quasi-steady

region, although the magnitude is significantly different. But these trends differ from each other at the higher region. Over $\omega = 100$, the profile tends to have a second mode oscillation as the pressure varies in the flame zone. It must be emphasized that the admittance function alone is not sufficient to describe the stability of the system unless the velocity coupling is concerned.

Temperature distributions are given in Fig. 4.6. Since the temperature is related to the density by Eq. (3.5), it can be analyzed easily by comparing the results with those in Fig. 4.5. Accordingly, the distribution of the temperature shows the profile opposed to that of the density. Temperature rises are predominant along the reaction region for $\omega > 1$. Note that no significant temperature changes occur at the interface as imposed by the boundary conditions. Negative amplitude near the flame edge may be caused by the stagnation phenomena in which the density increases. Because of the pressure unity, the imaginary parts of the temperature are given as reciprocals of those of the density.

The fuel consumption at a given frequency is shown in Fig. 4.7. Trends for species distributions are opposite to those for temperature distributions in that negative maximum occurs along the reaction region. Note that linearly diminishing the fuel near the flame edge affects the temperature changes slowly (Fig. 4.6).

The results of the second order perturbation are shown

in Figs. 4.10-4.28. As previously indicated, each variable of the second order response to acoustic disturbance has two components: one time-dependent component that oscillates at twice the fundamental frequency and one that is time-independent. The latter represents a shift in the mean value, thus causing a shift of the mean burning rate. It should be noted that the variations for the second order system may be characterized by the sum of those two parts, with the factor $e^{i2\omega t}$ ranging between -1 and 1 and zero indicating the case of time-independence.

Figures 4.10-4.15 show the distributions in the second order time-independent case. The calculations are also conducted by imposing the pressure of unity at the flame edge as the Dirichlet condition. General trends show that shifts in the mean values are evident.

In Fig. 4.10, the pressure varies from $\omega = 5$, which is half of that in the first order system. For the higher frequency region, the oscillatory motion is significant, which may affect the velocity distribution. Figure 4.11 shows all of the variables for $\omega = 1$, indicating that shifts in mean values may have the affect of damping; however, the opposite may be true for higher frequencies as demonstrated in Figs. 4.12-4.15. The trends are roughly similar to those of the first order illustrated in Fig. 4.4a, but they have different amplitudes because of the nonlinearities in the higher order system. In Figs. 4.12-4.15, the distributions of field variables in lower

frequencies appear to vary negligibly along the flame thickness, while the opposite is true for $\omega > 1$. In particular, since the pressure varies at $\omega > 5$, the velocity changes significantly at those frequencies, implying that the system is unstable at higher frequencies. As mentioned earlier, a shift of the mean burning rate is the most significant effect in the time-independent system. This result will be discussed in Fig. 4.28.

The distributions in the second order time-dependent case are shown in Figs. 4.16-4.21. Here, the pressure also varies from $\omega = 5$ and oscillates for higher frequencies. Note that the amplitude variations are smaller than those in the time-independent case. The trends seem to reduce the total effect of the second order system.

Figures 4.22-4.27 show the variations of field variables in the second order system by summing time-independent and time-dependent effects, with the factor $e^{i2\omega t} = 1$ for time-dependent effects. Note that amplitude variations of each variable in the flame zone are significant at $\omega = 1$, which is the same result obtained for the case of the first order system. Finally, Fig. 4.28 reveals that the shift in burning rate versus frequency is consistently negative, as asserted by other investigators. The offset is relatively small in the quasi-steady region, but increases with oscillatory motion along the frequencies. The variations of the acoustic admittance are similar to those of the first order system, except that

oscillatory deviations are more predominant at higher frequencies in both time-independent and time-dependent cases.

Parameter studies are conducted for the first order and are summarized as follows. Decreasing the density ratio ß affects the variables shifted slightly to the negative direction, keeping the distribution profiles constant. Changing the latent heat of solid L exerts a negligible effect on the variables, but a very small value of L shifts the system toward instability. Increasing the surface activation energy E_s or the gas phase activation energy E reduces the magnitude of the variables, keeping the same profiles. Changes of the rate constant and viscosity effect coefficient strongly affect the system, such that every aspect discussed herein will change.

The present study could be extended to the multi-dimensional case by introducing the appropriate axial mean flow field. It is well recognized that fluctuation of the gas velocity parallel to the propellant surface affects the burning rate in terms of velocity coupling; therefore, this quantity must be considered together with pressure coupling for a satisfactory measure of stability.

A simple calculation has been accomplished using the artificial axial flow velocity in Eq. (3.22). However, difficulties of the boundary conditions could not be eliminated. A test run shows that the existence of a small amount of the axial flow reduces differences between the

variable amplitudes in each frequency considered, thus leading the system toward stability.

CHAPTER V

CONCLUSION

A multi-dimensional numerical model for the premixed flame acoustic instability is proposed and solved using the finite element method. The governing equations are perturbed to the second order and formulated with the Galerkin finite elements. The results have direct bearing on the validity of published theories of solid propellant combustion instability at the lower frequency region where the uniform pressure assumption is valid. Extended studies are made on the higher frequency region and some new results are obtained.

Under the restricted boundary conditions, the following conclusions, based on numerical computations, are reached:

(1) The stability characteristics for the low frequency range in the first order system have been verified to be the same as those reported in the literature. For example, the acoustic admittance is controlled by the burning rate, negative for low frequencies, whereas the opposite is true for high frequencies.

(2) Instabilities are likely to occur at high frequencies ($\omega > 10$).

(3) For the second order system, the trend is similar to the first order system for low frequencies, but

instabilities may appear at frequencies lower than those of the first order system.

(4) The most significant effect of the second order system is that the admittance is extremely oscillatory between $\omega = 1$ and $\omega = 10$.

REFERENCES

1. Hart, R.W. and McClure, F.T., "Combustion Instability: Acoustic Interaction with a Burning Propellant Surface", J. Chem. Phys., Vol. 30, Sept. 1959, pp. 1501-1514.

2. Denison, M.R. and Baum, E., "A Simplified Model of Unstable Burning in Solid Propellants", ARS J., Vol. 31, Aug. 1961, pp. 1112-1122.

3. Culick, F.E.C., "A Review of Calculations for Unstable Burning of a Solid Propellant", AIAA J., Vol. 6, Dec. 1968, pp. 2241-2254.

4. T'ien, J.S., "Oscillatory Burning of Solid Propellants Including Gas Phase Time Lag", Combustion Science and Technology, Vol. 5, 1972, pp. 47-54.

5. Culick, F.E.C., "Nonlinear Behavior of Acoustic Waves in Combustion Chambers-I", Acta Astronautica, Vol. 3, 1976, pp. 715-734.

6. Culick, F.E.C., "Nonlinear Behavior of Acoustic Waves in Combustion Chambers-II", Acta Astronautica, Vol. 3, 1976, pp. 735-757.

7. Baum, J.D., Levine, J.N., and Lovine, R.L., "Pulse-Triggered Instability in Solid Rocket Motors", AIAA J., Vol. 22, No. 10, Oct. 1984, pp. 1413-1419.

8. Yang, V., Kim, S.I., and Culick, F.E.C., "Third-order Nonlinear Acoustic Oscillations in Combustion Chambers, Part I", AIAA paper 87-1873, June 1987.

9. Flandro, G.A., "Nonlinear Time-Dependent Combustion of a Solid Rocket Propellant", 19th JANNAF Combustion Meeting, Oct. 1982.

10. Chung, T.J. and Kim, P.K., "Unsteady Response of Burning Surface in Solid Propellant Combustion", AIAA paper 85-0234, Jan. 1985.

11. Chung, T.J., Finite Element Analysis in Fluid Dynamics, McGraw-Hill Book Co., 1978.

12. Cantrell, R.H., Hart, R.W., and McClure, F.T., "Linear Acoustic Gains and Losses in Solid Propellant Rocket Motors", AIAA J., Vol. 2, No. 6, June 1964, pp. 1100-1105.

13. Brown, R.S., Dunlap, R., Young, S.W., and Waugh, R.C., "Vortex Shedding as a Source of Acoustic Energy in Segmented Rockets", J. of Spacecraft and Rockets, Vol. 18, July-August 1981, pp. 312-319.

14. Flandro, G.A., "Rotating Flows in Acoustically Unstable Rocket Motors", AIAA J., Vol. 2. July 1964, pp. 1305-1306.

15. Hegde, U.G. and Strahle, W.C., "The Generation of Sound by Turbulence Inside Rocket Motor Cavities", AIAA paper 84-0287, 1984.

16. Friedly, J.C. and Petersen, E.E., "Influence of Combustion Parameters on Instability in Solid Propellant Motors, Part I: Development of Model and Linear Analysis", AIAA J., Vol. 4, No. 9, Sept. 1966, pp. 1605-1610.

17. Friedly, J.C. and Petersen, E.E., "Influence of Combustion Parameters on Instability in Solid Propellant Motors, Part II: Nonlinear Analysis", AIAA J., Vol. 4, No. 11, Nov. 1966, pp. 1932-1937.

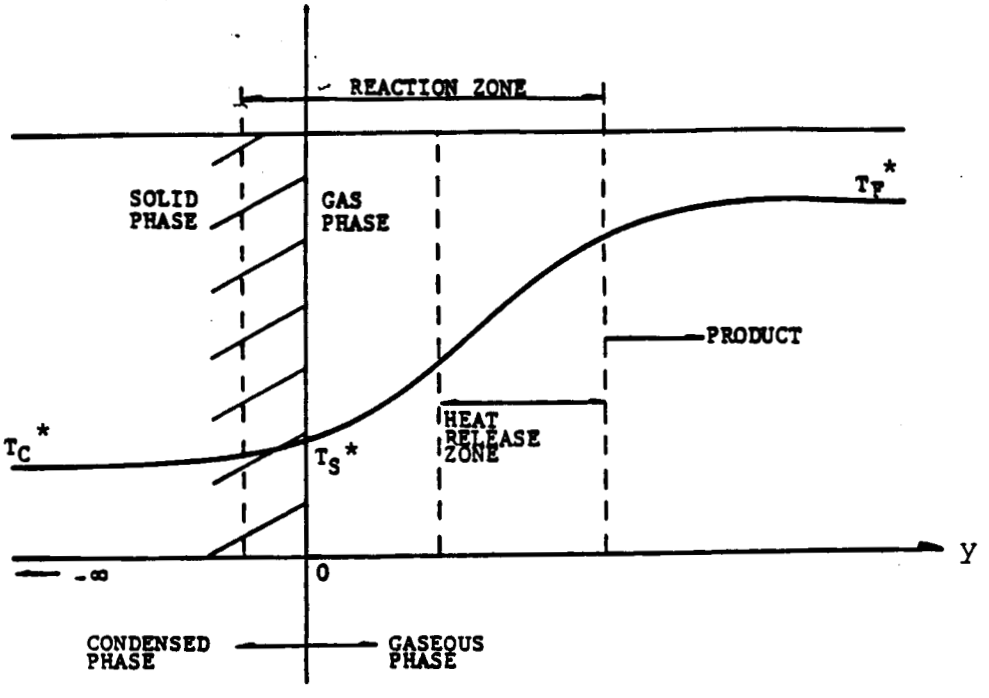

Fig. 3.1 Domain of study for one-dimensional case.

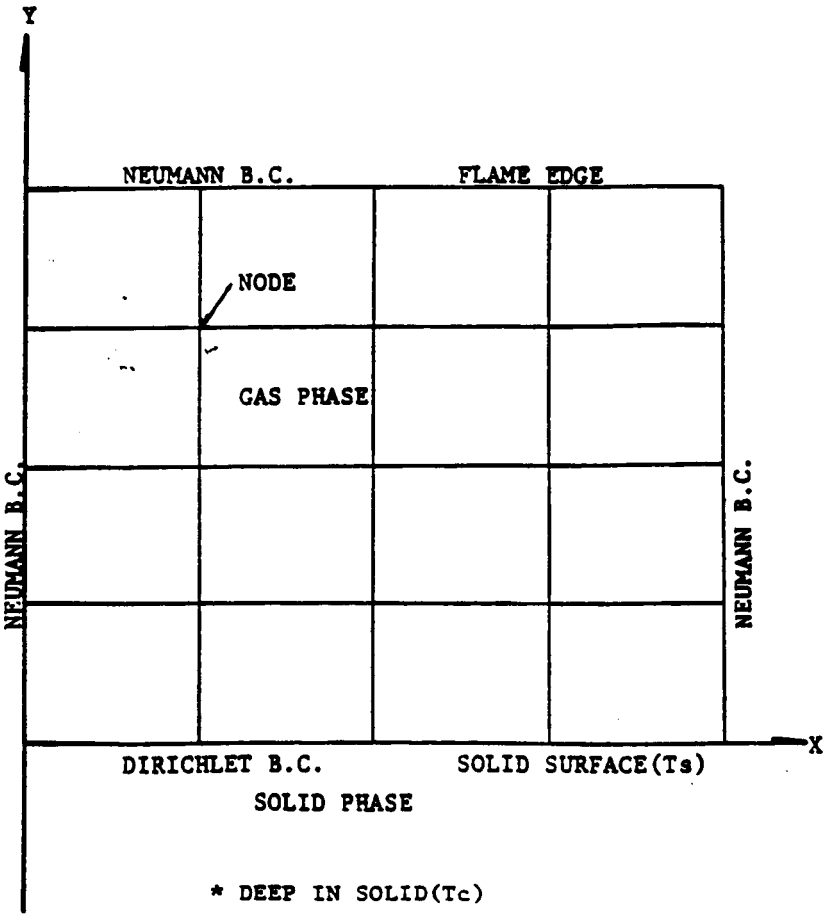

Fig. 4.1 Finite element geometry.

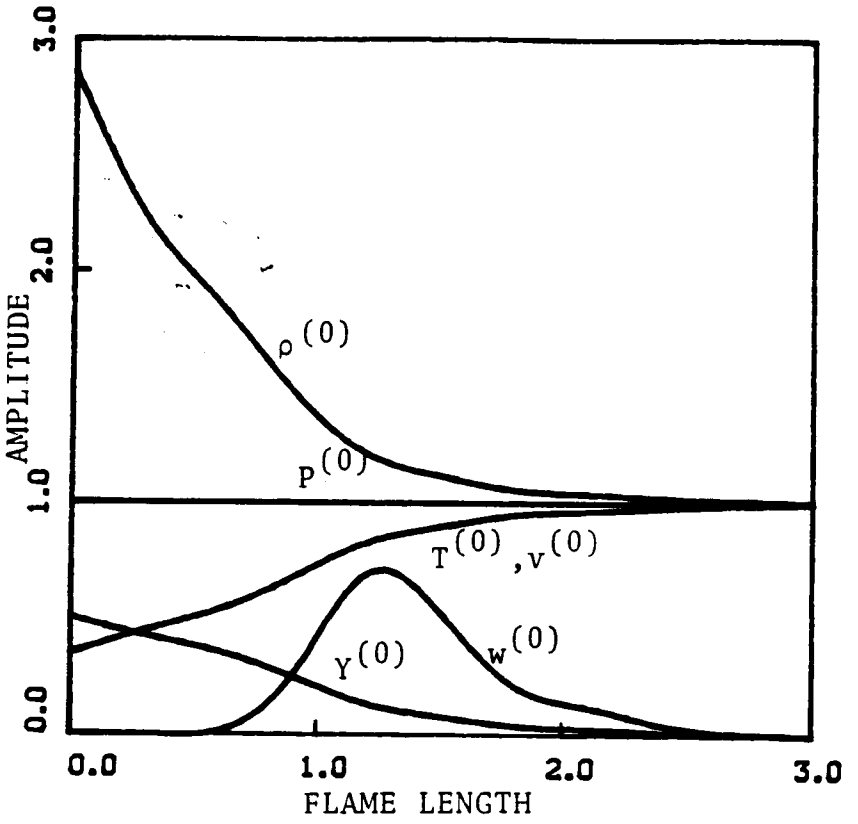

Fig. 4.2 Steady-state distributions of field variables in flame zone. Parameters used in the calculations are given in Table 1, including Pr=1 and Mb= 0.003. Reference values for non-dimensionalization are chosen from the flame edge. (ρ:density,T:temperature, Y:species of fuel, v:velocity, P:pressure, and w:reaction rate).

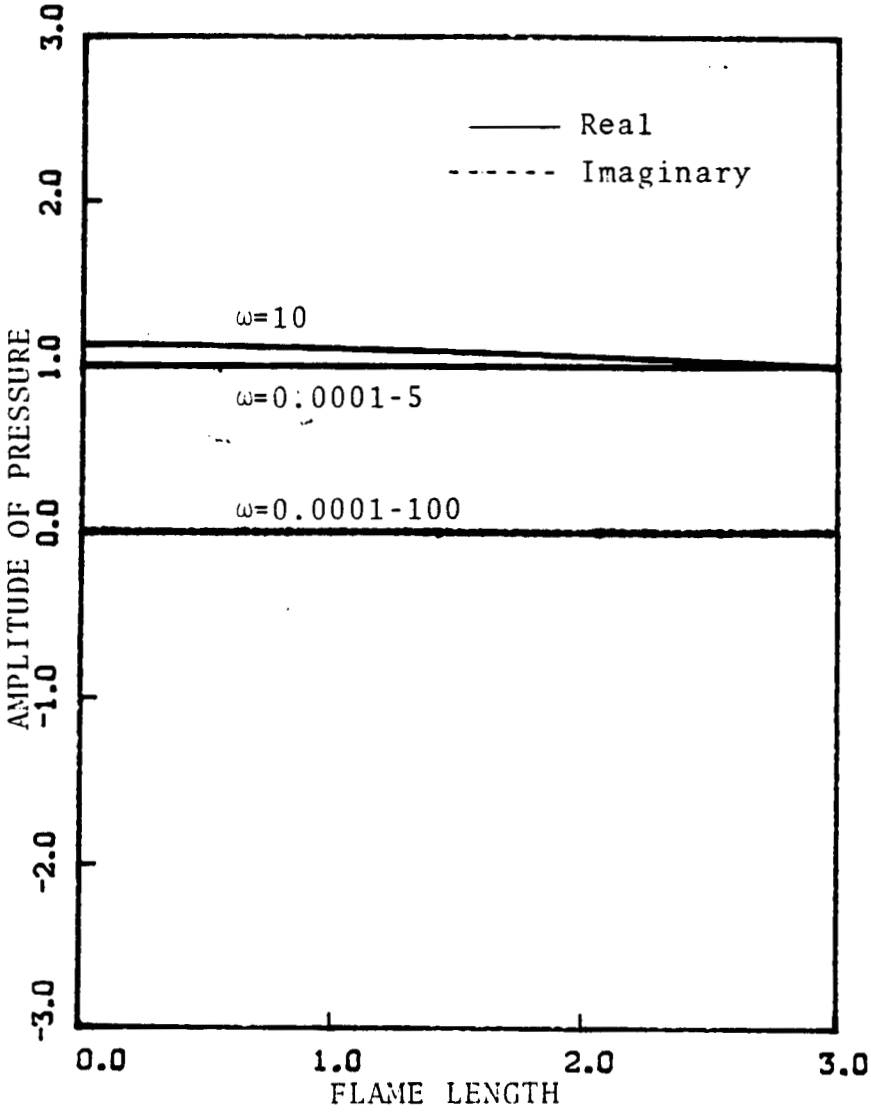

Fig. 4.3 First order pressure distributions vs. frequency(Dirichlet condition is imposed at the flame edge).

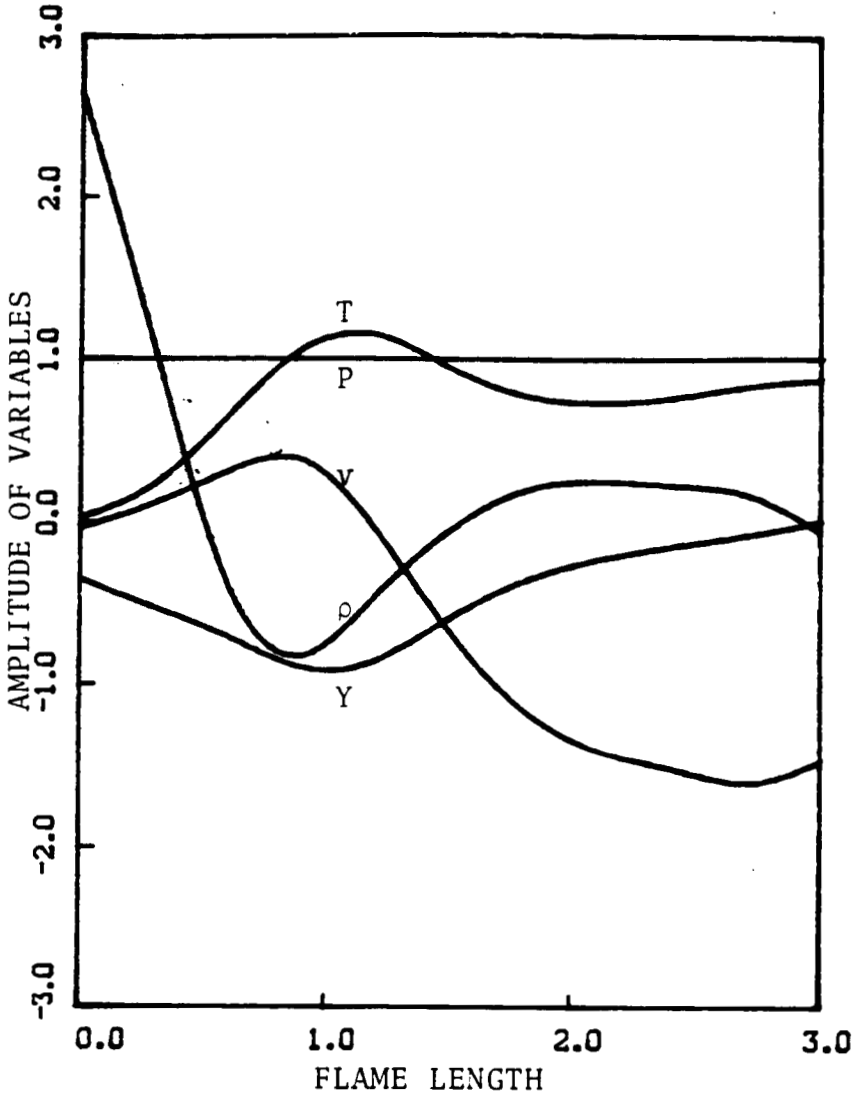

Fig. 4.4a First order distributions of field variables at ω=1(real parts).

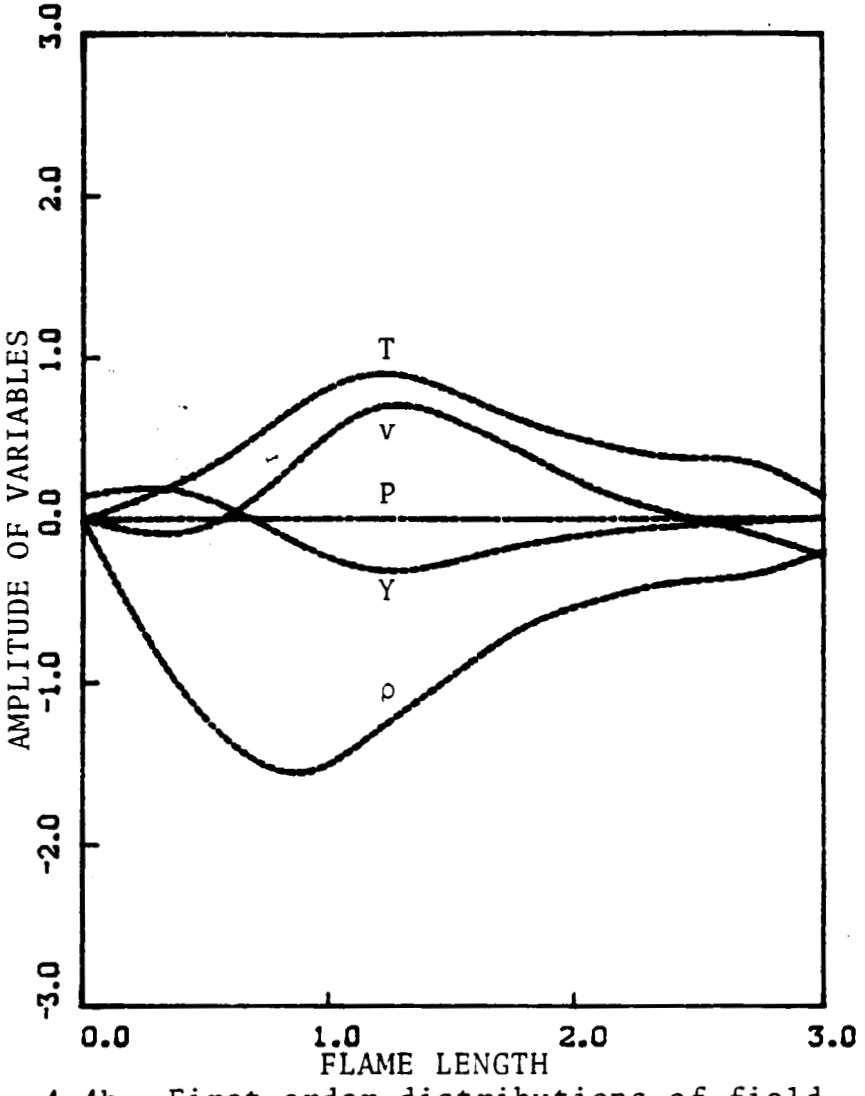

Fig. 4.4b First order distributions of field variables at $\omega = 1$(imaginary parts).

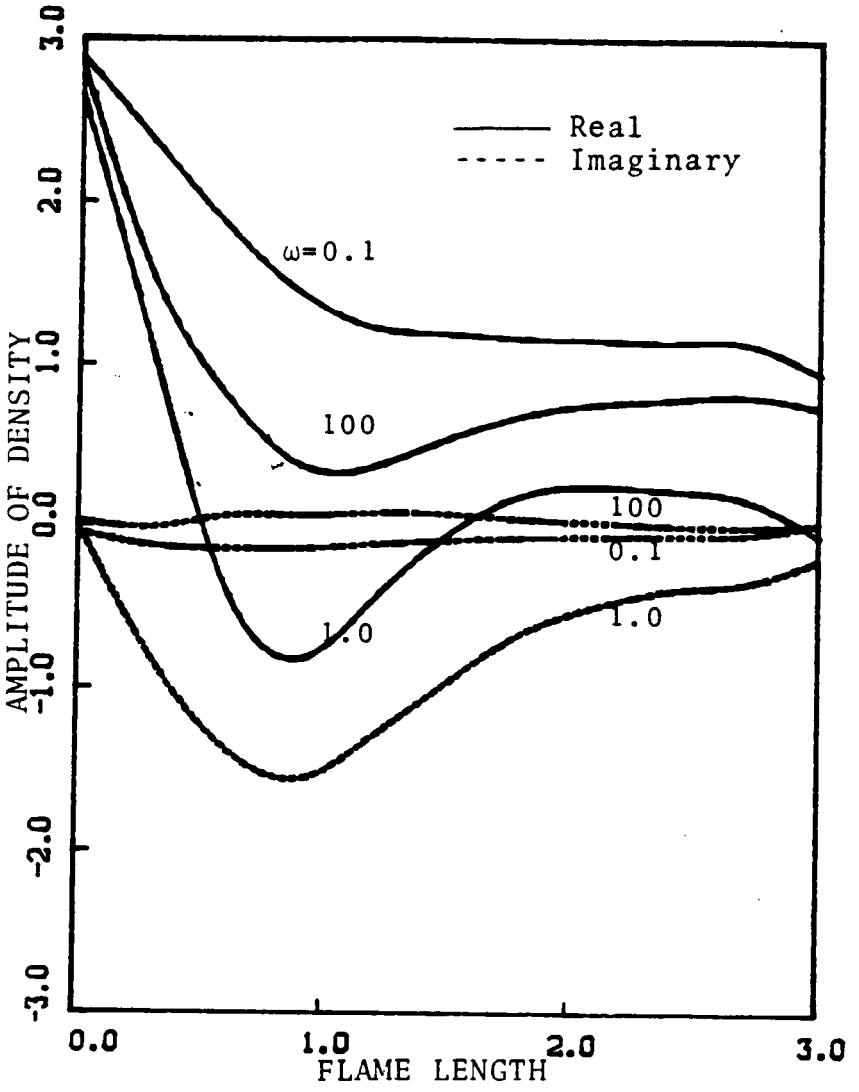

Fig. 4.5 First order density distributions vs. frequency.

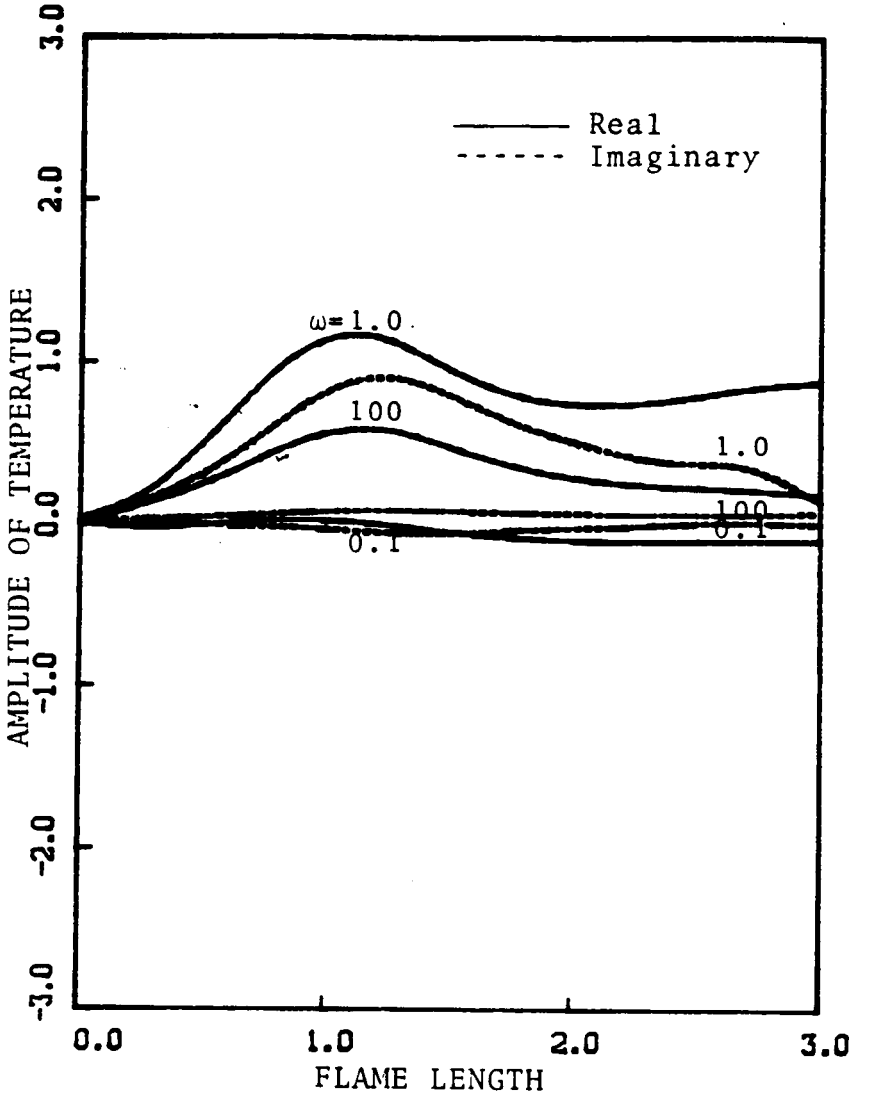

Fig. 4.6 First order temperature distributions vs. frequency.

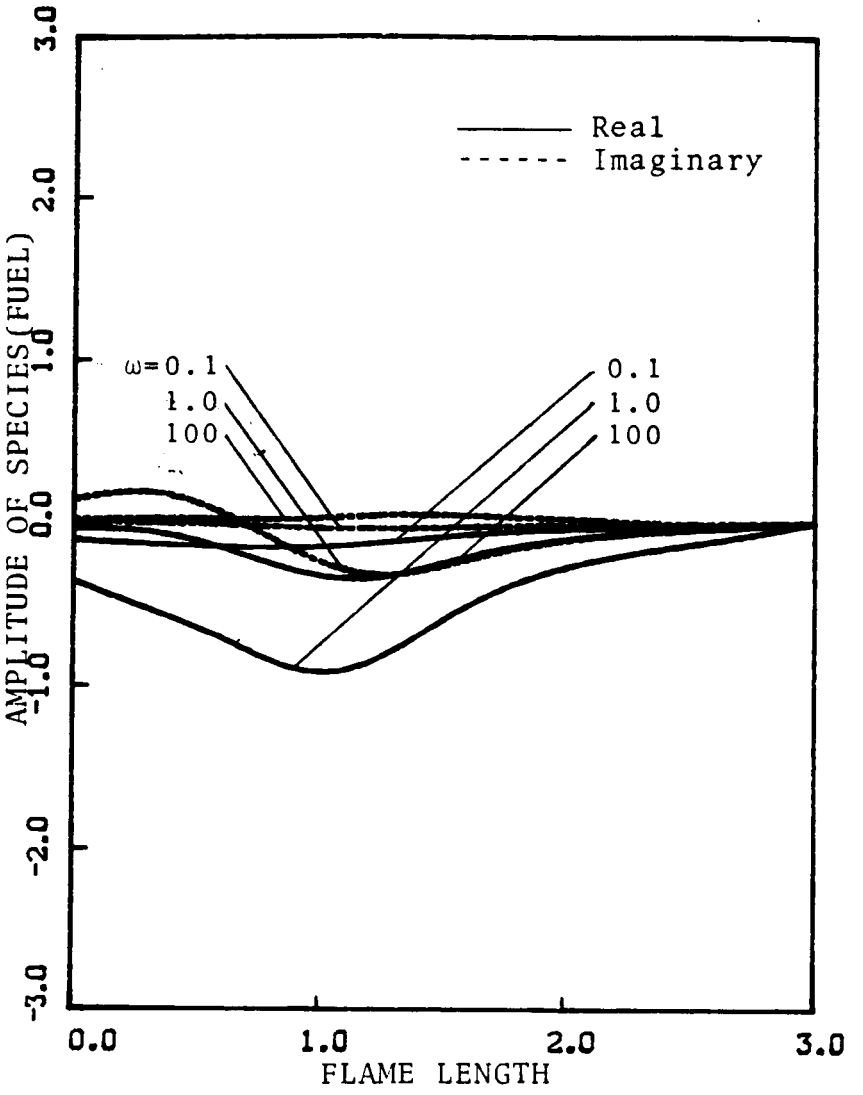

Fig. 4.7 First order species(fuel) distributions vs. frequency.

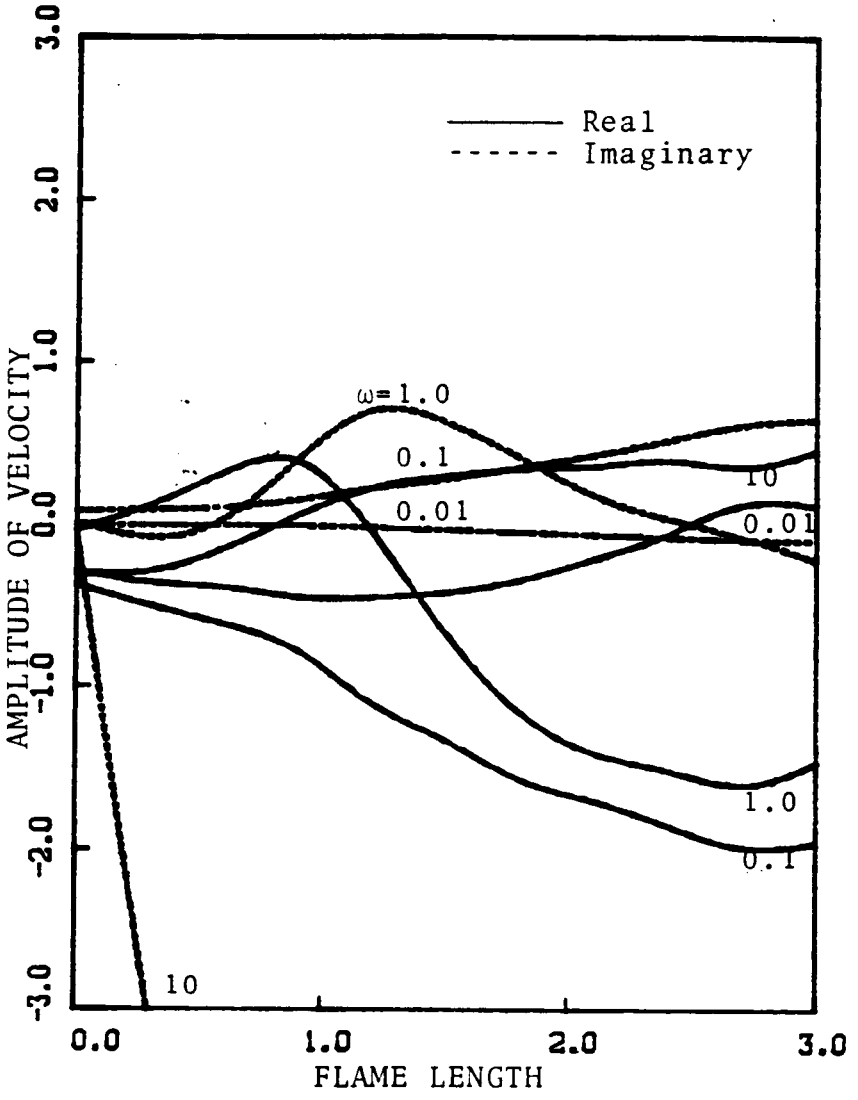

Fig. 4.8 First order velocity distributions vs. frequency.

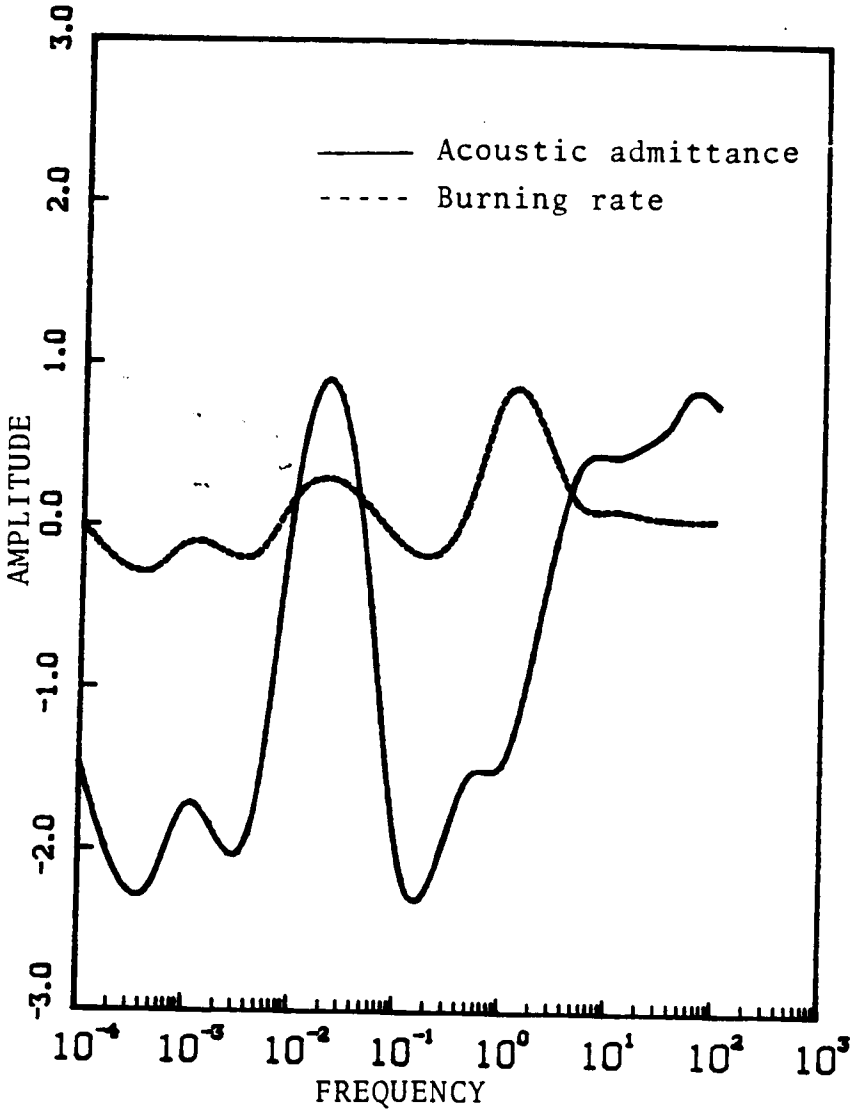

Fig. 4.9a First order acoustic admittance and burning rate vs. frequency. Positive peak near $\omega = 0.01$ resembles the results of Denison and Baum(2) and T'ien(4).

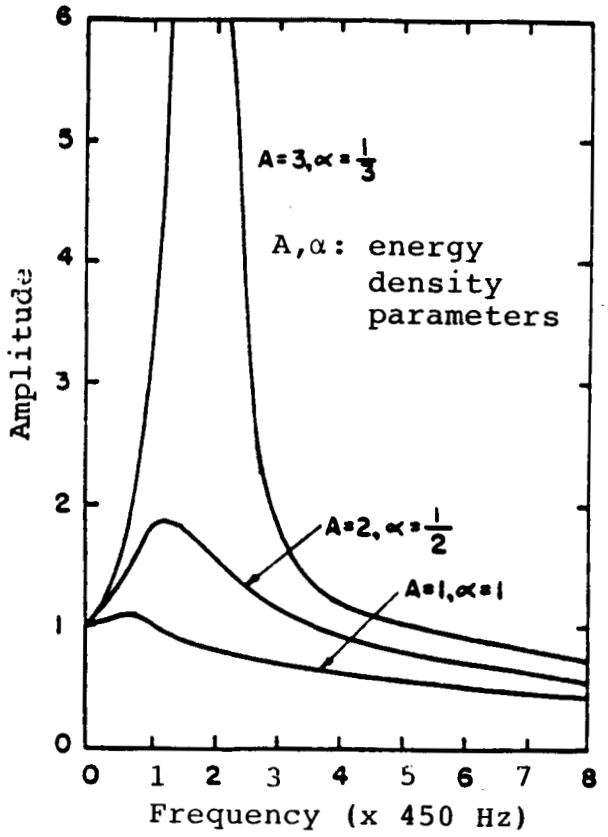

Fig. 4.9b Steady oscillatory mode: typical dependence of amplitude on frequency of pressure oscillation [Denison and Baum, 1961].

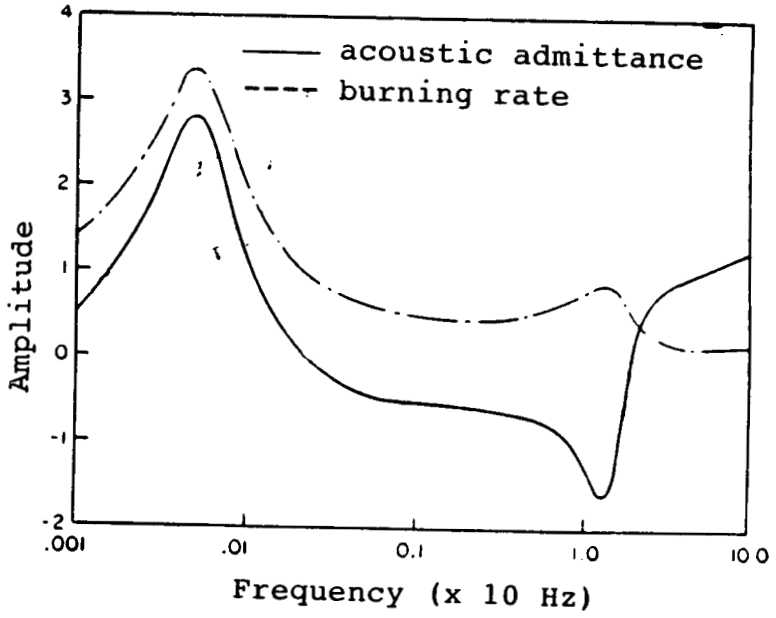

Fig. 4.9c Real parts of acoustic admittance and burning rate vs. frequency [T'ien, 1972].

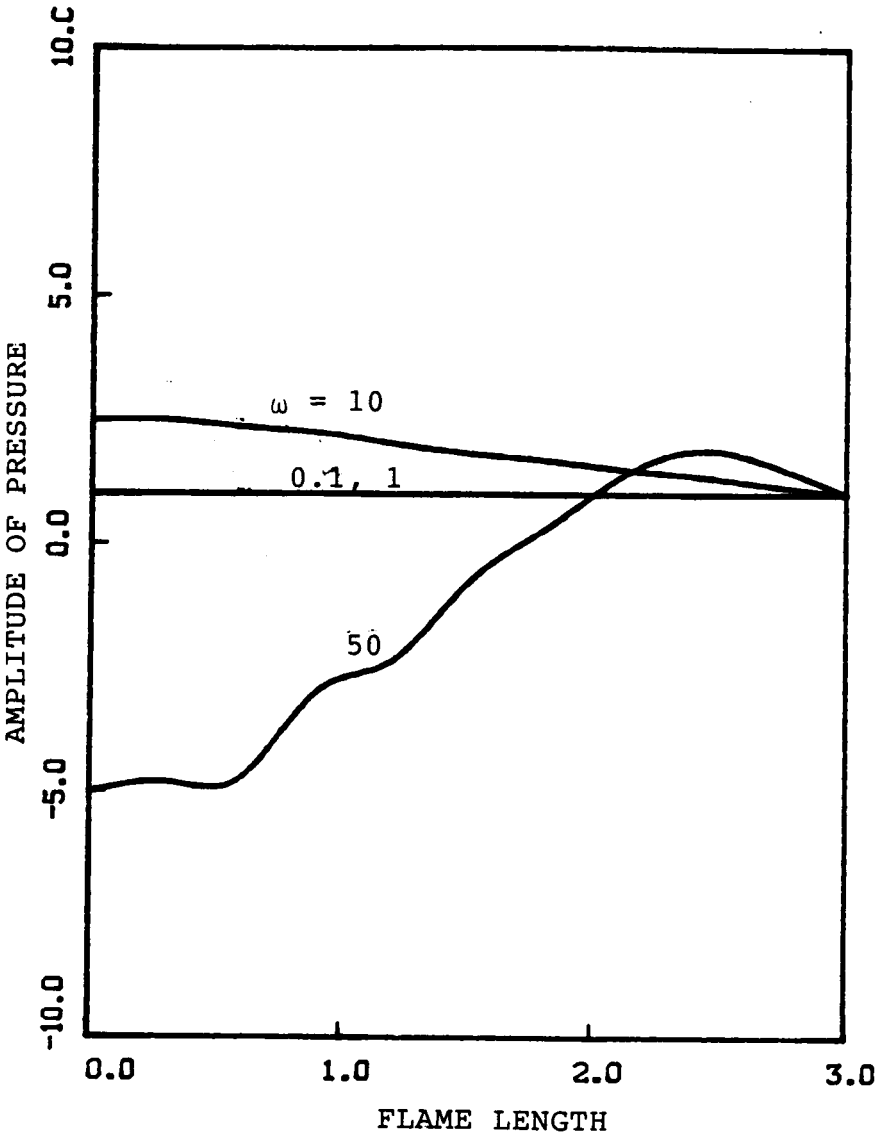

Fig. 4.10 Second order time-independent pressure distributions vs. frequency.

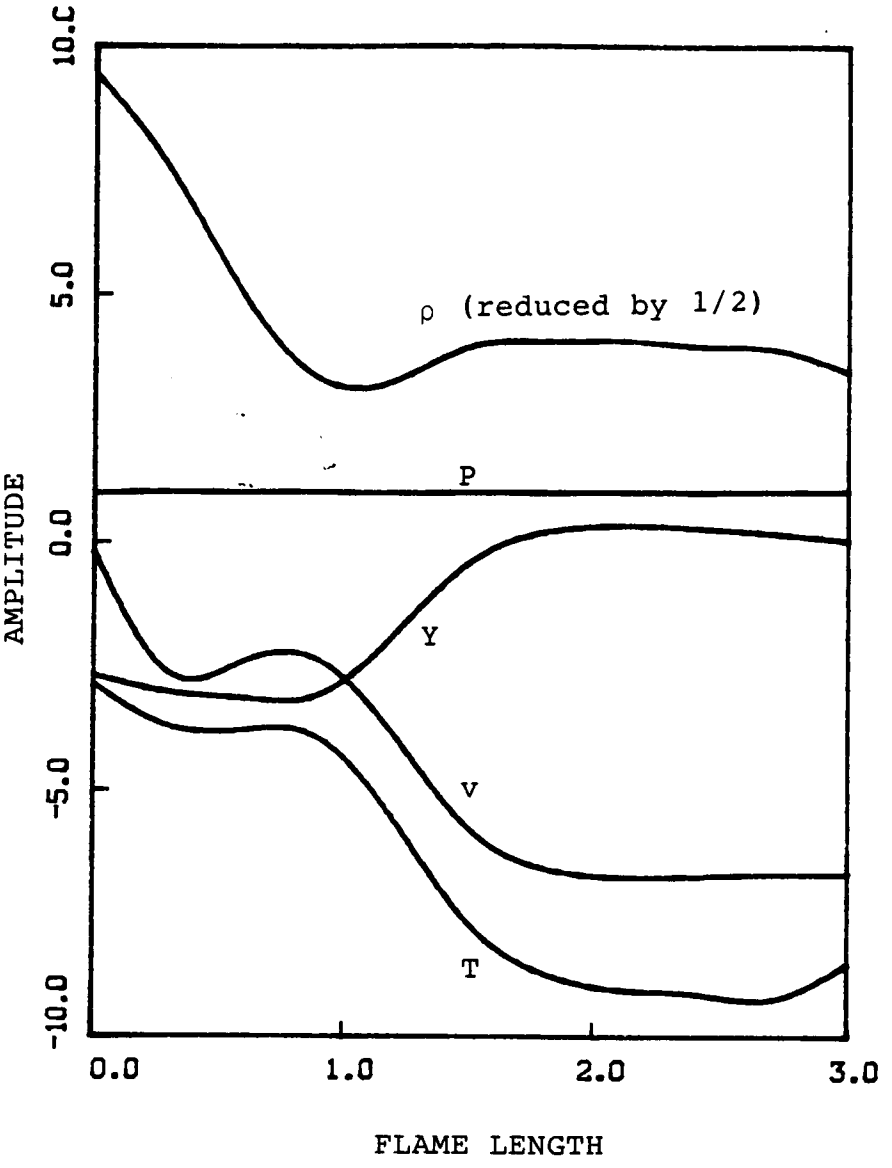

Fig. 4.11 Second order time-independent distributions of field variables at $\omega = 1$.

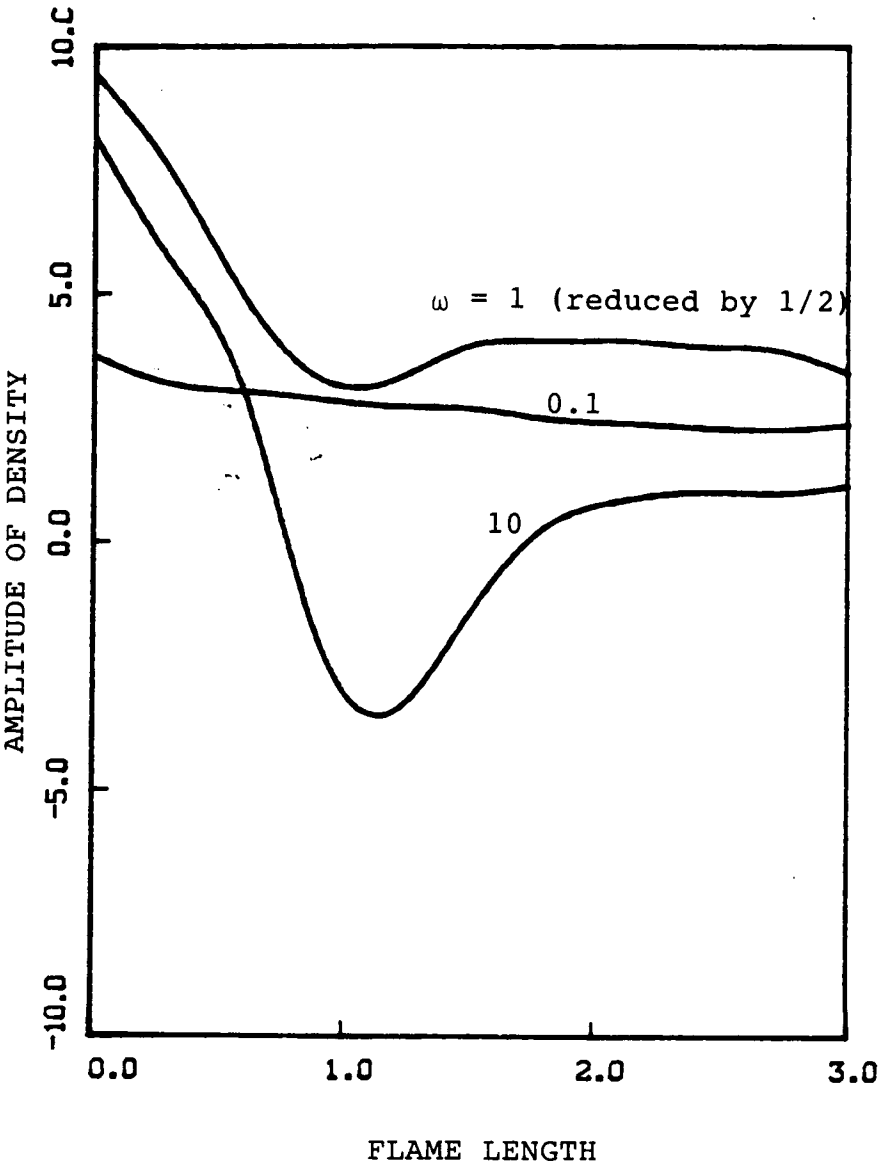

Fig. 4.12 Second order time-independent density distributions vs. frequency.

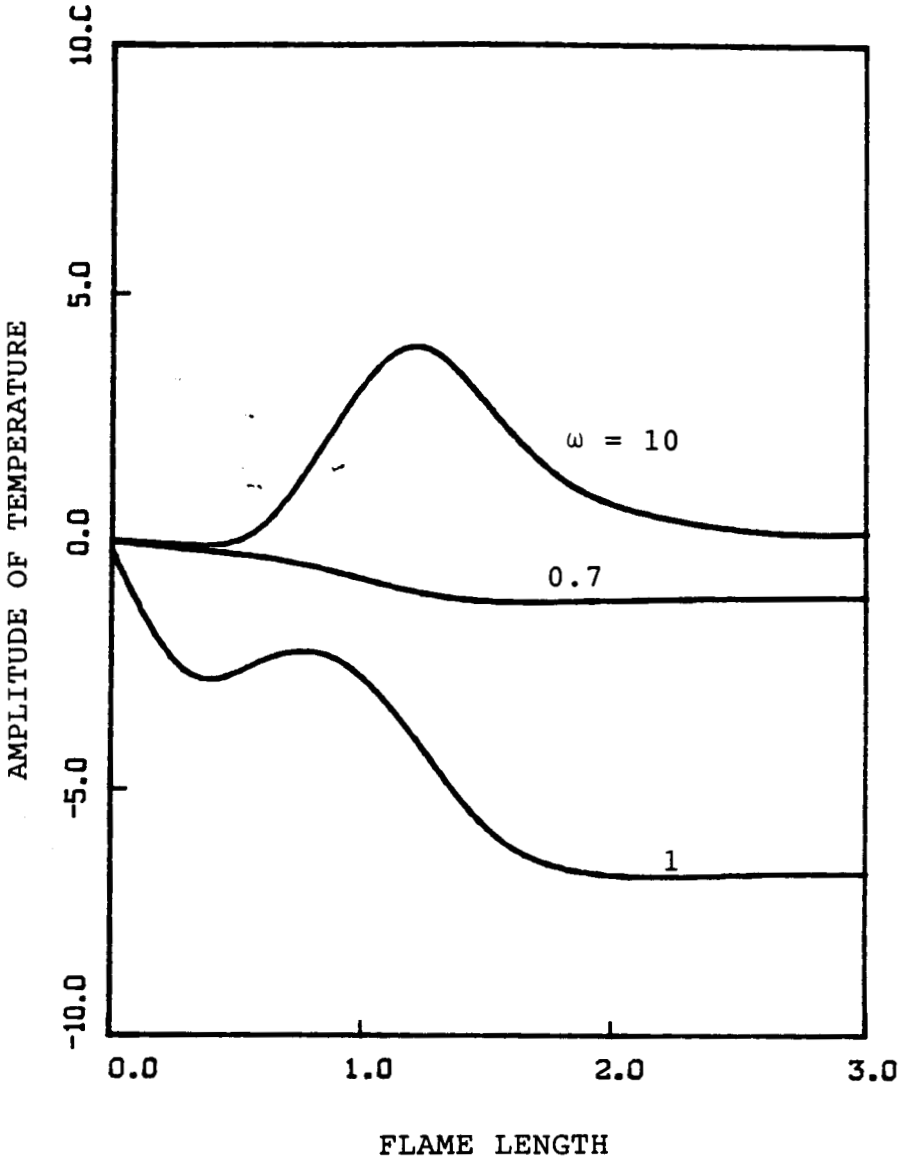

Fig. 4.13 Second order time-independent temperature distributions vs. frequency.

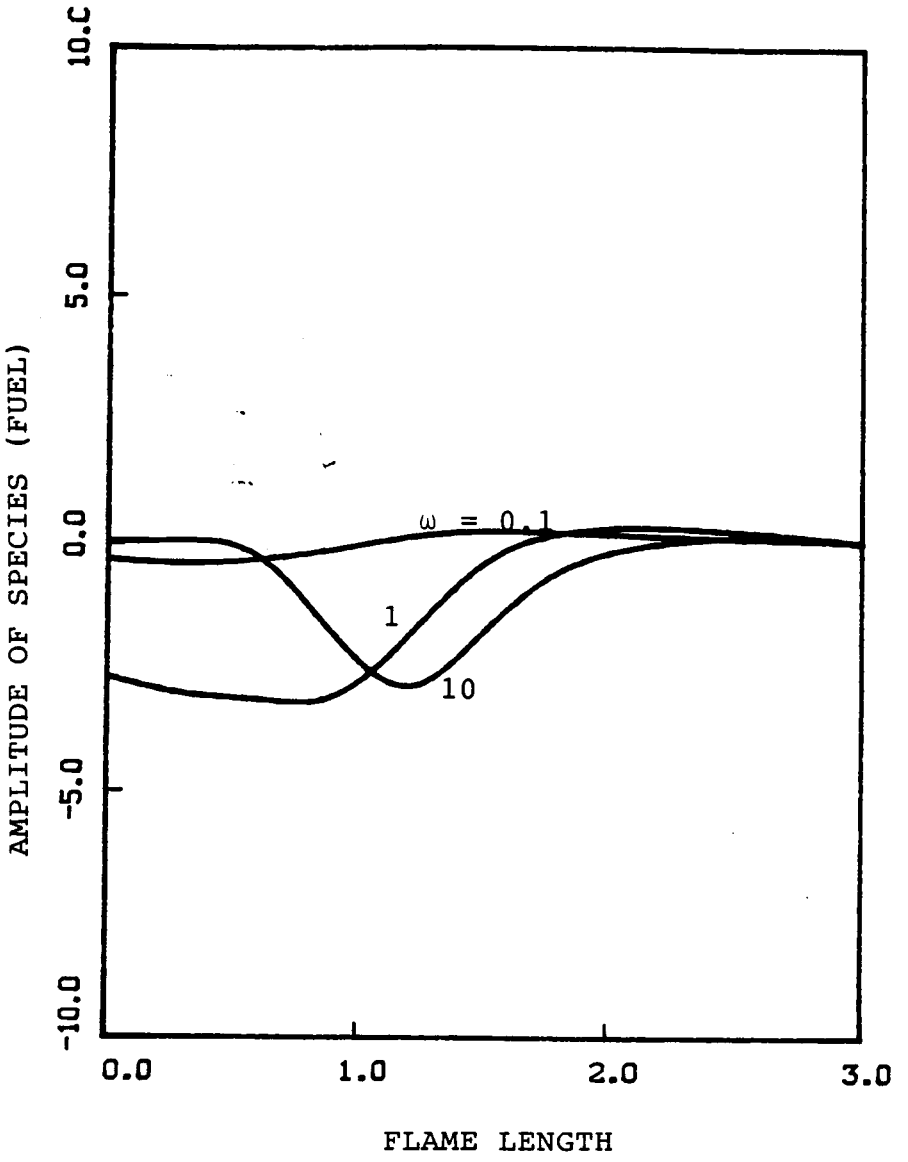

Fig. 4.14 Second order time-independent species (fuel) distributions vs. frequency.

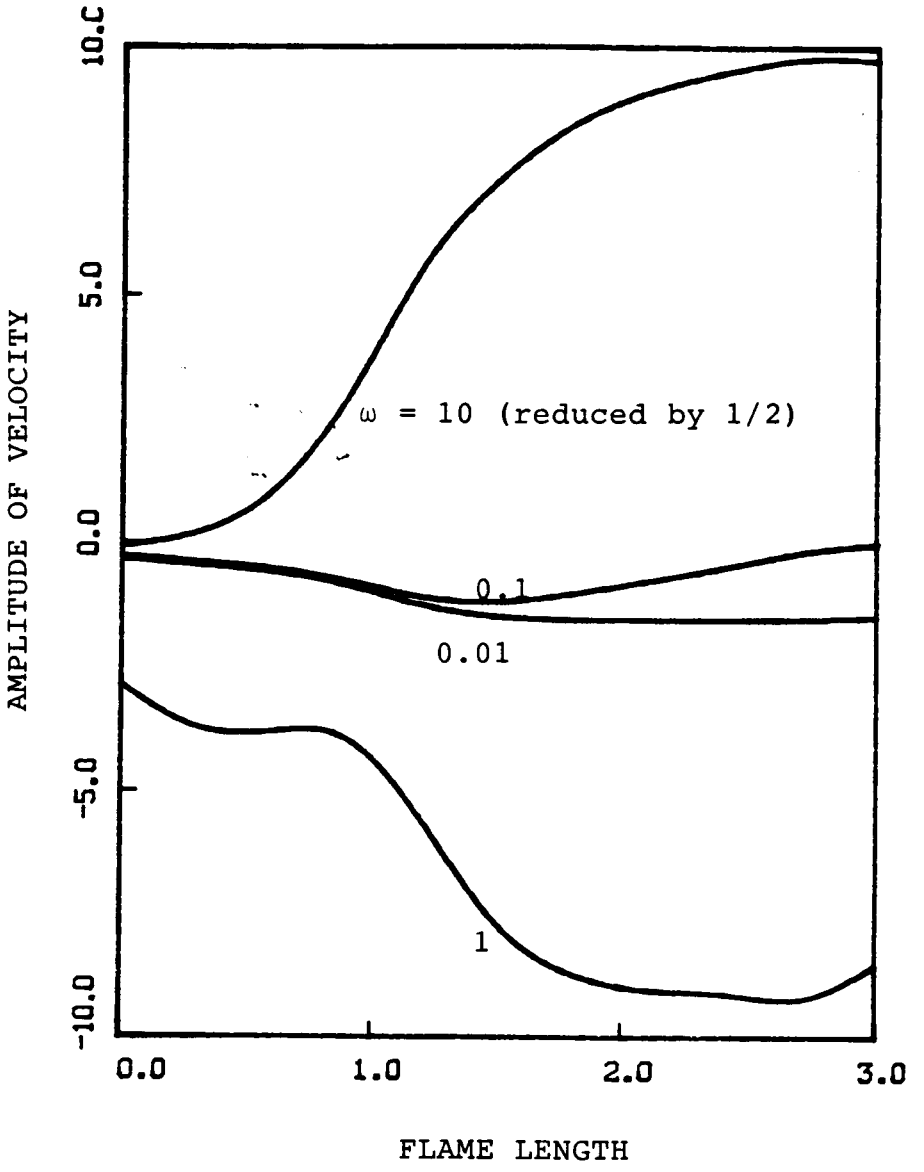

Fig. 4.15 Second order time-independent velocity distributions vs. frequency.

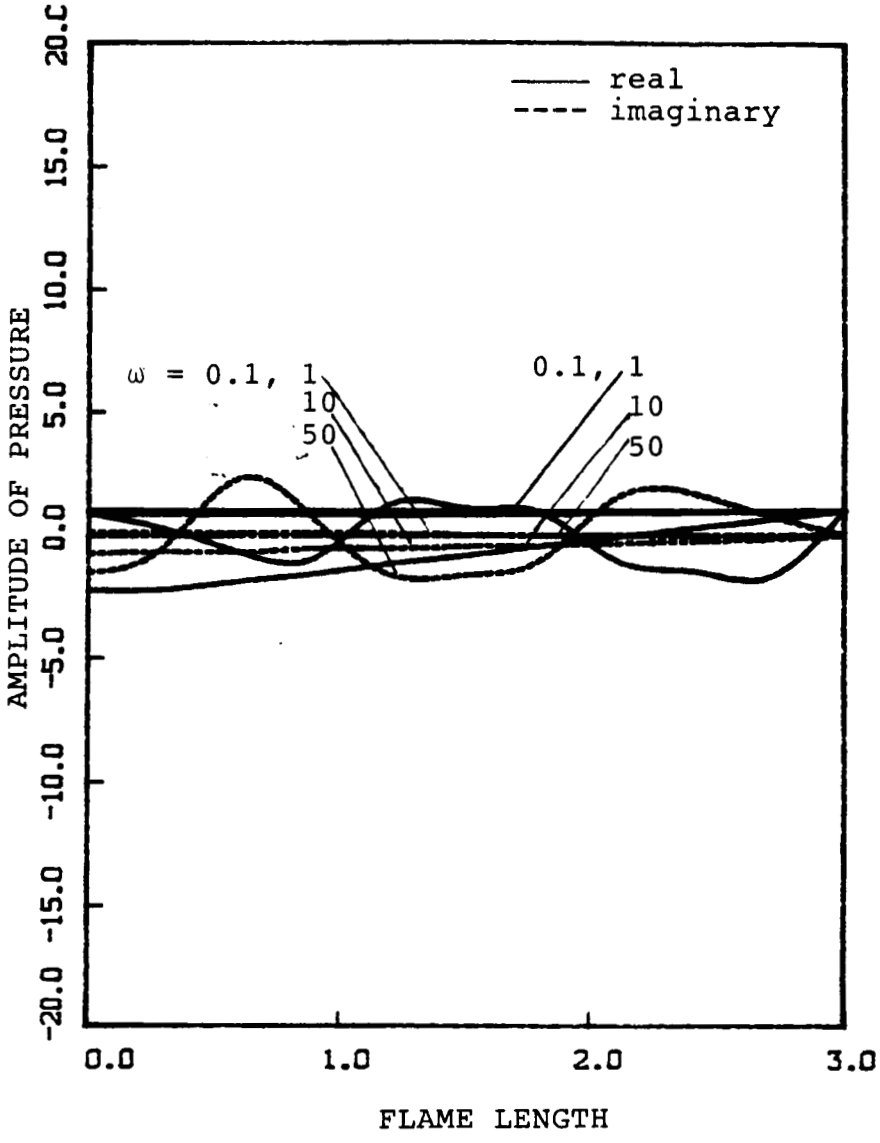

Fig. 4.16 Second order time-dependent pressure distributions vs. frequency.

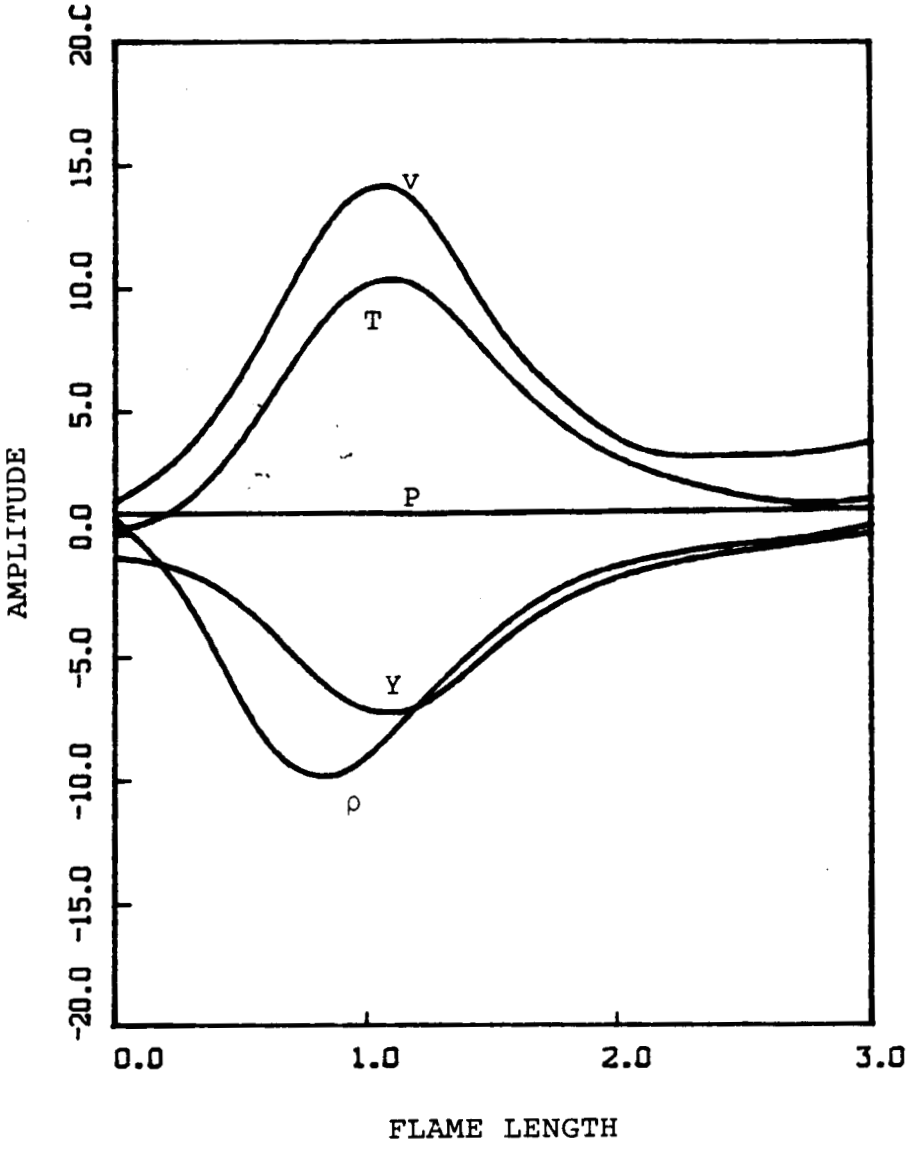

Fig. 4.17a Second order time-dependent distributions of field variables at $\omega = 1$ (real parts).

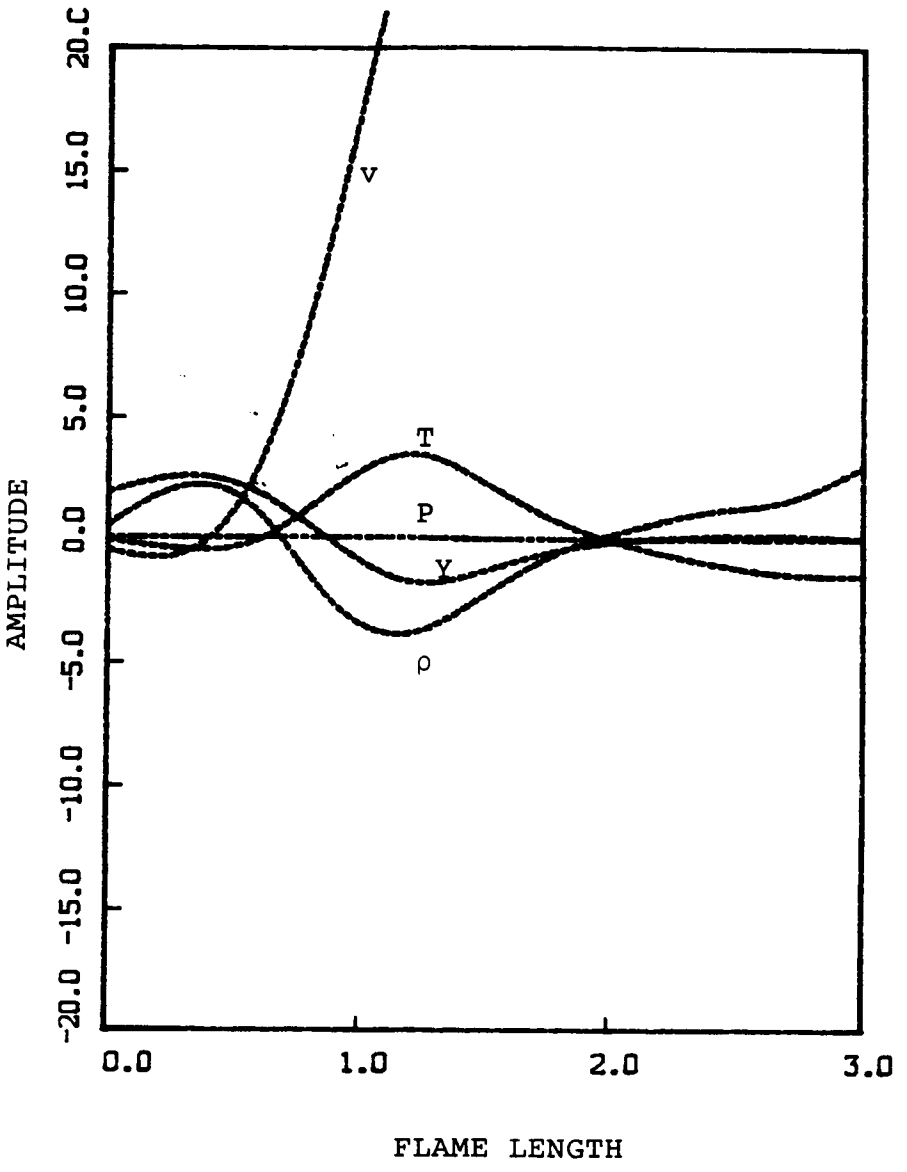

Fig. 4.17b Second order time-dependent distributions of field variables at $\omega = 1$ (imaginary parts).

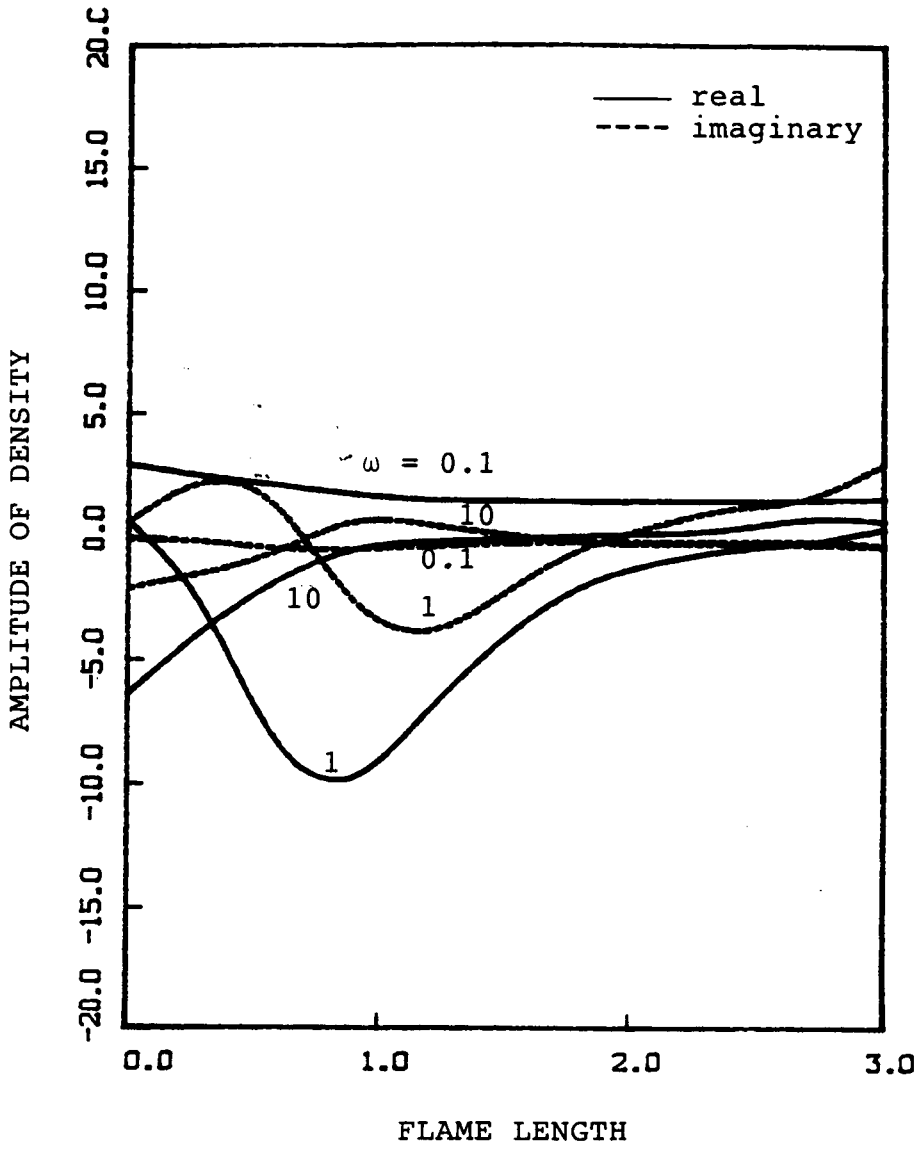

Fig. 4.18 Second order time-dependent density distributions vs. frequency.

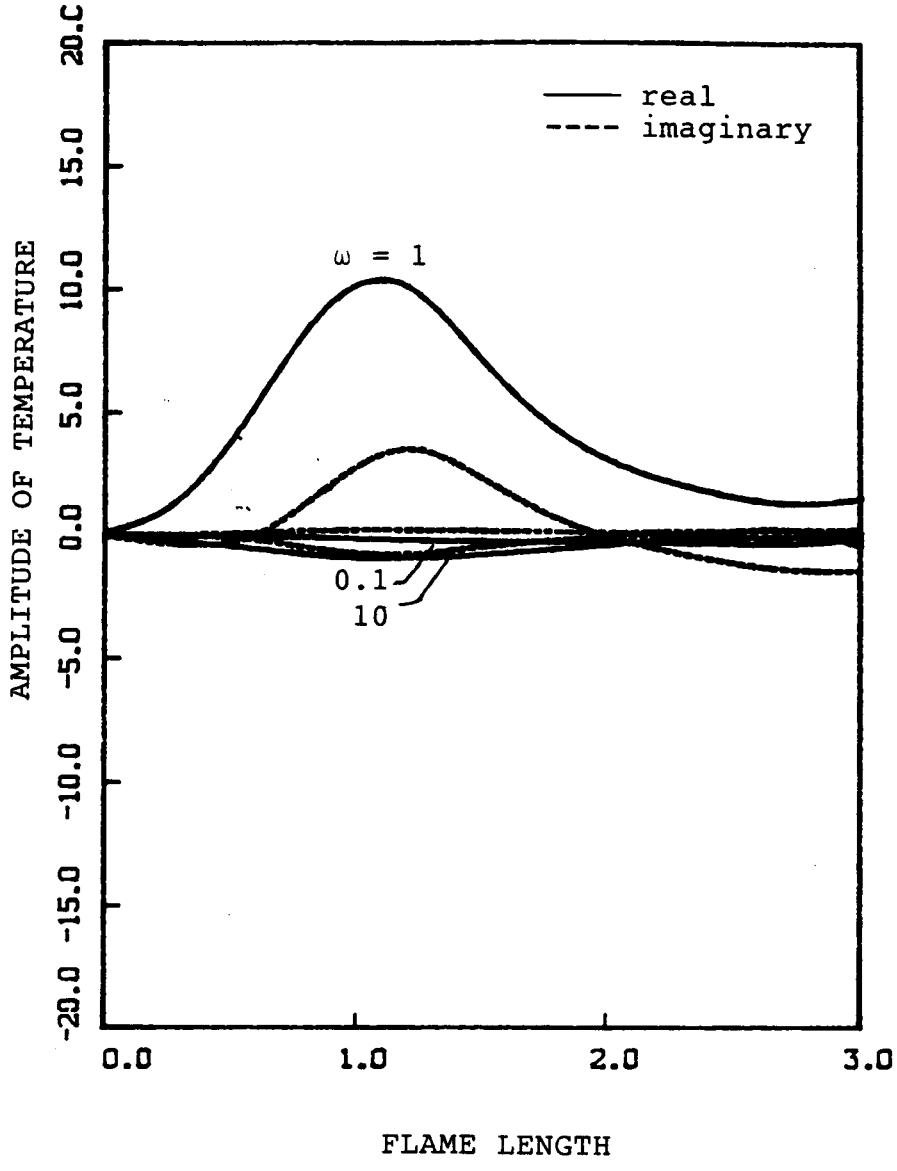

Fig. 4.19 Second order time-dependent temperature distributions vs. frequency.

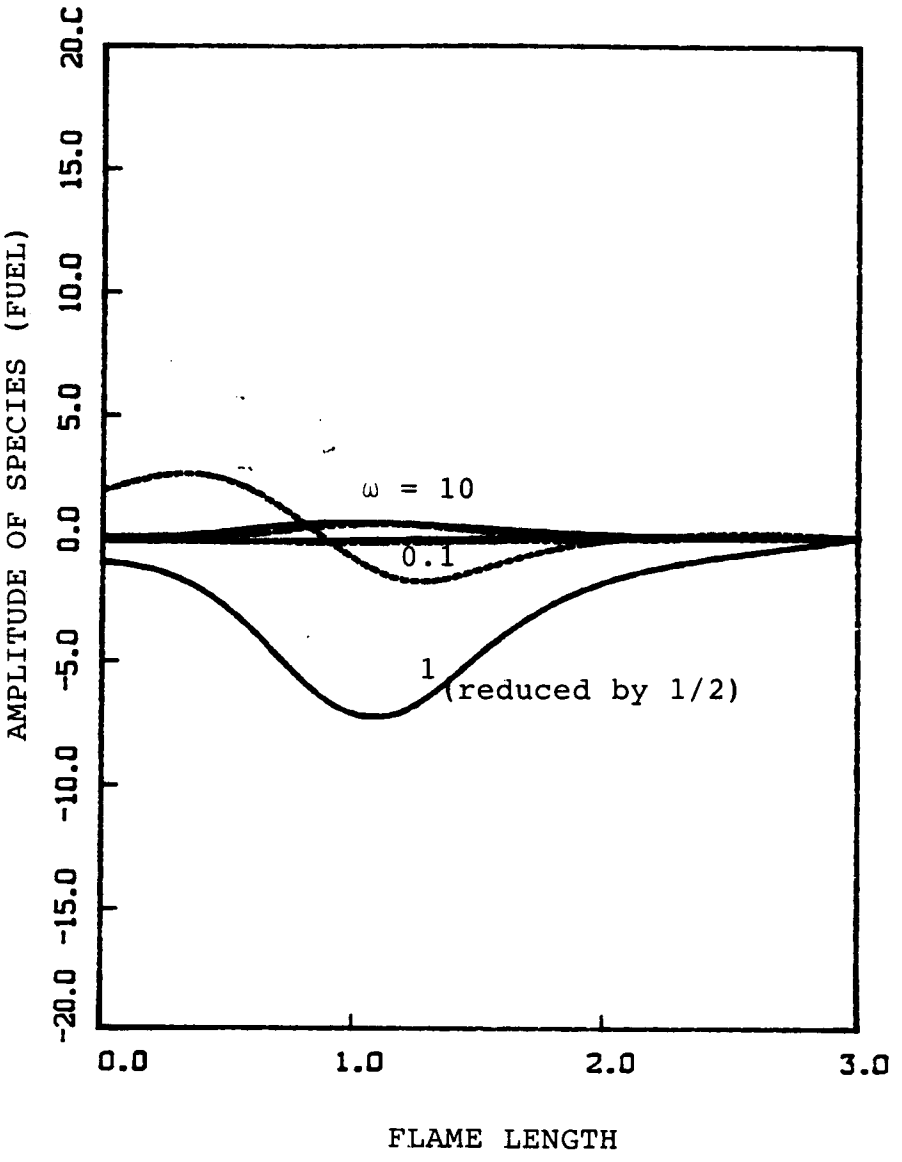

Fig. 4.20 Second order time-dependent species (fuel) distributions vs. frequency.

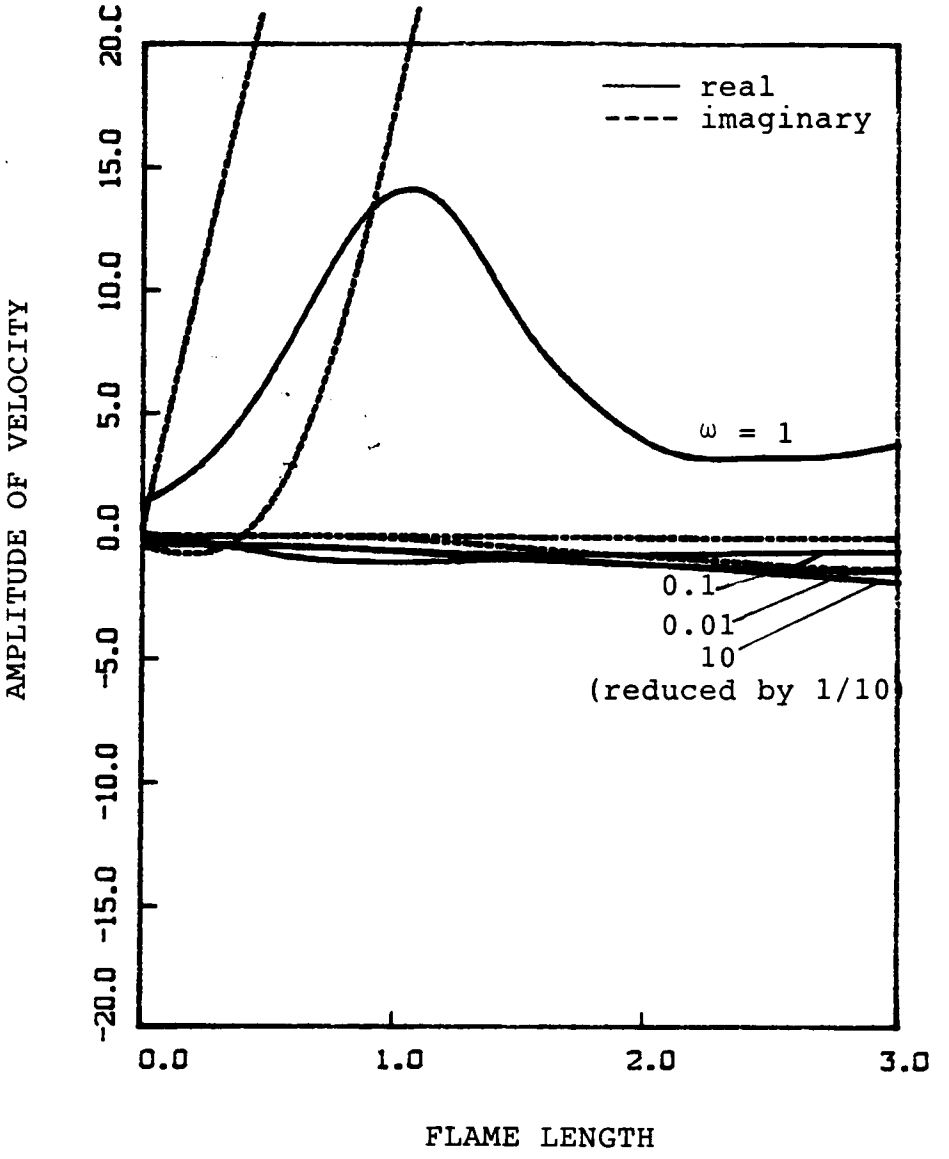

Fig. 4.21 Second order time-dependent velocity distributions vs. frequency.

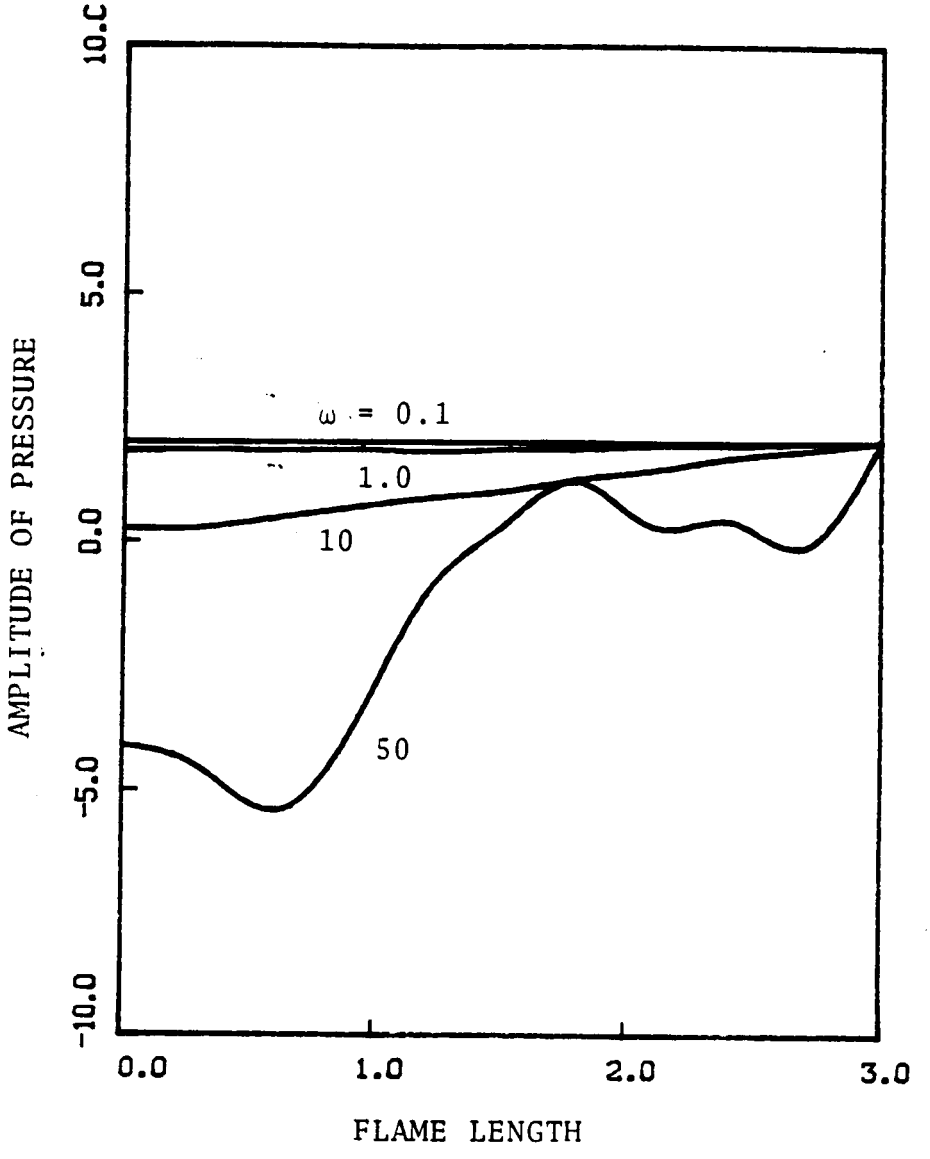

Fig. 4.22 Second order pressure distributions vs. frequency. Both time-dependent and time-independent coefficients are added for denoting the maximum deviation from mean value.

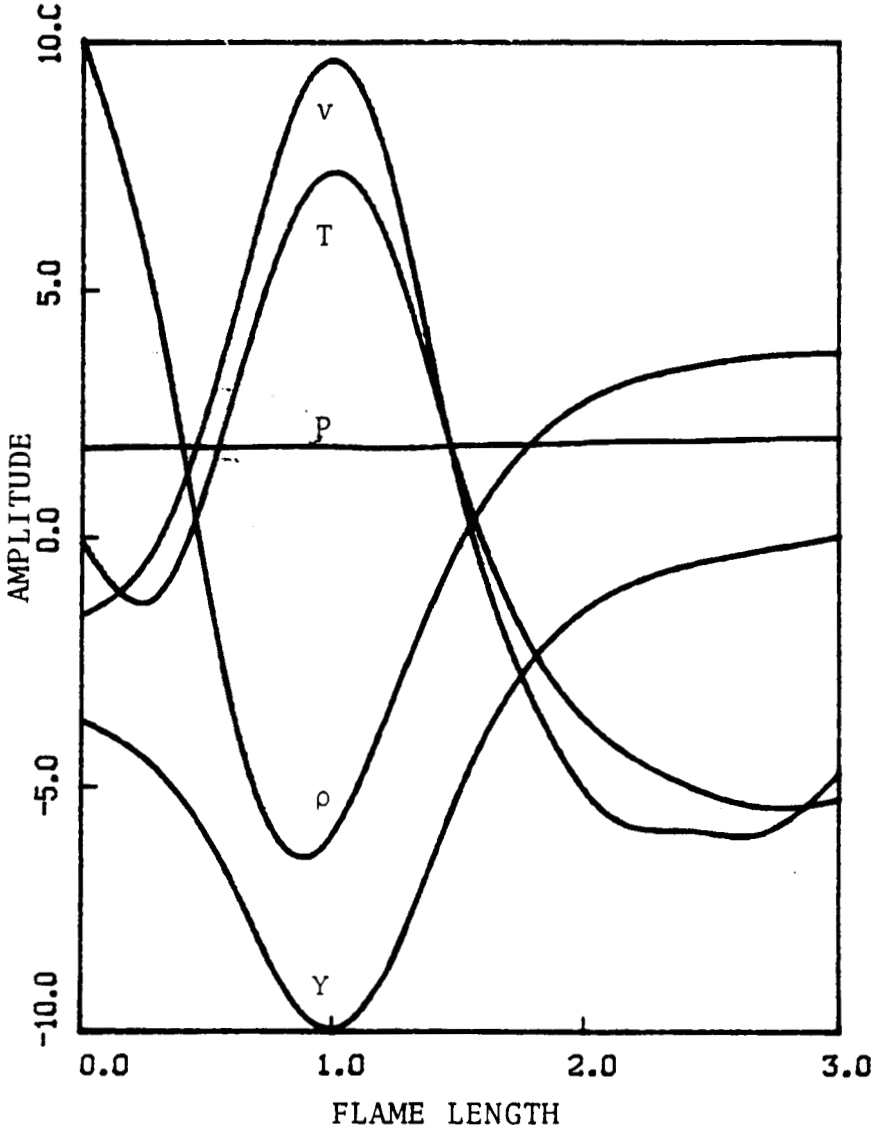

Fig. 4.23 Second order distributions of field variables at $\omega = 1$.

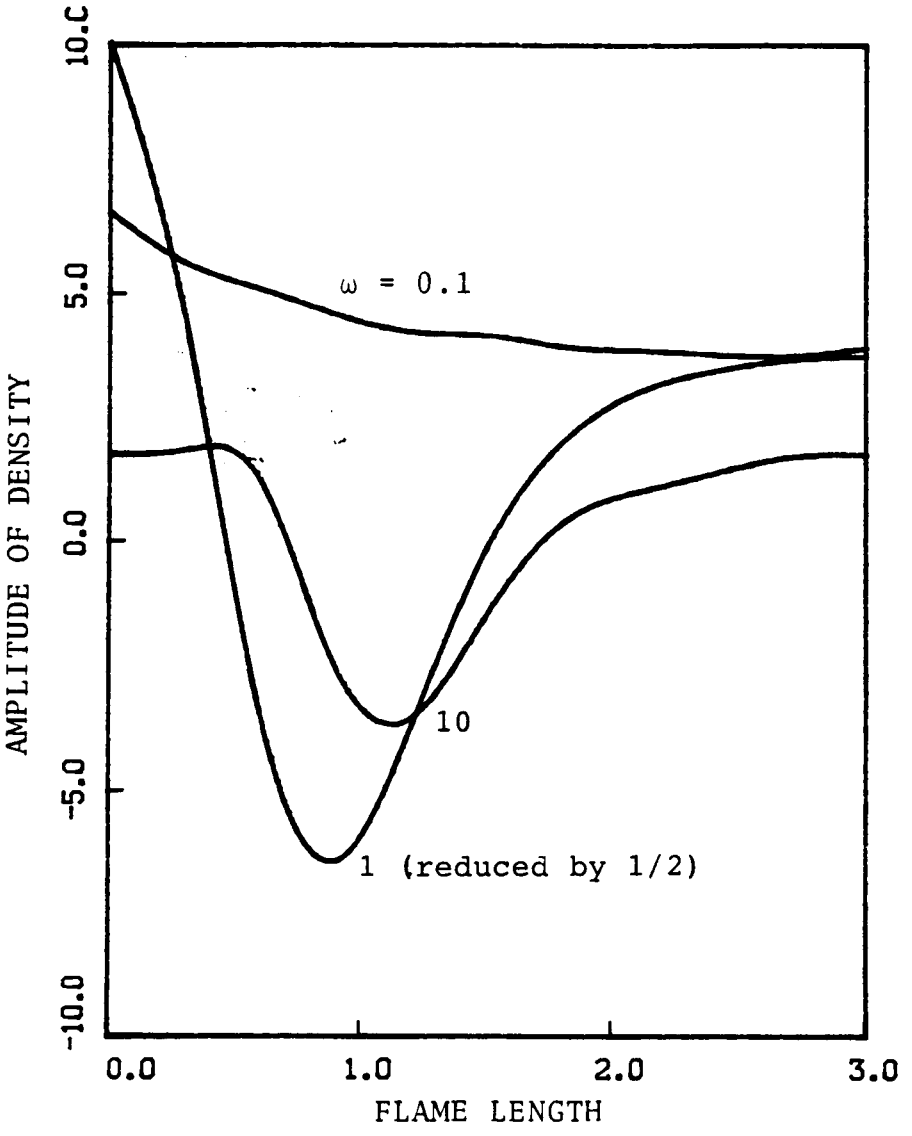

Fig. 4.24 Second order density distributions vs. frequency.

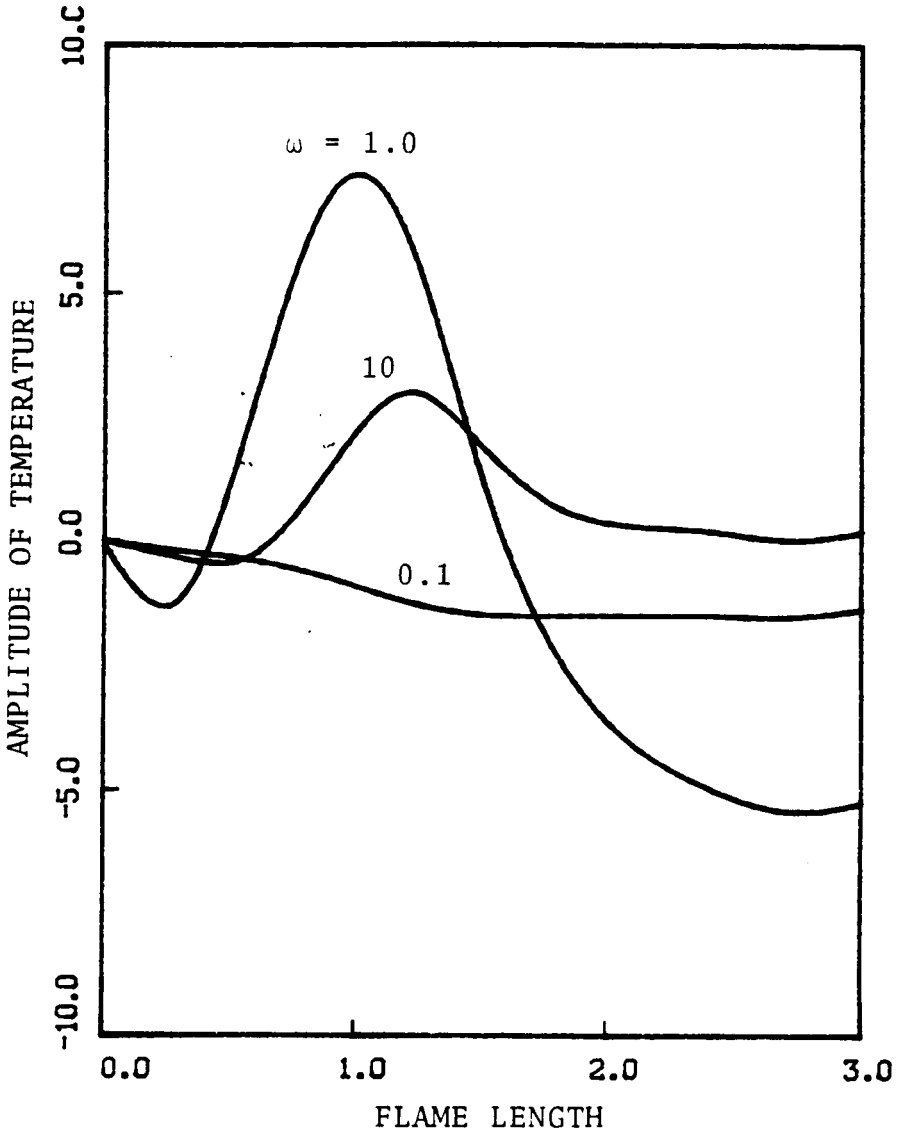

Fig. 4.25 Second order temperature distributions vs. frequency.

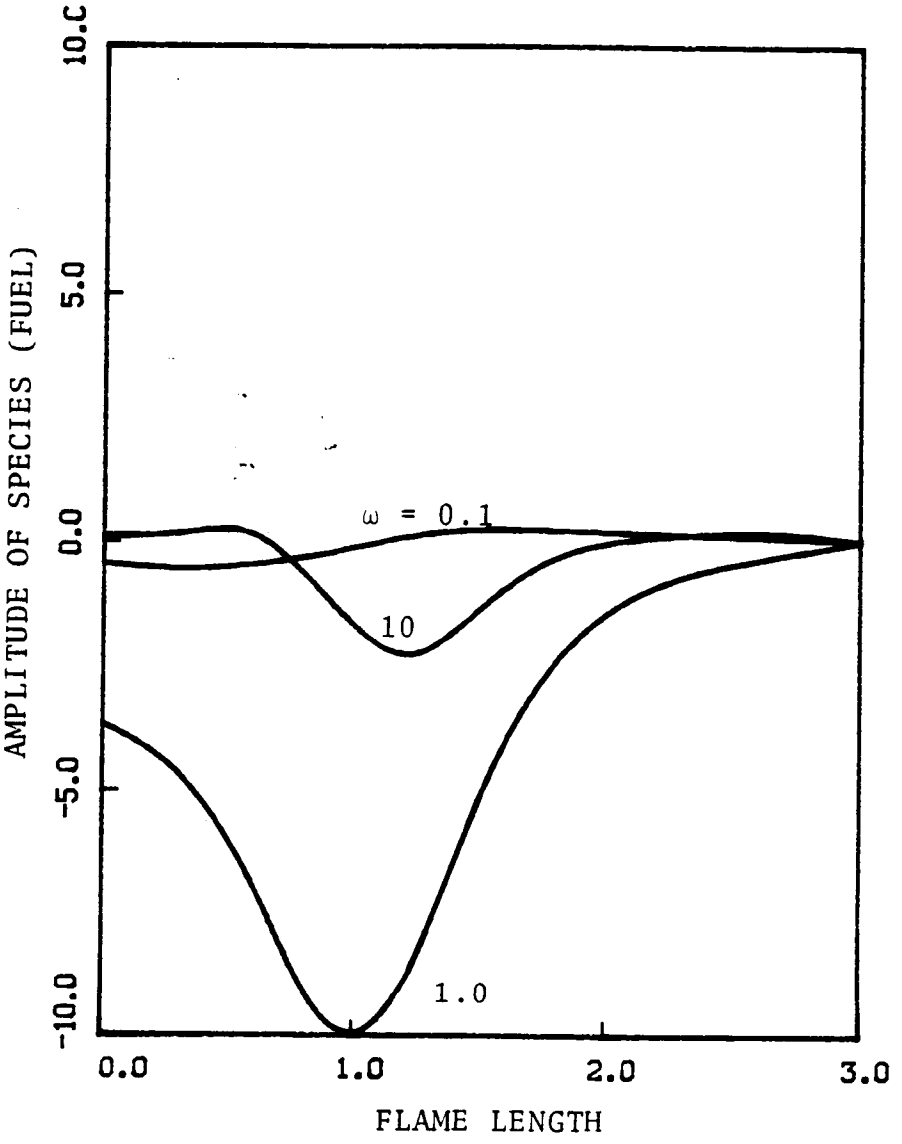

Fig. 4.26 Second order species (fuel) distributions vs. frequency.

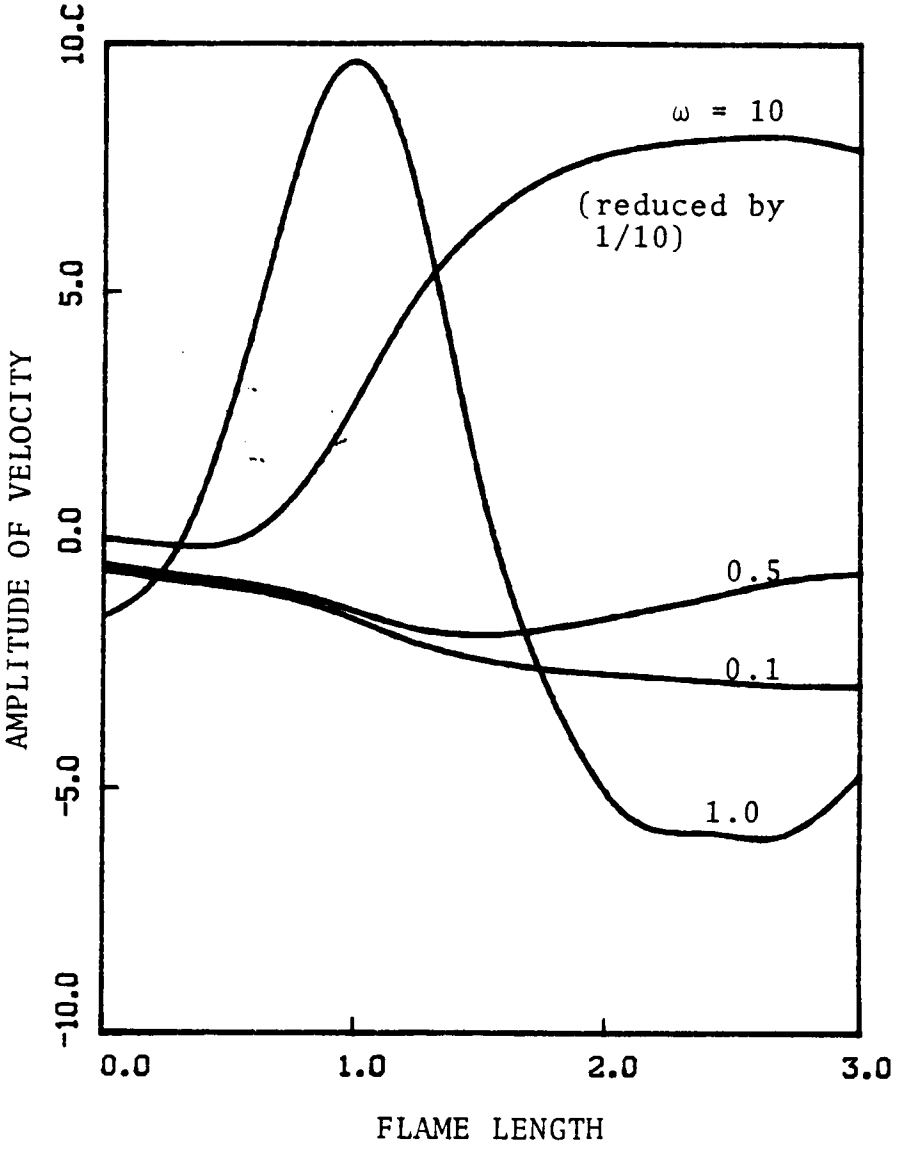

Fig. 4.27 Second order velocity distributions vs. frequency.

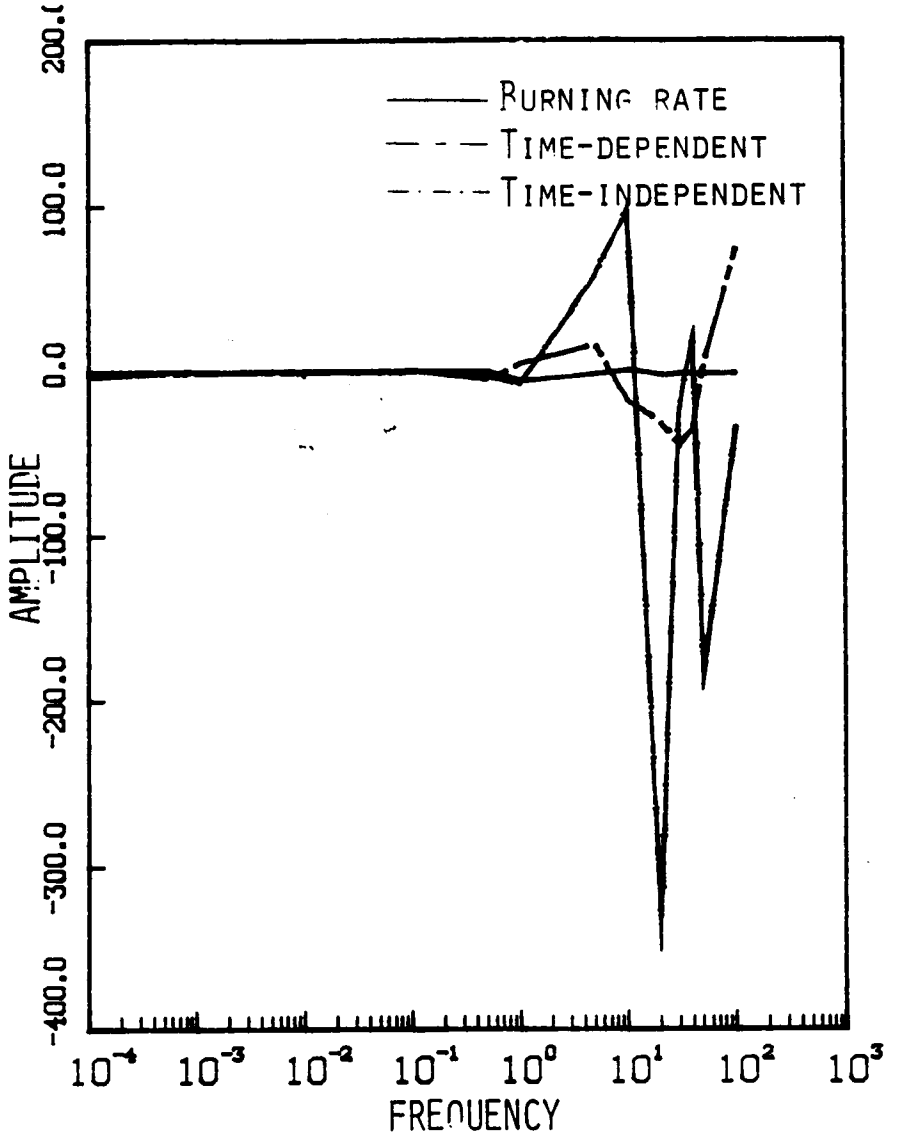

Fig. 4.28 Offset burning rate and acoustic admittances of the second order time-dependent and time-independent systems. Negative value of the burning rate at the frequency region verifies the past investigations.

APPENDIX A

DERIVATION OF NON-DIMENSIONAL GOVERNING EQUATIONS

1. Continuity Equation

The dimensional continuity equation is of the form

$$\frac{\partial \rho^*}{\partial t^*} + (\rho^* u_i^*)_{,i} = 0 \tag{A.1}$$

Substituting Eq. (3.6) yields

$$\frac{\rho_0^* v_0^*}{\ell^*} \frac{\partial \rho}{\partial t} + \frac{1}{\ell^*} (\rho_0^* v_0^* \rho u_i)_{,i} = 0 \tag{A.2}$$

Dividing (A.2) by $\rho_0^* v_0^* / \ell^*$ yields

$$\frac{\partial \rho}{\partial t} + (\rho u_i)_{,i} = 0 \tag{A.3}$$

which is equivalent to Eq. (3.1).

2. Momentum Equation

Neglecting the body forces, the dimensional governing equation is given by

$$\rho^* \frac{\partial u_i^*}{\partial t^*} + \rho^* u_{i,j}^* u_j^* + P_{,i}^* - \mu^* \left(u_{i,jj}^* + \frac{1}{3} u_{j,ij}^* \right) = 0 \tag{A.4}$$

Substituting Eq. (3.6) gives

$$\rho_0^* \frac{v_0^{*2}}{\ell^*} \rho \frac{\partial u_i}{\partial t} + \rho_0^* \frac{v_0^{*2}}{\ell^*} \rho u_{i,j} u_j + \frac{P_0^*}{\ell^*} P_{,i}$$

$$- \mu^* \left(\frac{v_0^*}{\ell^{*2}} u_{i,jj} + \frac{v_0^*}{3\ell^{*2}} u_{j,ij} \right) = 0 \qquad (A.5)$$

Dividing the equation by $\rho_0^* v_0^{*2}/\ell^*$ results in

$$\rho \frac{\partial u_i}{\partial t} + \rho u_{i,j} u_j + \frac{P_0^*}{\rho_0^* v_0^{*2}} P_{,i} - \frac{\mu^*}{\rho_0^* v_0^* \ell^*} \left(u_{i,jj} + \frac{1}{3} u_{j,ij} \right) = 0 \qquad (A.6)$$

Since

$$M_b^2 = \left(\frac{v_0^*}{a_0^*} \right)^2 = \frac{\rho_0^* v_0^{*2}}{\gamma P_0^*}$$

where M_b is the Mach number at the reference point, then

$$\frac{P_0^*}{\rho_0^* v_0^{*2}} = \frac{1}{\gamma M_b^2} \qquad (A.7)$$

For the last term,

$$\ell^* = \frac{\alpha^*}{v_0^*} = \frac{k^*}{\rho_0^* C_p^* v_0^*}$$

with α^* being the thermal diffusivity. Thus,

$$\frac{\mu^*}{\rho_0^* v_0^* \ell^*} = \frac{\mu^* \rho_0^* C_p^* v_0^*}{\rho_0^* v_0^* k^*} = \frac{\mu^* C_p^*}{k^*} = Pr \qquad (A.8)$$

Substituting Eqs. (A.7) and (A.8) yields

$$\rho \frac{\partial u_i}{\partial t} + \rho u_{i,j} u_j + \frac{1}{\gamma M_b^2} P_{,i} - Pr \left(u_{i,jj} + \frac{1}{3} u_{j,ij} \right) = 0 \qquad (A.9)$$

which is equivalent to Eq. (3.2).

3. Energy Equation

Neglecting the radiation effect, the dimensional governing equation is given by

$$\rho^* C_p^* \frac{\partial T^*}{\partial t^*} + \rho^* C_p^* T_{,i}^* u_i^* - \frac{\partial P^*}{\partial t} - k^* T_{,ii}^* - \sum_{\alpha=1}^{n} w_\alpha^* h_\alpha^* = 0 \quad \text{(A.10)}$$

Substituting Eq. (3.6) yields

$$\rho_0^* C_p^* v_0^* T_0^* \frac{1}{\ell^*} \rho \frac{\partial T}{\partial t} + \rho_0^* C_p^* \frac{v_0^* T_0^*}{\ell^*} \rho T_{,i} u_i - \frac{P_0^* v_0^*}{\ell^*} \frac{\partial P}{\partial t}$$

$$- k^* \frac{T_0^*}{\ell^{*2}} T_{,ii} - \frac{\rho_0^* v_0^{*2}}{\alpha^*} C_p^* T_0^* \sum_\alpha w_\alpha h_\alpha = 0 \quad \text{(A.11)}$$

Dividing Eq. (A.11) by $\rho_0^* C_p^* v_0^* T_0^* / \ell^*$ gives

$$\rho \frac{\partial T}{\partial t} + \rho T_{,i} u_i - \frac{P_0^*}{\rho_0^* T_0^* C_p^*} \frac{\partial P}{\partial t} - T_{,ii} - \sum_\alpha w_\alpha h_\alpha = 0 \quad \text{(A.12)}$$

Since $P_0^* = \rho_0^* R T_0^*$,

$$\frac{P_0^*}{\rho_0^* T_0^* C_p^*} = \frac{R}{C_p^*} = 1 - \frac{C_v^*}{C_p^*} = \frac{\gamma - 1}{\gamma}$$

where $R = C_p^* - C_v^*$ and $\gamma = C_p^*/C_v^*$ are used. Therefore, the non-dimensional governing equation is of the form

$$\rho \frac{\partial T}{\partial t} + \rho T_{,i} u_i - \frac{\gamma - 1}{\gamma} \frac{\partial P}{\partial t} - T_{,ii} - wh = 0 \quad \text{(A.13)}$$

in which the last term is obtained from Eq. (A.30). Equation

(A.13) is equivalent to Eq. (3.3).

4. Species Equation

The dimensional governing equation is of the form

$$\rho^* \frac{\partial Y_\alpha}{\partial t^*} + \rho^* Y_{\alpha,i} u_i^* - \frac{k^*}{C_p^*} Y_{\alpha,ii} - w_\alpha^* = 0 \ , \quad \alpha = 1,2,\ldots,N \tag{A.14}$$

where N denotes the total number of species considered.

Substituting Eq. (3.6) yields

$$\rho_o^* \frac{v_o^*}{\ell^*} \rho \frac{\partial Y_\alpha}{\partial t} + \rho_o^* \frac{v_o^*}{\ell^*} \rho Y_{\alpha,i} u_i - \frac{k^*}{C_p^*} \frac{1}{\ell^{*2}} Y_{\alpha,ii} - \frac{\rho_o^* v_o^{*2}}{\alpha^*} w_\alpha = 0 \tag{A.15}$$

Dividing Eq. (A.15) by $\rho_o^* v_o^* / \ell^*$ gives the following

$$\rho \frac{\partial Y_\alpha}{\partial t} + \rho Y_{\alpha,i} u_i - \frac{k^*}{C_p^* \ell^* \rho_o^* v_o^*} Y_{\alpha,ii} - \frac{v_o^* \ell^*}{\alpha^*} w_\alpha = 0 \tag{A.16}$$

Since

$$\ell^* = \frac{\alpha^*}{v_o^*} = \frac{k^*}{\rho_o^* v_o^* C_p^*}$$

The coefficient of the third and the last terms are to be unity. Therefore,

$$\rho \frac{\partial Y_\alpha}{\partial t} + \rho Y_{\alpha,i} u_i - Y_{\alpha,ii} - \nu_\alpha w_\alpha = 0, \quad \alpha = f,o,p \tag{A.17}$$

where ν_α is defined by

$$\nu_\alpha = \frac{W_\alpha(\nu_\alpha'' - \nu_\alpha')}{W_f \nu_f'} \tag{A.18}$$

The three mass fraction equations for the fuel, oxidizer, and product in Eq. (A.17) are similar to one another, allowing treatment of the fuel equation alone with the following relation

$$\frac{Y_\alpha}{\nu_\alpha} - \frac{Y_f}{\nu_f} = \text{constant} \tag{A.19}$$

Therefore, Eq. (A.17) for the fuel only is enough to describe the whole system and is given as

$$\rho \frac{\partial Y_f}{\partial t} + \rho Y_{f,i} u_i - Y_{f,ii} + w_f = 0 \tag{A.20}$$

This is equivalent to Eq. (3.4).

5. Reaction Rate of Fuel Species

For a one-step forward chemical reaction,

$$\nu_f'[f] + \nu_o'[O] \rightarrow \nu_p''[P] \tag{A.21}$$

where ν denotes the stoichiometric coefficient, and f,o,p represent fuel, oxidizer, and product, respectively. Using the Arrhenius law, the reaction rate of the fuel can be expressed by

$$w^* = B^* T^{*\delta} \left(\frac{P^*}{RT^*} \right)^n \prod_{j=1}^{N} \left(\frac{Y_j}{W_j} \right)^{n_j} e^{-(E^*/RT^*)} \tag{A.22}$$

in which B^* is the frequency factor for the gas phase; R, the gas

constant; W_j, the molecular weight of the species; E^*, the activiation energy; and δ and n are constants. For the oxidizer and products, the reaction rate can be written as follows:

$$w_\alpha^* = \frac{\nu_\alpha'' - \nu_\alpha'}{\nu_f'} w^* \quad , \quad \alpha = o,p \tag{A.23}$$

The the last term of Eq. (A.12) becomes

$$- \Sigma\, w_\alpha^* h_\alpha^o = w^* h^* \tag{A.24}$$

where

$$h^* = \frac{\Sigma\, W_\alpha(\nu_\alpha' - \nu_\alpha'')h_\alpha^o}{W_f \nu_f'}$$

is the heat of combustion per unit mass of fuel consumed. Using the definition in Eq. (A.18),

$$\nu_\alpha = \frac{W_\alpha(\nu_\alpha'' - \nu_\alpha')}{W_f \nu_f'} \tag{A.25}$$

and the following relation in Eq. (A.19)

$$\frac{Y_\alpha}{\nu_\alpha} - \frac{Y_f}{\nu_f} = \text{constant} \tag{A.26}$$

the reaction rate term can be non-dimensionalized.

Since both the fuel and oxidizer must vanish at the flame edge,

$$\frac{Y_o}{\nu_o} - \frac{Y_f}{\nu_f} = 0 \tag{A.27}$$

Therefore,

$$Y_o = \frac{\nu_o}{\nu_f} Y_f \tag{A.28}$$

From Eq. (A.25), $\nu_f = -1$; thus,

$$Y_o = -\nu_o Y_f$$

or

$$Y_o = \frac{W_o \nu_o'}{W_f \nu_f} Y_f \tag{A.29}$$

The non-dimensional reaction rate can then be written as

$$w = BzT^{\delta}\left(\frac{P}{T}\right)^{n} Y_f{}^{n} e^{-E/T} \tag{A.30}$$

where

$$z = \frac{W_o \nu_o'}{W_f \nu_f'}$$

$$B = \frac{B^* k^* T_o{}^{*\delta} \rho_o{}^{*n}}{\rho_o{}^{*2} v_o{}^{*2} C_p \prod_{j=1}^{N} W_j{}^{n_j}}$$

$$E = \frac{E^*}{RT_o{}^*}$$

and this is equivalent to Eq. (3.7).

6. Heat Transfer Equation in Solid Phase

The dimensional governing equation is given as

$$\rho_s^* c_s^* \frac{\partial T_s^*}{\partial t^*} + \rho_s^* c_s^* T_{s,i}^* u_i^* - k_s^* T_{s,ii}^* = 0 \qquad \text{(A.31)}$$

with c_s^* and k_s^* being the specific heat and the thermal conductivity of the propellant, respectively, and $y = 0$ is attached to the surface. Substituting Eq. (3.6) yields

$$\rho_s^* c_s^* T_0^* \frac{v_0^*}{\ell^*} \frac{\partial T_s}{\partial t} + \rho_s^* c_s^* \frac{T_0^*}{\ell^*} v_0^* T_{s,i} u_i - k_s^* \frac{T_0^{*2}}{\ell^{*2}} T_{s,ii} = 0 \qquad \text{(A.32)}$$

Dividing Eq. (A.32) by $\rho_0^* c_s^* T_0^* v_0^* / \ell^*$ results in

$$\beta \frac{\partial T_s}{\partial t} + \beta T_{s,i} u_i - \frac{k_s^* T_0^*}{\rho_0^* c_s^* v_0^* \ell^*} T_{s,ii} = 0 \qquad \text{(A.33)}$$

Since $\ell^* = k^*/\rho_0^* v_0^* C_p^*$, the last term can be written as

$$\frac{k_s^* T_0^*}{\rho_0^* c_s^* v_0^* \ell^*} = \frac{k_s^* C_p^*}{k^* c_s^*} \equiv \zeta \qquad \text{(A.34)}$$

Therefore, Eq. (A.33) becomes

$$\beta \frac{\partial T_s}{\partial t} + \beta T_{s,i} u_i - \zeta T_{s,ii} = 0 \qquad \text{(A.35)}$$

In the one-dimensional case, since $\rho_0^* v_0^* = \rho_s^* \bar{r}^*$ if r is defined by $r = r^*/\bar{r}^*$ (actually r^* is the same as u_i^* in Eq. (A.31)), then

$$\beta \frac{\partial T_s}{\partial t} + r \frac{\partial T_s}{\partial y} - \zeta \frac{\partial^2 T_s}{\partial y^2} = 0 \qquad \text{(A.36)}$$

which is equivalent to Eq. (3.8).

7. Solid-Gas Interface Boundary Condition

The surface energy balance across the interface can be expressed as follows:

$$-k^*\left(\frac{\partial T^*}{\partial y^*}\right)_+ + \rho^* v^* H_+^* = -k_s^*\left(\frac{\partial T^*}{\partial y^*}\right)_- + \rho_s^* r^* H_-^* \qquad (A.37)$$

with subscripts + and - being used to indicate the gas and solid side of the interface, respectively, and H^* denotes the enthalpy. Using Eq. (3.6) and defining $\xi = k/k_s^*$ and $L = (H_+^* - H_-^*)/C_p^* T_0^*$ yield

$$-k^* \frac{T_0^*}{\ell^*}\left(\frac{\partial T}{\partial y}\right)_+ + \rho_s^* \bar{r}^* C_p^* T_0^* rL = -k_s^* \frac{T_0^*}{\ell^*}\left(\frac{\partial T}{\partial y}\right)_-$$

or

$$-\frac{k^*}{k_s^*}\left(\frac{\partial T}{\partial y}\right)_+ + \frac{\rho_s^* \bar{r}^* C_p^* \ell^*}{k_s^*} rL = -\left(\frac{\partial T}{\partial y}\right)_- \qquad (A.38)$$

Since $\rho_s^* \bar{r}^* = \rho_0^* v_0^*$ and $\ell^* = k^*/\rho_0^* v_0^* C_p^*$, then

$$-\xi\left(\frac{\partial T}{\partial y}\right)_+ + \xi rL = -\left(\frac{\partial T}{\partial y}\right)_-$$

or

$$\left(\frac{\partial T}{\partial y}\right)_+ = \frac{1}{\xi}\left(\frac{\partial T}{\partial y}\right)_- + rL \qquad (A.39)$$

which is equivalent to Eq. (3.10).

APPENDIX B

PERTURBATION OF MODEL EQUATIONS

1. Perturbation of Reaction Rate

The dimensionless reaction rate equation is given by Eq. (3.7). After taking $\delta = 0$ and $n = 2$, we have

$$w^{(0)} + \epsilon\hat{w}^{(1)} + \epsilon^2\hat{w}^{(2)} = Bz[P^{(0)} + \epsilon\hat{P}^{(1)} + \epsilon^2\hat{P}^{(2)}]^2[T^{(0)} + \epsilon\hat{T}^{(1)} + \epsilon^2\hat{T}^{(2)}]^{-2}[Y^{(0)} + \epsilon\hat{Y}^{(1)} + \epsilon^2\hat{Y}^{(2)}]\exp\left[-\frac{E}{T^{(0)}}\left(1 + \epsilon\frac{\hat{T}^{(1)}}{T^{(0)}} + \epsilon^2\frac{\hat{T}^{(2)}}{T^{(0)}}\right)^{-1}\right]$$

$$= Bz\left(\frac{P^{(0)}}{T^{(0)}}\right)^2 Y^{(0)2}e^{-E/T^{(0)}}\left[1 + \epsilon\frac{2\hat{P}^{(1)}}{P^{(0)}} + \epsilon^2\left(\frac{2\hat{P}^{(2)}}{P^{(0)}} + \frac{\hat{P}^{(1)2}}{P^{(0)2}}\right) + O(\epsilon^3)\right]\left[1 - \epsilon\frac{2\hat{T}^{(1)}}{T^{(0)}} - \epsilon^2\left(\frac{2\hat{T}^{(2)}}{T^{(0)}} - \frac{3\hat{T}^{(1)2}}{T^{(0)2}}\right) + O(\epsilon^3)\right]\left[1 + \epsilon\frac{2\hat{Y}^{(1)}}{Y^{(0)}} + \epsilon^2\left(\frac{2\hat{Y}^{(2)}}{Y^{(0)}} + \frac{\hat{Y}^{(1)2}}{Y^{(0)2}}\right) + O(\epsilon^3)\right]\exp\left[\frac{E}{T^{(0)}}\left\{\epsilon\frac{\hat{T}^{(1)}}{T^{(0)}} + \epsilon^2\left(\frac{\hat{T}^{(2)}}{T^{(0)}} - \frac{\hat{T}^{(1)2}}{T^{(0)2}}\right) + O(\epsilon^3)\right\}\right]$$

$$= w^{(0)}[1 - 2\epsilon T_1' - \epsilon^2(2T_2' - 3T_1'^2) + 2\epsilon P_1' + \epsilon^2(2P_2' + P_1'^2) - 4\epsilon^2 T_1'P_1'][1 + 2\epsilon Y_1' + \epsilon^2(2Y_2' + Y_1'^2)]\left[1 + \epsilon\frac{E}{T^{(0)}}T_1' + \frac{1}{2}\epsilon^2\left(\frac{E}{T^{(0)}}\right)^2 T_1'^2\right]\left[1 + \epsilon^2\frac{E}{T^{(0)}}(T_2' - T_1'^2)\right]$$

$$= w^{(0)}[1 + \epsilon(-2T_1' + 2P_1') + \epsilon^2(-2T_2' + 3T_1'^2 + 2P_2'$$

$$+ P_1'^2 - 4T_1'P_1')][1 + 2\epsilon Y_1' + \epsilon^2(2Y_2' + Y_1'^2)]\left[1 + \epsilon\frac{E}{T^{(0)}}T_1' + \frac{1}{2}\epsilon^2\left(\frac{E}{T^{(0)}}\right)^2 T_1'^2 + \epsilon^2\frac{E}{T^{(0)}}(T_2' - T_1'^2)\right]$$

$$= w^{(0)}\left[1 + \epsilon(-2T_1' + 2P_1') + \epsilon^2(-2T_2' + 3T_1'^2 + 2P_2' + P_1'^2 - 4T_1'P_1') + \epsilon\left(2Y_1' + \frac{E}{T^{(0)}}T_1'\right) + \epsilon^2\left(2Y_1' + \frac{E}{T^{(0)}}T_1'\right)(-2T_1' + 2P_1') + 2\epsilon^2\frac{E}{T^{(0)}}Y_1'T_1' + \epsilon^2(2Y_2' + Y_1'^2) + \frac{1}{2}\epsilon^2\left(\frac{E}{T^{(0)}}\right)^2 T_1'^2 + \epsilon^2\frac{E}{T^{(0)}}(T_2' - T_1'^2)\right]$$

$$= w^{(0)}\left[1 + \epsilon\left(-2T_1' + 2P_1' + 2Y_1' + \frac{E}{T^{(0)}}T_1'\right) + \epsilon^2(-2T_2' + 3T_1'^2 + 2P_2' + P_1'^2 - 4T_1'P_1' - 4Y_1'T_1' + 4Y_1'P_1' - \frac{2E}{T^{(0)}}T_1'^2 + \frac{2E}{T^{(0)}}T_1'P_1' + \frac{2E}{T^{(0)}}Y_1'T_1' + 2Y_2' + Y_1'^2 + \frac{1}{2}\left(\frac{E}{T^{(0)}}\right)^2 T_1'^2 + \frac{E}{T^{(0)}}T_2' - \frac{E}{T^{(0)}}T_1'^2\right)\right] \qquad (B.1)$$

where $F_1' = \hat{F}^{(1)}/F^{(0)}$ and $F_2' = \hat{F}^{(2)}/F^{(0)}$ are used. Therefore,

$$w^{(0)} = Bz\left(\frac{P^{(0)}}{T^{(0)}}\right)^2 Y^{(0)2}e^{-E/T^{(0)}} \qquad (B.2)$$

$$\hat{w}^{(1)} = w^{(0)}\left[\left(\frac{E}{T^{(0)}} - 2\right)\frac{\hat{T}^{(1)}}{T^{(0)}} + \frac{2\hat{Y}^{(1)}}{Y^{(0)}} + \frac{2\hat{P}^{(1)}}{P^{(0)}}\right] \qquad (B.3)$$

$$\hat{w}^{(2)} = w^{(0)}\left[\left(\frac{E}{T^{(0)}} - 2\right)\frac{\hat{T}^{(2)}}{T^{(0)}} + \frac{2\hat{Y}^{(2)}}{Y^{(0)}} + \frac{2\hat{P}^{(2)}}{P^{(0)}} + 3\left(1 - \frac{E}{T^{(0)}}\right.\right.$$

$$+ \frac{E^2}{6T^{(0)2}} \Bigg) \frac{\hat{T}^{(1)2}}{T^{(0)2}} + \frac{\hat{Y}^{(1)2}}{Y^{(0)2}} + \frac{\hat{P}^{(1)2}}{P^{(0)2}} + \left(\frac{2E}{T^{(0)}} - 4 \right) \frac{\hat{T}^{(1)}}{T^{(0)}} \frac{\hat{P}^{(1)}}{P^{(0)}}$$

$$+ \left(\frac{2E}{T^{(0)}} - 4 \right) \frac{\hat{T}^{(1)}}{T^{(0)}} \frac{\hat{Y}^{(1)}}{Y^{(0)}} + 4 \frac{\hat{P}^{(1)}}{P^{(0)}} \frac{\hat{Y}^{(1)}}{Y^{(0)}} \Bigg] \qquad \text{(B.4)}$$

Since

$$\hat{P}^{(1)} = \rho^{(0)}\hat{T}^{(1)} + \hat{\rho}^{(1)}T^{(0)} = \frac{\hat{T}^{(1)}}{T^{(0)}} + \hat{\rho}^{(1)}T^{(0)}$$

and $$\qquad \text{(B.5)}$$

$$\hat{P}^{(2)} = \rho^{(0)}\hat{T}^{(2)} + \hat{\rho}^{(1)}\hat{T}^{(1)} + \hat{\rho}^{(2)}T^{(0)}$$

$$= \frac{\hat{T}^{(2)}}{T^{(0)}} + \hat{\rho}^{(1)}\hat{T}^{(1)} + \hat{\rho}^{(2)}T^{(0)}$$

we have another form of the reaction rate such that

$$\hat{w}^{(1)} = w^{(0)} \left[\frac{2}{\rho^{(0)}} \hat{\rho}^{(1)} + \frac{E}{T^{(0)2}} \hat{T}^{(1)} + \frac{2}{Y^{(0)}} \hat{Y}^{(1)} \right] \qquad \text{(B.6)}$$

$$\hat{w}^{(2)} = w^{(0)} \Bigg[\frac{2}{\rho^{(0)}} \hat{\rho}^{(2)} + \frac{E}{T^{(0)2}} \hat{T}^{(2)} + \frac{2}{Y^{(0)}} \hat{Y}^{(2)} + \frac{\hat{\rho}^{(1)2}}{\rho^{(0)2}}$$

$$+ \frac{E}{T^{(0)}} \left(\frac{E}{2T^{(0)}} - 1 \right) \frac{\hat{T}^{(1)2}}{T^{(0)2}} + \frac{\hat{Y}^{(1)2}}{Y^{(0)2}} + \frac{2E}{T^{(0)}} \frac{\hat{\rho}^{(1)}}{\rho^{(0)}} \frac{\hat{T}^{(1)}}{T^{(0)}}$$

$$+ 4 \frac{\hat{\rho}^{(1)}}{\rho^{(0)}} \frac{\hat{Y}^{(1)}}{Y^{(0)}} + \frac{2E}{T^{(0)}} \frac{\hat{T}^{(1)}}{T^{(0)}} \frac{\hat{Y}^{(1)}}{Y^{(0)}} \Bigg] \qquad \text{(B.7)}$$

If we substitute $T^{(0)}$ for $1/\rho^{(0)}$ and $(1/h)(1 - T^{(0)})$ for $Y^{(0)}$, then

$$\hat{w}^{(1)} = w^{(0)} \left[2T^{(0)}\hat{\rho}^{(1)} + \frac{E}{T^{(0)2}} \hat{T}^{(1)} + \frac{2h}{1 - T^{(0)}} \hat{Y}^{(1)} \right] \qquad \text{(B.8)}$$

$$\hat{w}^{(2)} = w^{(0)}\Bigg[2T^{(0)}\hat{\rho}^{(2)} + \frac{E}{T^{(0)2}}\hat{T}^{(2)} + \frac{2h}{1 - T^{(0)}}\hat{Y}^{(2)} + T^{(0)2}\hat{\rho}^{(1)2} + \frac{E}{T^{(0)3}}\left(\frac{E}{2T^{(0)}} - 1\right)\hat{T}^{(1)2} + \frac{h^2}{(1 - T^{(0)})^2}\hat{Y}^{(1)2} + \frac{2E}{T^{(0)}}\hat{\rho}^{(1)}\hat{T}^{(1)} + \frac{4hT^{(0)}}{1-T^{(0)}}\hat{\rho}^{(1)}\hat{Y}^{(1)} + \frac{2hE}{(1-T^{(0)})T^{(0)2}}\hat{T}^{(1)}\hat{Y}^{(1)}\Bigg] \tag{B.9}$$

Combining Eqs. (B.6) and (B.7) yields Eq. (3.33).

2. Perturbation of Burning Rate

From Eq. (3.9), the burning rate r can be perturbed in the form

$$r^{(0)} + \epsilon\hat{r}^{(1)} + \epsilon^2\hat{r}^{(2)} = \exp[-E_s(T_s^{(0)} + \epsilon\hat{T}_s^{(1)} + \epsilon^2\hat{T}_s^{(2)})^{-1}]e^{E_s/\bar{T}_s} = e^{E_s/\bar{T}_s}\exp\Bigg[\frac{-E_s}{T_s^{(0)}}\Bigg\{1 - \epsilon\frac{\hat{T}_s^{(1)}}{T_s^{(0)}} - \epsilon^2\left(\frac{\hat{T}_s^{(2)}}{T_s^{(0)}} - \frac{\hat{T}_s^{(1)2}}{T_s^{(0)2}}\right)\Bigg\}\Bigg]$$

$$= e^{E_s/\bar{T}_s}\, e^{-E_s/T_s^{(0)}}\exp\left[\frac{E_s}{T_s^{(0)}}\epsilon\frac{\hat{T}_s^{(1)}}{T_s^{(0)}}\right]\exp\left[\frac{E_s}{T_s^{(0)}}\epsilon^2\left(\frac{\hat{T}_s^{(2)}}{T_s^{(0)}} - \frac{\hat{T}_s^{(1)2}}{T_s^{(0)2}}\right)\right] = e^{E_s/\bar{T}_s}\, e^{-E_s/T_s^{(0)}}\Bigg[1 + \epsilon\frac{E_s}{T_s^{(0)}}\frac{\hat{T}_s^{(1)}}{T_s^{(0)}} + \epsilon^2\left\{\frac{E_s}{T_s^{(0)}}\left(\frac{\hat{T}_s^{(2)}}{T_s^{(0)}} - \frac{\hat{T}_s^{(1)2}}{T_s^{(0)2}}\right) + \frac{1}{2}\left(\frac{E_s}{T_s^{(0)}}\frac{\hat{T}_s^{(1)}}{T_s^{(0)}}\right)^2\right\} + O(\epsilon^3)\Bigg] \tag{B.10}$$

Therefore,

$$r^{(0)} = \exp\left[-E_s\left(\frac{1}{T_s^{(0)}} - \frac{1}{\bar{T}_s}\right)\right] = 1 \tag{B.11}$$

where $T_s^{(0)} = \bar{T}_s$ at $y = 0$ is used,

$$\hat{r}^{(1)} = r^{(0)} \frac{E_s}{T_s^{(0)2}} \hat{T}_s^{(1)} = r^{(0)} c_1 \hat{T}_s^{(1)} \tag{B.12}$$

$$\hat{r}^{(2)} = r^{(0)} \frac{E_s}{T_s^{(0)2}} \left(\hat{T}_s^{(2)} - \frac{\hat{T}_s^{(1)2}}{T_s^{(0)}} + \frac{E_s}{2T_s^{(0)2}} \hat{T}_s^{(1)2} \right)$$

$$= r^{(0)} c_1 \left\{ \hat{T}_s^{(2)} + \left(\frac{c_1}{2} - \frac{1}{\bar{T}_s} \right) \hat{T}_s^{(1)2} \right\} \tag{B.13}$$

Combining Eqs. (B.12) and (B.13) yields Eq. (3.36).

APPENDIX C

DERIVATIONS OF BOUNDARY CONDITIONS

1. Temperature Condition at Interface

(a) First Order Condition

The first order solid phase energy equation (3.35) is rewritten as

$$i\omega\beta\tau + r^{(0)} \frac{\partial \tau}{\partial y} + \hat{r}^{(1)} \frac{\partial T_s^{(0)}}{\partial y} - \zeta \frac{\partial^2 \tau}{\partial y^2} = 0 \qquad (C.1)$$

where τ denotes $\hat{T}_s^{(1)}$ for convenience. Knowing that $r^{(0)} = 1$ and $\partial T_s^{(0)}/\partial y = (1/\zeta)(\bar{T}_s - T_c)e^{Y/\zeta}$ from Eq. (3.25), we have

$$\zeta \frac{\partial^2 \tau}{\partial y^2} - \frac{d\tau}{dy} - iI\omega\beta\tau = c_2 \hat{r}^{(1)} e^{Y/\zeta} \qquad (C.2)$$

in which

$$c_2 = \frac{1}{\zeta} (\bar{T}_s - T_c)$$

The general solution of Eq. (C.2) has the form

$$\tau = \tau_h + \tau_p \qquad (C.3)$$

with subscripts h and p denoting homogeneous and particular solution, respectively. The characteristic equation is then given by

$$\zeta\lambda^2 - \lambda - i\omega\beta = 0 \qquad (C.4)$$

Thus,

$$\lambda_1 = \frac{1}{2\zeta}\left(1 + \sqrt{1 + 4i\omega\beta\zeta}\right)$$
$$\lambda_1' = \frac{1}{2\zeta}\left(1 - \sqrt{1 - 4i\omega\beta\zeta}\right) \tag{C.5}$$

which gives the homogeneous solution such as

$$\tau_h = A_0 e^{\lambda_1 y} \tag{C.6}$$

where $\tau_h \to 0$ at deep in solid ($y \to -\infty$) is considered.

The particular solution τ_p is of the form

$$\tau_p = A_1 e^{y/\zeta} \tag{C.7}$$

Since $\partial\tau_p/\partial y = (1/\zeta)\tau_p$ and $\partial^2\tau_p/\partial y^2 = (1/\zeta^2)\tau_p$, we have

$$A_1 = -\frac{\hat{r}^{(1)} c_2}{i\omega\beta} \tag{C.8}$$

Therefore, from Eqs. (C.3), (C.6), (C.7), and (C.8), τ is given by

$$\tau = A_0 e^{\lambda_1 y} - \frac{\hat{r}^{(1)} c_2}{i\omega\beta} e^{y/\zeta} \tag{C.9}$$

From the fact that $\tau = \tau_s$ at $y = 0$,

$$A_0 = \tau_s + \frac{\hat{r}^{(1)} c_2}{i\omega\beta} \tag{C.10}$$

which yields

$$\tau = \left(\tau_s + \frac{\hat{r}^{(1)} c_2}{i\omega\beta} \right) e^{\lambda_1 y} - \frac{\hat{r}^{(1)} c_2}{i\omega\beta} e^{y/\zeta} \tag{C.11}$$

and

$$\frac{\partial \tau}{\partial y} = \lambda_1 \left(\tau_s + \frac{\hat{r}^{(1)} c_2}{i\omega\beta} \right) e^{\lambda_1 y} - \frac{\hat{r}^{(1)} c_2}{i\omega\beta\zeta} e^{y/\zeta} \tag{C.12}$$

At $y = 0$,

$$\left. \frac{\partial \tau}{\partial y} \right|_{y=0} = \lambda_1 \left(\tau_s + \frac{\hat{r}^{(1)} c_2}{i\omega\beta} \right) - \frac{\hat{r}^{(1)} c_2}{i\omega\beta\zeta} \tag{C.13}$$

Substituting Eq. (C.13) into Eq. (3.10) yields

$$\begin{aligned} \left(\frac{\partial \hat{T}^{(1)}}{\partial y} \right)_+ &= \frac{1}{\xi} \left(\frac{\partial \tau}{\partial y} \right)_{y=0} + \hat{r}^{(1)} L \\ &= \frac{\lambda_1}{\xi} \left(\hat{T}_s{}^{(1)} + \frac{\hat{r}^{(1)} c_2}{i\omega\beta} \right) - \frac{\hat{r}^{(1)} c_2}{i\omega\beta\zeta\xi} + \hat{r}^{(1)} L \\ &= \frac{\lambda_1}{\xi} \left(\hat{T}_s{}^{(1)} + \frac{c_1 c_2}{i\omega\beta} \hat{T}_s{}^{(1)} \right) - \frac{c_1 c_2}{i\omega\beta\zeta\xi} \hat{T}_s{}^{(1)} + c_1 L \hat{T}_s{}^{(1)} \end{aligned} \tag{C.14}$$

where $\hat{r}^{(1)} = r^{(0)} (E_s / \bar{T}_c{}^2) \hat{T}_s{}^{(1)} = c_1 \hat{T}_s{}^{(1)}$ is used. Therefore,

$$\hat{T}_+{}^{(1)} = \frac{\left(\frac{\partial \hat{T}^{(1)}}{\partial y} \right)_+}{\left[\frac{\lambda_1}{\xi} \left(1 + \frac{c_1 c_2}{i\omega\beta} \right) - \frac{c_1 c_2}{i\omega\beta\zeta\xi} + c_1 L \right]} \tag{C.15}$$

(b) Second Order Condition

The second order solid phase energy equation is rewritten as

$$i2\omega\beta\tau + r^{(0)} \frac{\partial \tau}{\partial y} + \hat{r}^{(2)} \frac{\partial T_s^{(0)}}{\partial y} - \zeta \frac{\partial^2 \tau}{\partial y^2} = -\hat{r}^{(1)} \frac{\partial \hat{T}_s^{(1)}}{\partial y}$$

or

$$\zeta \frac{\partial^2 \tau}{\partial y^2} - \frac{\partial \tau}{\partial y} - i2\omega\beta\tau = \hat{r}^{(1)} \frac{\partial \hat{T}_s^{(1)}}{\partial y} + \hat{r}^{(2)} \frac{\partial T_s^{(0)}}{\partial y} \qquad (C.16)$$

With the same argument of the first order solution, the characteristic equation is given by

$$\zeta\lambda^2 - \lambda - i2\omega\beta = 0 \qquad (C.17)$$

of which solution is

$$\lambda_2 = \frac{1}{2\zeta} \left(1 + \sqrt{1 + 8i\omega\beta\zeta}\right)$$
$$\lambda_2' = \frac{1}{2\zeta} \left(1 - \sqrt{1 - 8i\omega\beta\zeta}\right) \qquad (C.18)$$

Therefore, the homogeneous solution is

$$\tau_h = B_0 e^{\lambda_2 Y} \qquad (C.19)$$

Substituting Eq. (C.11) into Eq. (C.16) yields the particular solution to be of the form

$$\tau_p = B_1 e^{\lambda_1 Y} + B_2 e^{Y/\zeta} \qquad (C.20)$$

Since

$$\frac{\partial \tau_p}{\partial y} = \lambda_1 B_1 e^{\lambda_1 Y} + \frac{B_2}{\zeta} e^{Y/\zeta}$$

and

$$\frac{\partial^2 \tau_p}{\partial y^2} = \lambda_1^2 B_1 e^{\lambda_1 Y} + \frac{B_2}{\zeta^2} e^{Y/\zeta}$$

we have, from Eq. (C.16), the following equations:

For the coefficient of the $e^{\lambda_1 Y}$ term,

$$i2\omega\beta B_1 + \lambda_1 B_1 + F - \zeta\lambda_1^2 B_1 = 0 \qquad \text{(C.21)}$$

where

$$F = \hat{r}^{(1)} \lambda_1 \left(\hat{T}_s^{(1)} + \frac{\hat{r}^{(1)} C_2}{i\omega\beta} \right)$$

For the coefficient of the $e^{Y/\zeta}$ term,

$$i2\omega\beta B_2 + \frac{B_2}{\zeta} + \hat{r}^{(2)} C_2 - \frac{\zeta}{\zeta^2} B_2 - \frac{\hat{r}^{(1)2} C_2}{i\omega\beta\zeta} = 0 \qquad \text{(C.22)}$$

Thus,

$$B_1 = \frac{F}{\zeta\lambda_1^2 - \lambda_1 - i2\omega\beta}$$

$$B_2 = \frac{-\hat{r}^{(2)} C_2 + \hat{r}^{(1)2} C_2 / i\omega\beta\zeta}{i2\omega\beta} \qquad \text{(C.23)}$$

and

$$\tau = \tau_h + \tau_p = B_0 e^{\lambda_2 Y} + \frac{F}{\zeta\lambda_1^2 - \lambda_1 - i2\omega\beta} e^{\lambda_1 Y} + \frac{-\hat{r}^{(2)}c_2 + \hat{r}^{(1)2}c_2/i\omega\beta\zeta}{i2\omega\beta} \tag{C.24}$$

Since $\tau = \tau_s$ at $y = 0$, then

$$B_0 = \tau_s - \frac{F}{\zeta\lambda_1^2 - \lambda_1 - i2\omega\beta} - \frac{-\hat{r}^{(2)}c_2 + \hat{r}^{(1)2}c_2/i\omega\beta\zeta}{i2\omega\beta} \tag{C.25}$$

which yields

$$\tau = \left(\tau_s - \frac{F}{\zeta\lambda_1^2 - \lambda_1 - i2\omega\beta} - \frac{-\hat{r}^{(2)}c_2 + \hat{r}^{(1)2}c_2/i\omega\beta\zeta}{i2\omega\beta}\right) e^{\lambda_2 Y} + \frac{F}{\zeta\lambda_1^2 - \lambda_1 - i2\omega\beta} e^{\lambda_1 Y} + \frac{-\hat{r}^{(2)}c_2 + \hat{r}^{(1)2}c_2/i\omega\beta\zeta}{i2\omega\beta} e^{Y/\zeta} \tag{C.26}$$

and

$$\frac{\partial\tau}{\partial y} = \lambda_2\left(\tau_s - \frac{F}{\zeta\lambda_1^2 - \lambda_1 - i2\omega\beta} - \frac{-\hat{r}^{(2)}c_2 + \hat{r}^{(1)2}c_2/i\omega\beta\zeta}{i2\omega\beta}\right) e^{\lambda_2 Y} + \frac{\lambda_1 F}{\zeta\lambda_1^2 - \lambda_1 - i2\omega\beta} e^{\lambda_1 Y} + \frac{-\hat{r}^{(2)}c_2 + \hat{r}^{(1)2}c_2/i\omega\beta\zeta}{i2\omega\beta\zeta} e^{Y/\zeta} \tag{C.27}$$

Substituting Eq. (C.27) into Eq. (3.10) yields

$$\left(\frac{\partial\hat{T}^{(2)}}{\partial y}\right)_+ = \frac{1}{\xi}\left(\frac{\partial\tau}{\partial y}\right)_{y=0} + \hat{r}^{(2)}L$$

$$= \frac{\lambda_2}{\xi}\left(\hat{T}_s{}^{(2)} - \frac{F}{\zeta\lambda_1^2 - \lambda_1 - i2\omega\beta} + \frac{\hat{r}^{(2)}c_2 - \hat{r}^{(1)2}c_2/i\omega\beta\zeta}{i2\omega\beta}\right)$$

$$+ \frac{1}{\xi} \frac{\lambda_1 F}{\zeta\lambda_1^2 - \lambda_1 - i2\omega\beta} - \frac{\hat{r}^{(2)}c_2 - \hat{r}^{(1)2}c_2/i\omega\beta\zeta}{i2\omega\beta\zeta\xi} + \hat{r}^{(2)}L \tag{C.28}$$

Since

$$\hat{r}^{(2)} = \frac{E_s}{\bar{T}_s^2}\left[\hat{T}_s^{(2)} + \frac{1}{\bar{T}_s}\left(\frac{1}{2}\frac{E_s}{\bar{T}_s} - 1\right)\hat{T}_s^{(1)2}\right.$$

$$= c_1\left[\hat{T}_s^{(2)} + \left(\frac{c_1}{2} - \frac{1}{\bar{T}_s}\right)\hat{T}_s^{(1)2}\right]$$

$$\left(\frac{\partial\hat{T}^{(2)}}{\partial y}\right)_+ = \frac{\lambda_2}{\xi}\left[\hat{T}_s^{(2)} - \frac{F}{\zeta\lambda_1^2 - \lambda_1 - i2\omega\beta} + \frac{c_1c_2\hat{T}_s^{(2)}}{i2\omega\beta}\right.$$

$$+ \frac{c_1c_2\left(\frac{c_1}{2} - \frac{1}{\bar{T}_s}\right)}{i2\omega\beta}\hat{T}_s^{(1)2} + \left.\frac{\hat{r}^{(1)2}c_2}{2\omega^2\beta^2\zeta}\right] + \frac{1}{\xi}\frac{\lambda_1 F}{\zeta\lambda_1^2 - \lambda_1 - i2\omega\beta}$$

$$- \frac{c_1c_2\hat{T}_s^{(2)}}{i2\omega\beta\zeta\xi} - \frac{c_1c_2\left(\frac{c_1}{2} - \frac{1}{\bar{T}_s}\right)}{i2\omega\beta\zeta\xi}\hat{T}_s^{(1)2} - \frac{\hat{r}^{(1)2}c_2}{2\omega^2\beta^2\zeta^2\xi}$$

$$+ c_1\left[\hat{T}_s^{(2)} + \left(\frac{c_1}{2} - \frac{1}{\bar{T}_s}\right)\hat{T}_s^{(1)2}\right]L \tag{C.29}$$

Therefore,

$$\hat{T}_+^{(2)} = \left[\left(\frac{\partial\hat{T}^{(2)}}{\partial y}\right)_+ + \frac{\lambda_2 F}{\xi(\zeta\lambda_1^2 - \lambda_1 - i2\omega\beta)} - \frac{\lambda_2 c_1 c_2\left(\frac{c_1}{2} - \frac{1}{\bar{T}_s}\right)}{i2\omega\beta\xi}\hat{T}_s^{(1)2}\right.$$

$$- \frac{\lambda_2\hat{r}^{(1)2}c_2}{2\omega^2\beta^2\zeta\xi} - \frac{\lambda_1 F}{\xi(\zeta\lambda_1^2 - \lambda_1 - i2\omega\beta)} + \left.\frac{c_1c_2\left(\frac{c_1}{2} - \frac{1}{\bar{T}_s}\right)}{i2\omega\beta\zeta\xi}\hat{T}_s^{(1)2}\right.$$

$$+ \frac{\hat{r}^{(1)2}c_2}{2\omega^2\beta^2\zeta^2\xi} - c_1\left(\frac{c_1}{2} - \frac{1}{\bar{T}_s}\right)\hat{T}_s{}^{(1)2}L\Bigg]\Bigg[\frac{\lambda_2}{\xi}\left(1 + \frac{c_1c_2}{i2\omega\beta}\right) - \frac{c_1c_2}{i2\omega\beta\zeta\xi} + c_1L\Bigg]^{-1}$$

$$= \Bigg[\left(\frac{\partial\hat{T}^{(2)}}{\partial y}\right)_+ + \frac{c_3c_2}{i2\omega\beta\xi}\left(-\lambda_2 + \frac{1}{\zeta}\right) + \frac{1}{\xi}\frac{(\lambda_2 - \lambda_1)F}{(\zeta\lambda_1{}^2 - \lambda_1 - i2\omega\beta)}$$

$$+ \frac{1}{\xi}\cdot\frac{-c_2\hat{r}^{(1)2}}{2\omega^2\beta^2\zeta}\left(\lambda_2 - \frac{1}{\zeta}\right) - c_3L\Bigg]\Bigg[\frac{\lambda_2}{\xi}\left(1 + \frac{c_1c_2}{i2\omega\beta}\right) - \frac{c_1c_2}{i2\omega\beta\zeta\xi} + c_1L\Bigg]^{-1}$$

$$= \Bigg[\left(\frac{\partial\hat{T}^{(2)}}{\partial y}\right)_+ + \frac{c_3c_2}{i2\omega\beta\xi}\left(-\lambda_2 + \frac{1}{\zeta}\right) + \frac{1}{\xi}\left(\lambda_2c_4 + c_5 - \frac{c_4}{\zeta}\right)$$

$$- c_3L\Bigg]\Bigg[\frac{\lambda_2}{\xi}\left(1 + \frac{c_1c_2}{i2\omega\beta}\right) - \frac{c_1c_2}{i2\omega\beta\zeta\xi} + c_1L\Bigg]^{-1}$$

$$= \Bigg[\left(\frac{\partial\hat{T}^{(2)}}{\partial y}\right)_+ + G_9\Bigg]\Bigg[\frac{\lambda_2}{\xi}\left(1 + \frac{c_1c_2}{i2\omega\beta}\right) - \frac{c_1c_2}{i2\omega\beta\zeta\xi} + c_1L\Bigg]^{-1} \qquad \text{(C.30)}$$

where

$$c_3 = c_1\left(\frac{c_1}{2} - \frac{1}{\bar{T}_s}\right)\hat{T}^{(1)2}$$

$$c_4 = -\frac{c_2\hat{r}^{(1)2}}{2\omega^2\beta^2\zeta}$$

$$c_5 = \frac{\lambda_1(\lambda_2 - \lambda_1)}{(\zeta\lambda_1{}^2 - \lambda_1 - i2\omega\beta)}\hat{r}^{(1)}\left(\hat{T}_s{}^{(1)} + \frac{c_2\hat{r}^{(1)}}{i\omega\beta}\right)$$

$$= \frac{(\lambda_2 - \lambda_1)F}{(\zeta\lambda_1{}^2 - \lambda_1 - i2\omega\beta)}$$

and

$$G_9 = \frac{c_3c_2}{i2\omega\beta\xi}\left(-\lambda_2 + \frac{1}{\zeta}\right) + \frac{1}{\xi}\left(\lambda_2c_4 + c_5 - \frac{c_4}{\zeta}\right) - c_3L$$

are used. Combining Eqs. (C.15) and (C.30) yields Eq. (3.37).

Note that for the time dependent condition, the term $\hat{T}_s^{(1)2}$ has to be substituted by half of its value as indicated in Eq. (3.13).

If the second order time independent solution is required, then the boundary equation is different from the previous one and it is given as follows: From Eq. (3.35),

$$\hat{r}^{(0)} \frac{\partial \tau}{\partial y} + \hat{r}^{(2)} \frac{\partial T_s^{(0)}}{\partial y} - \zeta \frac{\partial^2 \tau}{\partial y^2} = -\hat{r}^{(1)} \frac{\partial \hat{T}_s^{(1)}}{\partial y} \tag{C.31}$$

The characteristic equation in this case is given by

$$\lambda(1 - \zeta\lambda) = 0 \tag{C.32}$$

Therefore, the homogeneous solution is of the form

$$\tau_h = D_0 + D_1 e^{Y/\zeta} \tag{C.33}$$

and the particular solution is

$$\tau_p = D_2 e^{\lambda_1 Y} + D_3 y e^{Y/\zeta} \tag{C.34}$$

Substituting Eq. (C.34) into Eq. (C.31) and investigating the coefficients gives the following relationships, i.e.,

$$\begin{aligned} D_2 &= \frac{F}{\zeta\lambda_1^2 - \lambda_1} \\ D_3 &= \hat{r}^{(2)} C_2 - \frac{\hat{r}^{(1)2} C_2}{i\omega\beta\zeta} \end{aligned} \tag{C.35}$$

Now, the solution τ is of the form

$$\tau = \tau_h + \tau_p = D_0 + D_1 e^{Y/\zeta} + \frac{F}{\zeta\lambda_1^2 - \lambda_1} e^{\lambda_1 Y}$$
$$+ c_2\left(\hat{r}^{(2)} - \frac{\hat{r}^{(1)2}}{i\omega\beta\zeta}\right) y e^{Y/\zeta} \qquad (C.36)$$

Since $\tau = \tau_s$ at $y = 0$ and $\tau = 0$ at $y = -\infty$, then

$$D_0 = 0$$
$$D_1 = \hat{T}_s^{(2)} - \frac{F}{\zeta\lambda_1^2 - \lambda_1} \qquad (C.37)$$

Finally,

$$\tau = \left(\hat{T}_s^{(2)} - \frac{F}{\zeta\lambda_1^2 - \lambda_1}\right) e^{Y/\zeta} + \frac{F}{\zeta\lambda_1^2 - \lambda_1} e^{\lambda_1 Y}$$
$$+ c_2\left(\hat{r}^{(2)} - \frac{\hat{r}^{(1)2}}{i\omega\beta\zeta}\right) y e^{Y/\zeta} \qquad (C.38)$$

and

$$\frac{\partial\tau}{\partial y} = \frac{1}{\zeta}\left(\hat{T}_s^{(2)} - \frac{F}{\zeta\lambda_1^2 - \lambda_1}\right) e^{Y/\zeta} + \frac{\lambda_1 F}{\zeta\lambda_1^2 - \lambda_1} e^{\lambda_1 Y}$$
$$+ c_2\left(\hat{r}^{(2)} - \frac{\hat{r}^{(1)2}}{i\omega\beta\zeta}\right) e^{Y/\zeta} + \frac{c_2}{\zeta}\left(\hat{r}^{(2)} - \frac{\hat{r}^{(1)2}}{i\omega\beta\zeta}\right) y e^{Y/\zeta} \qquad (C.39)$$

At $y = 0$,

$$\left.\frac{\partial\tau}{\partial y}\right|_{y=0} = \frac{1}{\zeta}\left(\hat{T}_s^{(2)} - \frac{F}{\zeta\lambda_1^2 - \lambda_1}\right) + \frac{\lambda_1 F}{\zeta\lambda_1^2 - \lambda_1} + c_2\left(\hat{r}^{(2)} - \frac{\hat{r}^{(1)2}}{i\omega\beta\zeta}\right) \qquad (C.40)$$

and then from Eq. (3.10)

$$\left(\frac{\partial \hat{T}^{(2)}}{\partial y} \right)_+ = \frac{1}{\zeta\xi} \left(\hat{T}_s^{(2)} - \frac{F}{\zeta\lambda_1^2 - \lambda_1} \right) + \frac{\lambda_1 F}{\xi(\zeta\lambda_1^2 - \lambda_1)}$$

$$+ \frac{c_2}{\xi} \left(\hat{r}^{(2)} - \frac{\hat{r}^{(1)2}}{i\omega\beta\zeta} \right) + \hat{r}^{(2)} L$$

$$= \frac{1}{\zeta\xi} \left(\hat{T}_s^{(2)} - \frac{F}{\zeta\lambda_1^2 - \lambda_1} \right) + \frac{\lambda_1 F}{\xi(\zeta\lambda_1^2 - \lambda_1)} - \frac{c_2 \hat{r}^{(1)2}}{i\omega\beta\zeta\xi}$$

$$+ \left(\frac{c_2}{\xi} + L \right) c_1 \left[\hat{T}_s^{(2)} + \left(\frac{c_1}{2} - \frac{1}{\bar{T}_s} \right) \hat{T}_s^{(1)2} \right] \qquad \text{(C.41)}$$

Therefore,

$$\hat{T}_s^{(2)} = \left[\left(\frac{\partial \hat{T}^{(2)}}{\partial y} \right)_+ + \frac{F}{\xi(\zeta\lambda_1 - 1)} \left(\frac{1}{\zeta\lambda_1} - 1 \right) - \frac{c_2 c_3}{\xi} \right.$$

$$\left. - c_3 L \right] \left[\frac{1}{\zeta\xi} + \frac{c_1 c_2}{\xi} + c_1 L \right]^{-1} \qquad \text{(C.42)}$$

Note that in actual calculation the term $\hat{T}_s^{(1)2}$ has to be substituted by $(1/2)\hat{T}_s^{(1)\dagger}\hat{T}_s^{(1)}$ as indicated in Eq. (3.13).

2. Temperature Conditions at Flame Edge

The temperature at the flame edge can be obtained by assuming that the flow very close to the flame is isentropic (see [21]). Writing this expression in terms of temperature and pressure yields

$$\frac{P}{P^{(0)}} = \left(\frac{\rho}{\rho^{(0)}} \right)^{\gamma} = \left(\frac{T}{T^{(0)}} \right)^{(\gamma/\gamma-1)} \tag{C.43}$$

Therefore,

$$\frac{T}{T^{(0)}} = \left(\frac{P}{P^{(0)}} \right)^{(\gamma-1)/\gamma}$$

or

$$\ell n\left(\frac{T}{T^{(0)}} \right) = \frac{\gamma - 1}{\gamma} \ell n\left(\frac{P}{P^{(0)}} \right) \tag{C.44}$$

Perturbing both sides yields

$$\ell n\left(1 + \epsilon \frac{\hat{T}^{(1)}}{T^{(0)}} + \epsilon^2 \frac{\hat{T}^{(2)}}{T^{(0)}} \right) = \frac{\gamma - 1}{\gamma} \ell n\left(1 + \epsilon \frac{\hat{P}^{(1)}}{P^{(0)}} + \epsilon^2 \frac{\hat{P}^{(2)}}{P^{(0)}} \right) \tag{C.45}$$

Since $\ell n(1 + \lambda) = \lambda - (1/2)\lambda^2 + (1/3)\lambda^3 - \ldots$ for $|\lambda| < 1$, Eq. (C.45) can be rewritten as follows:

$$\epsilon \frac{\hat{T}^{(1)}}{T^{(0)}} + \epsilon^2 \left(\frac{\hat{T}^{(2)}}{T^{(0)}} - \frac{1}{2} \frac{\hat{T}^{(1)2}}{T^{(0)2}} \right) + O(\epsilon^3) = \frac{\gamma - 1}{\gamma} \left[\epsilon \frac{\hat{P}^{(1)}}{P^{(0)}} + \epsilon^2 \left(\frac{\hat{P}^{(2)}}{P^{(0)}} - \frac{1}{2} \frac{\hat{P}^{(1)2}}{P^{(0)2}} \right) \right] + O(\epsilon^3) \tag{C.46}$$

Thus, for the first order term, we have

$$\frac{\hat{T}^{(1)}}{T^{(0)}} = \frac{\gamma - 1}{\gamma} \frac{\hat{P}^{(1)}}{P^{(0)}} \tag{C.47}$$

and for the second order term

$$\frac{\hat{T}^{(2)}}{T^{(0)}} - \frac{1}{2} \frac{\hat{T}^{(1)2}}{T^{(0)2}} = \frac{\gamma - 1}{\gamma} \left(\frac{\hat{P}^{(2)}}{P^{(0)}} - \frac{1}{2} \frac{\hat{P}^{(1)2}}{P^{(0)2}} \right) \tag{C.48}$$

Since DS/Dt = 0, where S denotes the entropy, which means that the entropy is conserved for each fluid particle convected away from the flame, Eq. (C.47) is of the form

$$\frac{1}{T^{(0)}} [\hat{T}^{(1)}(y + \Delta y, x + \Delta x, t) - \hat{T}^{(1)}(y, x, t - \Delta t)] = \frac{\gamma - 1}{\gamma} \frac{1}{P^{(0)}} [\hat{P}^{(1)}(y + \Delta y, x + \Delta x, t) - \hat{P}^{(1)}(y, x, t - \Delta t)] \tag{C.49}$$

Assuming that $\partial\hat{T}^{(1)}/\partial y >> \partial\hat{T}^{(1)}/\partial x$ and $\hat{P}^{(1)}$ is constant at $y = \ell$ (flame edge), then

$$\frac{1}{T^{(0)}} \left(\frac{\partial\hat{T}^{(1)}}{\partial y} + i\omega\hat{T}^{(1)} \right) = \frac{\gamma - 1}{\gamma} i\omega \frac{\hat{P}^{(1)}}{P^{(0)}} \tag{C.50}$$

Substituting Eq. (C.47) into Eq. (C.48) shows

$$\frac{\hat{T}^{(2)}}{T^{(0)}} = \frac{\gamma - 1}{\gamma} \left(\frac{\hat{P}^{(2)}}{P^{(0)}} - \frac{1}{2\gamma} \frac{\hat{P}^{(1)2}}{P^{(0)2}} \right) \tag{C.51}$$

and using the same argument about the entropy conservation,

$$\frac{1}{T^{(0)}}\left(\frac{\partial \hat{T}^{(2)}}{\partial y} + i2\omega\hat{T}^{(2)}\right) = \frac{\gamma - 1}{\gamma}\left(i2\omega\frac{\hat{P}^{(2)}}{P^{(0)}} - \frac{i\omega}{\gamma P^{(0)2}}\hat{P}^{(1)2}\right) \tag{C.52}$$

Combining Eqs. (C.50) and (C.52) yields

$$\frac{1}{T^{(0)}}\left(\frac{\partial \hat{T}^{(I)}}{\partial y} + iI\omega\hat{T}^{(I)}\right) - iI\omega\frac{\gamma - 1}{\gamma}\frac{\hat{P}^{(I)}}{P^{(0)}} = -\frac{(\gamma - 1)}{\gamma^2}\frac{i\omega}{P^{(0)2}}\hat{P}^{(1)2}$$

or

$$iI\omega\hat{T}^{(I)} + \frac{\partial \hat{T}^{(I)}}{\partial y} - iI\omega\frac{\gamma - 1}{\gamma}\hat{P}^{(I)} = -\frac{(\gamma - 1)}{\gamma^2}i\omega\hat{P}^{(1)2} \tag{C.53}$$

which is equivalent to Eq. (3.39).

3. Fuel Species Condition at Interface

Since the mass flux fraction of the fuel and oxidizer is fixed by the propellant composition, the species boundary condition at the gas-solid interface can be derived from Eq. (3.4). After neglecting the unsteady and reaction terms, the governing equation yields

$$\rho u_i Y_{,i} - Y_{,ii} = 0 \tag{C.54}$$

For one-dimensional consideration, Eq. (C.54) can be integrated with respect to y and the results show

$$m_f = Y - \frac{1}{m}\frac{dY}{dy} \tag{C.55}$$

where m is the mass flux and m_f is the fuel mass flux fraction. Perturbing Eq. (C.55) yields

$$m_f^{(0)} + \epsilon\hat{m}_f^{(1)} + \epsilon^2\hat{m}_f^{(2)} = [Y^{(0)} + \epsilon\hat{Y}^{(1)} + \epsilon^2\hat{Y}^{(2)}]$$

$$- [m^{(0)} + \epsilon\hat{m}^{(1)} + \epsilon^2\hat{m}^{(2)}]^{-1} \frac{d}{dy} (Y^{(0)} + \epsilon\hat{Y}^{(1)} + \epsilon^2\hat{Y}^{(2)})$$

$$= \left[Y^{(0)} - \frac{1}{m^{(0)}} \frac{dY^{(0)}}{dy} \right] + \epsilon \left[\hat{Y}^{(1)} - \frac{1}{m^{(0)}} \left\{ \frac{d\hat{Y}^{(1)}}{dy} \right.\right.$$

$$\left.\left. - \frac{\hat{m}^{(1)}}{m^{(0)}} \frac{dY^{(0)}}{dy} \right\} \right] + \epsilon^2 \left[\hat{Y}^{(2)} - \frac{1}{m^{(0)}} \left\{ \frac{d\hat{Y}^{(2)}}{dy} - \frac{\hat{m}^{(1)}}{m^{(0)}} \frac{d\hat{Y}^{(1)}}{dy} \right.\right.$$

$$\left.\left. + \left(\frac{\hat{m}^{(1)2}}{m^{(0)2}} - \frac{\hat{m}^{(2)}}{m^{(0)}} \right) \frac{dY^{(0)}}{dy} \right\} \right] - \frac{1}{m^{(0)}} O(\epsilon^3) \qquad \text{(C.56)}$$

Therefore,

$$m_f^{(0)} = Y^{(0)} - \frac{1}{m^{(0)}} \frac{dY^{(0)}}{dy}$$

$$\hat{m}_f^{(1)} = \hat{Y}^{(1)} - \frac{1}{m^{(0)}} \left(\frac{dY^{(1)}}{dy} - \frac{\hat{m}^{(1)}}{m^{(0)}} \frac{dY^{(0)}}{dy} \right) \qquad \text{(C.57)}$$

$$\hat{m}_f^{(2)} = \hat{Y}^{(2)} - \frac{1}{m^{(0)}} \left(\frac{d\hat{Y}^{(2)}}{dy} - \frac{\hat{m}^{(2)}}{m^{(0)}} \frac{dY^{(0)}}{dy} \right)$$

$$+ \frac{1}{m^{(0)}} \left(\frac{\hat{m}^{(1)}}{m^{(0)}} \frac{d\hat{Y}^{(1)}}{dy} - \frac{\hat{m}^{(1)2}}{m^{(0)2}} \frac{dY^{(0)}}{dy} \right)$$

Since $\hat{m}_f^{(1)} = \hat{m}_f^{(2)} = 0$, and using Eqs. (B.12) - (B.13), we have

$$\hat{Y}^{(1)} - \left(\frac{d\hat{Y}^{(1)}}{dy} - \rho_s r^{(0)} c_1 \hat{T}_s^{(1)} \frac{dY^{(0)}}{dy} \right) = 0 \qquad \text{(C.58)}$$

$$\hat{Y}^{(2)} - \left[\frac{d\hat{Y}^{(2)}}{dy} - \rho_s r^{(0)} c_1 \left\{ \hat{T}_s^{(2)} + \left(\frac{c_1}{2} - \frac{1}{\bar{T}_s} \right) \hat{T}_s^{(1)2} \right\} \frac{dY^{(0)}}{dy} \right]$$

$$+ \rho_s r^{(0)} c_1 \hat{T}_s^{(1)} \frac{d\hat{Y}^{(1)}}{dy} - (\rho_s r^{(0)} \hat{T}_s^{(1)})^2 \frac{dY^{(0)}}{dy} = 0 \qquad \text{(C.59)}$$

Knowing that $\rho_s r^{(0)} = \rho_0 v^{(0)} = 1$, we have

$$\hat{Y}^{(1)} = \frac{d\hat{Y}^{(1)}}{dy} - c_1 \frac{dY^{(0)}}{dy} \hat{T}_s^{(1)} \tag{C.60}$$

$$\hat{Y}^{(2)} = \frac{d\hat{Y}^{(2)}}{dy} - c_1 \frac{dY^{(0)}}{dy} \left\{ \hat{T}_s^{(2)} + \left(\frac{c_1}{2} - \frac{1}{\bar{T}_s} \right) \hat{T}_s^{(1)2} \right\}$$

$$- c_1 \hat{T}_s^{(1)} \frac{d\hat{Y}^{(1)}}{dy} + \hat{T}_s^{(1)2} \frac{dY^{(0)}}{dy} \tag{C.61}$$

Combining the two equations yields Eq. (3.43).

4. Normal Velocity Condition at Interface

The boundary condition of the normal velocity component is decided using the mass balance condition at the interface. For the first order mass balance, we have

$$\rho_s \hat{r}^{(1)} = \rho^{(0)} \hat{v}^{(1)} + \hat{\rho}^{(1)} v^{(0)} \tag{C.62}$$

Therefore,

$$\hat{v}^{(1)} = T^{(0)} (\rho_s \hat{r}^{(1)} - \hat{\rho}^{(1)} r^{(0)})$$

$$= T^{(0)} \left[\rho_s r^{(0)} \frac{E_s}{\bar{T}_s^2} \hat{T}_s^{(1)} - \left(\hat{P}^{(1)} - \frac{\hat{T}^{(1)}}{T^{(0)}} \right) \right]$$

$$= \left(\frac{E_s}{\bar{T}_s} + 1 \right) \hat{T}_+^{(1)} - \bar{T}_s \hat{P}^{(1)} \tag{C.63}$$

where

$$\hat{r}^{(1)} = r^{(0)} \frac{E_s}{\bar{T}_s^2} \hat{T}_s^{(1)}$$

and

$$\hat{P}^{(1)} = \rho^{(0)}\hat{T}^{(1)} + \hat{\rho}^{(1)}T^{(0)}$$

are used. For the second order condition,

$$\rho_s\hat{r}^{(2)} = \rho^{(0)}\hat{v}^{(2)} + \hat{\rho}^{(1)}\hat{v}^{(1)} + \hat{\rho}^{(2)}v^{(0)}$$

or

$$\begin{aligned}
\hat{v}^{(2)} &= T^{(0)}[\rho_s\hat{r}^{(2)} - \hat{\rho}^{(1)}\hat{v}^{(1)} - \hat{\rho}^{(2)}T^{(0)}] \\
&= T^{(0)}\Bigg[\rho_s r^{(0)}\frac{E_s}{\bar{T}_s^2}\left\{\hat{T}_s^{(2)} + \frac{1}{\bar{T}_s}\left(\frac{1}{2}\frac{E_s}{\bar{T}_s} - 1\right)\hat{T}_s^{(1)2}\right\} \\
&\quad - \frac{1}{T^{(0)}}(\hat{P}^{(1)} - \rho^{(0)}\hat{T}^{(1)})\hat{v}^{(1)} - (\hat{P}^{(2)} - \hat{\rho}^{(1)}\hat{T}_s^{(1)} - \rho^{(0)}\hat{T}_s^{(2)})\Bigg] \\
&= \left(\frac{E_s}{\bar{T}_s} + 1\right)\hat{T}_s^{(2)} - \bar{T}_s\hat{P}^{(2)} + \frac{E_s}{\bar{T}_s^2}\left(\frac{1}{2}\frac{E_s}{\bar{T}_s} - 1\right)\hat{T}_s^{(1)2} \\
&\quad - (\hat{P}^{(1)} - \rho^{(0)}\hat{T}_s^{(1)})\hat{v}^{(1)} + (\hat{P}^{(1)} - \rho^{(0)}\hat{T}_s^{(1)})\hat{T}_s^{(1)} \\
&= \left(\frac{E_s}{\bar{T}_s} + 1\right)\hat{T}_+^{(2)} - \bar{T}_s\hat{P}^{(2)} + C_1\left(\frac{1}{2}\frac{E_s}{\bar{T}_s} - 1\right)\hat{T}_+^{(1)2} \\
&\quad + (\hat{T}_+^{(1)} - \hat{v}_+^{(1)})\left(\hat{P}^{(1)} - \frac{1}{\bar{T}_s}\hat{T}_+^{(1)}\right)
\end{aligned} \tag{C.64}$$

Combining Eqs. (C.63) and (C.64) yields Eq. (3.44).

5. Parallel Velocity Conditions at Interface

Since the parallel component of the velocity has to be zero at the actual solid surface in order to satisfy the no-slip condition, we can derive the higher order condition using the Taylor series expansion about the origin such that

$$u_+ = u_+^{(0)} + \frac{\partial u_+^{(0)}}{\partial y}\,\delta y + \frac{1}{2}\,\frac{\partial^2 u_+^{(0)}}{\partial y^2}\,\delta y^2 + \ldots \qquad \text{(C.65)}$$

Differentiating Eq. (C.65) with respect to t and multiplying ρ yields

$$\rho\,\frac{\partial u_+}{\partial t} = \rho v_+\,\frac{\partial u_+^{(0)}}{\partial y} + \frac{1}{2}\,\rho v_+\,\frac{\partial^2 u_+^{(0)}}{\partial y^2}\,\delta y + \ldots \qquad \text{(C.66)}$$

For the first order condition,

$$i\omega\hat{u}_+^{(1)} = \beta\hat{r}^{(1)}\,\frac{\partial u^{(0)}}{\partial y}\bigg|_+$$

or

$$\hat{u}_+^{(1)} = \frac{\beta}{i\omega\beta}\,\hat{r}^{(1)}\,\frac{\partial u^{(0)}}{\partial y}\bigg|_+ \qquad \text{(C.67)}$$

For the second order condition,

$$i2\omega\hat{u}_+^{(2)} = \beta\left[\hat{r}^{(1)}\,\frac{\partial\hat{u}^{(1)}}{\partial y}\bigg|_+ + \hat{r}^{(2)}\,\frac{\partial u^{(0)}}{\partial y}\bigg|_+\right] - \frac{i\beta^2}{4\omega}\,\hat{r}^{(1)2}\,\frac{\partial^2 u^{(0)}}{\partial y^2}\bigg|_+$$

or

$$\hat{u}_+^{(2)} = \frac{\beta}{i2\omega}\left[\hat{r}^{(1)}\,\frac{\partial\hat{u}^{(1)}}{\partial y}\bigg|_+ + \hat{r}^{(2)}\,\frac{\partial u^{(0)}}{\partial y}\bigg|_+\right] - \frac{\beta^2}{8\omega^2}\,\hat{r}^{(1)2}\,\frac{\partial^2 u^{(0)}}{\partial y^2}\bigg|_+$$

$$= \frac{\beta}{i2\omega} \frac{\partial \hat{u}^{(1)}}{\partial y} \Bigg|_{+} \hat{r}^{(2)} + \frac{\beta}{i2\omega} \frac{\partial \hat{u}^{(1)}}{\partial y} \Bigg|_{+} \hat{r}^{(1)}$$

$$- \frac{\beta^2}{8\omega^2} \frac{\partial^2 u^{(0)}}{\partial y^2} \Bigg|_{+} \hat{r}^{(1)2} \qquad \text{(C.68)}$$

Combining Eqs. (C.67) and (C.68) yields Eq. (3.45).

APPENDIX D

DERIVATIONS OF FINITE ELEMENT EQUATIONS

1. Zeroth Order Analysis

The formulation of the zeroth order governing equations (3.16) is

$$(ZA_{\alpha\beta} + ZB_{\alpha\beta})T_{\beta}^{(0)} = ZG_{\alpha} \tag{D.1}$$

where

$$ZA_{\alpha\beta} = \int_{\Omega} \phi_{\alpha}\phi_{\beta,i}\, d\Omega$$

$$ZB_{\alpha\beta} = \int_{\Omega} \phi_{\alpha,i}\phi_{\beta,i}\, d\Omega$$

$$ZG_{\alpha} = \int_{\Gamma} T_{,i}^{(0)} n_i \phi_{\alpha}^{*}\, d\Gamma + h \int_{\Omega} \phi_{\alpha}\phi_{\beta} W_{\beta}^{(0)}\, d\Omega$$

and

$$W_{\beta}^{(0)} = \left[\frac{1}{h^2}\, Bz \left(\frac{1 - T^{(0)}}{T^{(0)}}\right)^2 e^{-E/T^{(0)}}\right]_{\beta}$$

2. Higher Order Analysis

The finite element analogs for the higher order system are summarized below.

Continuity

$$[(iI\omega)FA_{\alpha\beta} + FB_{\alpha\beta} + FC_{\alpha\beta}]\hat{\rho}_{\beta}^{(I)} + [FD_{\alpha\beta} + FE_{\alpha\beta}]\hat{u}_{\beta}^{(I)}$$

$$+ [FF_{\alpha\beta} + FH_{\alpha\beta}]v_{\beta}^{(I)} = FG_{\alpha} \qquad (D.2)$$

where

$$FA_{\alpha\beta} = \int_{\Omega} \phi_{\alpha}\phi_{\beta}\, d\Omega$$

$$FB_{\alpha\beta} = \int_{\Omega} \phi_{\alpha}\phi_{\beta,i}\phi_{\gamma}u_{\gamma i}^{(0)}\, d\Omega$$

$$FC_{\alpha\beta} = \int_{\Omega} \phi_{\alpha}\phi_{\beta}\phi_{\gamma,i}u_{\gamma i}^{(0)}\, d\Omega$$

$$FD_{\alpha\beta} = \int_{\Omega} \phi_{\alpha}\phi_{\beta}\phi_{\gamma,i}\rho_{\gamma}^{(0)}\, d\Omega \quad , \quad (i = 1)$$

$$FE_{\alpha\beta} = \int_{\Omega} \phi_{\alpha}\phi_{\beta,i}\phi_{\gamma}\rho_{\gamma}^{(0)}\, d\Omega \quad , \quad (i = 1)$$

$$FF_{\alpha\beta} = \int_{\Omega} \phi_{\alpha}\phi_{\beta}\phi_{\gamma,i}\rho_{\gamma}^{(0)}\, d\Omega \quad , \quad (i = 2)$$

$$FH_{\alpha\beta} = \int_{\Omega} \phi_{\alpha}\phi_{\beta,i}\phi_{\gamma}\rho_{\gamma}^{(0)}\, d\Omega \quad , \quad (i = 2)$$

$$FG_{\alpha} = -\int_{\Omega} \phi_{\alpha}\phi_{\beta,i}\phi_{\gamma}\hat{\rho}_{\beta}^{(1)}\hat{u}_{\gamma i}^{(1)}\, d\Omega - \int_{\Omega} \phi_{\alpha}\phi_{\beta}\phi_{\gamma,i}\hat{\rho}_{\beta}^{(1)}\hat{u}_{\gamma i}^{(1)}\, d\Omega$$

Momentum Equation, (X-component)

$$[XA_{\alpha\beta}]\hat{\rho}_{\beta}^{(I)} + [(iI\omega)XB_{\alpha\beta} + XC_{\alpha\beta} + XD_{\alpha\beta} + XE_{\alpha\beta} + XF_{\alpha\beta}]\hat{u}_{\beta}^{(I)} + [XH_{\alpha\beta} + XI_{\alpha\beta}]\hat{v}_{\beta}^{(I)} + XJ_{\alpha\beta}\hat{P}_{\beta}^{(I)} = XG_{\alpha} \qquad (D.3)$$

where

$$XA_{\alpha\beta} = \int_{\Omega} \phi_\alpha \phi_\beta \phi_\gamma \phi_{\delta,j} u^{(0)}_{\gamma j} u^{(0)}_{\delta i} \, d\Omega$$

$$XB_{\alpha\beta} = \int_{\Omega} \phi_\alpha \phi_\beta \phi_\gamma \rho^{(0)}_\gamma \, d\Omega$$

$$XC_{\alpha\beta} = \int_{\Omega} \phi_\alpha \phi_{\beta,j} \phi_\gamma \phi_\delta \rho^{(0)}_\gamma u^{(0)}_{\delta j} \, d\Omega$$

$$XD_{\alpha\beta} = \int_{\Omega} \phi_\alpha \phi_\beta \phi_\gamma \phi_{\delta,j} \rho^{(0)}_\gamma u^{(0)}_{\delta i} \, d\Omega \quad , \quad (j = 1)$$

$$XE_{\alpha\beta} = Pr \int_{\Omega} \phi_{\alpha,j} \phi_{\beta,j} \, d\Omega$$

$$XF_{\alpha\beta} = \frac{1}{3} Pr \int_{\Omega} \phi_{\alpha,i} \phi_{\beta,j} \, d\Omega \quad , \quad (j = 1)$$

$$XH_{\alpha\beta} = \int_{\Omega} \phi_\alpha \phi_\beta \phi_\gamma \phi_{\delta,j} \rho^{(0)}_\gamma u^{(0)}_{\delta i} \, d\Omega \quad , \quad (j = 2)$$

$$XI_{\alpha\beta} = \frac{1}{3} Pr \int_{\Omega} \phi_{\alpha,i} \phi_{\beta,j} \, d\Omega \quad , \quad (j = 2)$$

$$XJ_{\alpha\beta} = \frac{1}{\gamma M_b^{\,2}} \int_{\Omega} \phi_\alpha \phi_{\beta,i} \, d\Omega$$

$$XG_\alpha = -\int_{\Omega} \phi_\alpha \phi_\beta \phi_\gamma \phi_{\delta,j} \rho^{(0)}_\beta \hat{u}^{(1)}_{\gamma j} u^{(1)}_{\delta i} \, d\Omega$$

$$- \int_{\Omega} \phi_\alpha \phi_\beta \phi_\gamma \phi_{\delta,j} \hat{\rho}^{(1)}_\beta u^{(0)}_{\gamma j} u^{(1)}_{\delta i} \, d\Omega$$

$$- \int_{\Omega} \phi_\alpha \phi_\beta \phi_\gamma \phi_{\delta,j} \hat{\rho}^{(1)}_\beta \hat{u}^{(1)}_{\gamma j} u^{(0)}_{\delta i} \, d\Omega + Pr \left[\int_{\Gamma} \hat{u}^{(I)}_{i,j} n_j \phi^*_\alpha \, d\Gamma \right.$$

$$+ \frac{1}{3}\int_{\Gamma} \hat{u}^{(I)}_{j,j} n_i \phi^*_\alpha \, d\Gamma \Big] \quad , \qquad (i = 1)$$

Here, all i = 1.

Momentum Equation, (Y-component)

$$[YA_{\alpha\beta}]\rho^{(I)}_\beta + [YB_{\alpha\beta} + YC_{\alpha\beta}]u^{(I)}_\beta + [(iI\omega)YD_{\alpha\beta} + YE_{\alpha\beta} + YF_{\alpha\beta} + YH_{\alpha\beta} + YI_{\alpha\beta}]v^{(I)}_\beta + YJ_{\alpha\beta}P^{(I)}_\beta = YG_\alpha \qquad (D.4)$$

where

$$YA_{\alpha\beta} = XA_{\alpha\beta} \quad , \qquad YB_{\alpha\beta} = XD_{\alpha\beta}$$

$$YC_{\alpha\beta} = XF_{\alpha\beta} \quad , \qquad YD_{\alpha\beta} = XB_{\alpha\beta}$$

$$YE_{\alpha\beta} = XC_{\alpha\beta} \quad , \qquad YF_{\alpha\beta} = XH_{\alpha\beta}$$

$$YH_{\alpha\beta} = XE_{\alpha\beta} \quad , \qquad YI_{\alpha\beta} = XI_{\alpha\beta}$$

$$YJ_{\alpha\beta} = XJ_{\alpha\beta} \quad , \qquad YG_\alpha = XG_\alpha$$

Here, all i = 2.

Energy Equation

$$[EA_{\alpha\beta} + EB_{\alpha\beta}]\rho^{(I)}_\beta + EC_{\alpha\beta}u^{(I)}_\beta + ED_{\alpha\beta}v^{(I)}_\beta + [(iI\omega)EE_{\alpha\beta} + EF_{\alpha\beta} + EH_{\alpha\beta} + EI_{\alpha\beta}]T^{(I)}_\beta + EJ_{\alpha\beta}Y^{(I)}_\beta + EK_{\alpha\beta}P^{(I)}_\beta = EG_\alpha \qquad (D.5)$$

where

$$EA_{\alpha\beta} = \int_{\Omega} \phi_\alpha \phi_\beta \phi_\gamma \phi_{\delta,i} u_{\gamma i}^{(0)} T_\delta^{(0)} d\Omega$$

$$EB_{\alpha\beta} = -h \int_{\Omega} \phi_\alpha \phi_\beta \phi_\gamma \left(\frac{2w^{(0)}}{\rho^{(0)}} \right)_\gamma d\Omega$$

$$EC_{\alpha\beta} = \int_{\Omega} \phi_\alpha \phi_\beta \phi_\gamma \phi_{\delta,i} \rho_\gamma^{(0)} T_\delta^{(0)} d\Omega \ , \quad (i = 1)$$

$$ED_{\alpha\beta} = \int_{\Omega} \phi_\alpha \phi_\beta \phi_\gamma \phi_{\delta,i} \rho_\gamma^{(0)} T_\delta^{(0)} d\Omega \ , \quad (i = 2)$$

$$EE_{\alpha\beta} = \int_{\Omega} \phi_\alpha \phi_\beta \phi_\gamma \rho_\gamma^{(0)} d\Omega$$

$$EF_{\alpha\beta} = \int_{\Omega} \phi_\alpha \phi_{\beta,i} \phi_\gamma \phi_\delta \rho_\gamma^{(0)} u_{\delta i}^{(0)} d\Omega$$

$$EH_{\alpha\beta} = \int_{\Omega} \phi_{\alpha,i} \phi_{\beta,i} \, d\Omega$$

$$EI_{\alpha\beta} = -h \int_{\Omega} \phi_\alpha \phi_\beta \phi_\gamma \left(\frac{E}{T^{(0)2}} w^{(0)} \right)_\gamma d\Omega$$

$$EJ_{\alpha\beta} = -h \int_{\Omega} \phi_\alpha \phi_\beta \phi_\gamma \left(\frac{2w^{(0)}}{Y^{(0)}} \right)_\gamma d\Omega$$

$$EK_{\alpha\beta} = -\frac{\gamma - 1}{\gamma} \int_{\Omega} \phi_\alpha \phi_\beta \, d\Omega$$

$$EG_\alpha = -\int_{\Omega} \phi_\alpha \phi_\beta \phi_\gamma \phi_{\delta,i} \rho_\beta^{(0)} u_{\gamma i}^{(1)} T_\delta^{(1)} d\Omega$$

$$- \int_{\Omega} \phi_\alpha \phi_\beta \phi_\gamma \phi_{\delta,i} \rho_\beta^{(1)} u_{\gamma i}^{(0)} T_\delta^{(1)} d\Omega$$

$$- \int_\Omega \phi_\alpha \phi_\beta \phi_\gamma \phi_{\delta,i} \rho_\beta^{(1)} u_{\gamma i}^{(1)} T_\delta^{(0)} d\Omega + \int_\Gamma T_{,i}^{(I)} n_i \phi_\alpha^* \, d\Gamma$$

$$+ h \int_\Omega \phi_\alpha \phi_\beta \phi_\gamma \phi_\delta \left[\frac{Ew^{(0)}}{T^{(0)}} \left(\frac{E}{2T^{(0)}} - 1 \right) \right]_\beta T_\gamma^{(1)} T_\delta^{(1)} d\Omega$$

$$+ h \int_\Omega \phi_\alpha \phi_\beta \phi_\gamma \phi_\delta \left(\frac{2Ew^{(0)}}{\rho^{(0)} T^{(0)2}} \right)_\beta \rho_\gamma^{(1)} T_\delta^{(1)} d\Omega$$

$$+ h \int_\Omega \phi_\alpha \phi_\beta \phi_\gamma \phi_\delta \left(\frac{2Ew^{(0)}}{Y^{(0)} T^{(0)2}} \right)_\beta Y_\gamma^{(1)} T_\delta^{(1)} d\Omega$$

$$+ h \int_\Omega \phi_\alpha \phi_\beta \phi_\gamma \phi_\delta \left(\frac{4w^{(0)}}{\rho^{(0)} Y^{(0)}} \right)_\beta \rho_\gamma^{(1)} Y_\delta^{(1)} d\Omega$$

$$+ h \int_\Omega \phi_\alpha \phi_\beta \phi_\gamma \phi_\delta \left(\frac{w^{(0)}}{\rho^{(0)2}} \right)_\beta \rho_\gamma^{(1)} \rho_\delta^{(1)} d\Omega$$

$$+ h \int_\Omega \phi_\alpha \phi_\beta \phi_\gamma \phi_\delta \left(\frac{w^{(0)}}{Y^{(0)2}} \right)_\beta Y_\gamma^{(1)} Y_\delta^{(1)} d\Omega$$

$$- i\omega \int_\Omega \phi_\alpha \phi_\beta \phi_\gamma \rho_\beta^{(1)} T_\gamma^{(1)} d\Omega$$

Species Equation

$$[SA_{\alpha\beta} + SB_{\alpha\beta}] \rho_\beta^{(I)} + SC_{\alpha\beta} u_\beta^{(I)} + SD_{\alpha\beta} v_\beta^{(I)} + SE_{\alpha\beta} T_\beta^{(I)}$$

$$+ [(iI\omega) SF_{\alpha\beta} + SH_{\alpha\beta} + SI_{\alpha\beta} + SJ_{\alpha\beta}] Y_\beta^{(I)} = SG_\alpha \qquad (D.6)$$

where

$$SA_{\alpha\beta} = \int_\Omega \phi_\alpha \phi_\beta \phi_\gamma \phi_{\delta,i} u_{\gamma i}^{(0)} Y_\delta^{(0)} d\Omega$$

$$SB_{\alpha\beta} = \int_\Omega \phi_\alpha \phi_\beta \phi_\gamma \phi_\delta \left(\frac{2w^{(0)}}{\rho^{(0)}} \right)_\gamma T_\delta^{(0)} d\Omega$$

$$SC_{\alpha\beta} = \int_{\Omega} \phi_\alpha \phi_\beta \phi_\gamma \phi_{\delta,i} \rho_\gamma^{(0)} Y_\delta^{(0)} d\Omega \ , \qquad (i = 1)$$

$$SD_{\alpha\beta} = \int_{\Omega} \phi_\alpha \phi_\beta \phi_\gamma \phi_{\delta,i} \rho_\gamma^{(0)} Y_\delta^{(0)} d\Omega \ , \qquad (i = 2)$$

$$SE_{\alpha\beta} = \int_{\Omega} \phi_\alpha \phi_\beta \phi_\gamma \left(\frac{Ew^{(0)}}{T^{(0)2}} \right)_\gamma d\Omega$$

$$SF_{\alpha\beta} = \int_{\Omega} \phi_\alpha \phi_\beta \phi_\gamma \rho_\gamma^{(0)} d\Omega$$

$$SH_{\alpha\beta} = \int_{\Omega} \phi_\alpha \phi_{\beta,i} \phi_\gamma \phi_\delta \rho_\gamma^{(0)} u_{\delta i}^{(0)} d\Omega$$

$$SI_{\alpha\beta} = \int_{\Omega} \phi_{\alpha,i} \phi_{\beta,i} \, d\Omega$$

$$SJ_{\alpha\beta} = \int_{\Omega} \phi_\alpha \phi_\beta \phi_\gamma \left(\frac{2w^{(0)}}{Y^{(0)}} \right)_\gamma d\Omega$$

$$SG_\alpha = -\int_{\Omega} \phi_\alpha \phi_\beta \phi_\gamma \phi_{\delta,i} \rho_\beta^{(0)} u_{\gamma i}^{(1)} Y_\delta^{(1)} d\Omega$$

$$- \int_{\Omega} \phi_\alpha \phi_\beta \phi_\gamma \phi_{\delta,i} \rho_\beta^{(1)} u_{\gamma i}^{(0)} Y_\delta^{(1)} d\Omega$$

$$- \int_{\Omega} \phi_\alpha \phi_\beta \phi_\gamma \phi_{\delta,i} \rho_\beta^{(1)} u_{\gamma i}^{(1)} Y_\delta^{(0)} d\Omega$$

$$- \int_{\Omega} \phi_\alpha \phi_\beta \phi_\gamma \phi_\delta \left[\frac{Ew^{(0)}}{T^{(0)3}} \left(\frac{E}{2T^{(0)}} - 1 \right) \right]_\beta T_\gamma^{(1)} T_\delta^{(1)} d\Omega$$

$$- \int_{\Omega} \phi_\alpha \phi_\beta \phi_\gamma \phi_\delta \left(\frac{2Ew^{(0)}}{\rho^{(0)} T^{(0)2}} \right)_\beta \rho_\gamma^{(1)} T_\delta^{(1)} d\Omega$$

$$
\begin{aligned}
&- \int_{\Omega} \phi_\alpha \phi_\beta \phi_\gamma \phi_\delta \left(\frac{2Ew^{(0)}}{Y^{(0)} T^{(0)2}} \right)_\beta Y_\gamma^{(1)} T_\delta^{(1)} \, d\Omega \\
&- \int_{\Omega} \phi_\alpha \phi_\beta \phi_\gamma \phi_\delta \left(\frac{4w^{(0)}}{\rho^{(0)} Y^{(0)}} \right)_\beta \rho_\gamma^{(1)} Y_\delta^{(1)} \, d\Omega \\
&- \int_{\Omega} \phi_\alpha \phi_\beta \phi_\gamma \phi_\delta \left(\frac{w^{(0)}}{\rho^{(0)2}} \right)_\beta \rho_\gamma^{(1)} \rho_\delta^{(1)} \, d\Omega \\
&- \int_{\Omega} \phi_\alpha \phi_\beta \phi_\gamma \phi_\delta \left(\frac{w^{(0)}}{Y^{(0)2}} \right)_\beta Y_\gamma^{(1)} Y_\delta^{(1)} \, d\Omega \\
&- i\omega \int_{\Omega} \phi_\alpha \phi_\beta \phi_\gamma \rho_\beta^{(1)} Y_\gamma^{(1)} \, d\Omega
\end{aligned}
$$